# APPARENT ADDITIONAL MASS

A THESIS

Submitted in partial fulfillment
of the requirements for the Degree
of Master of Science in Aeronautical Engineering

by

Melvyn Franklin Towsley

Georgia School of Technology
Atlanta, Georgia
1947

APPARENT ADDITIONAL MASS

Approved:

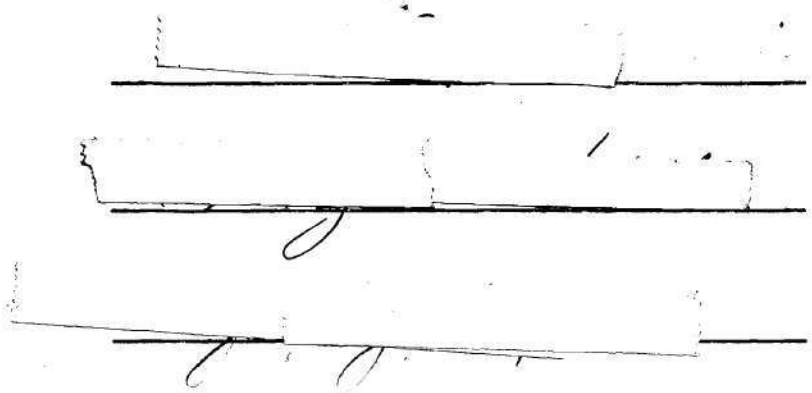

Date Approved by Chairman May 20th, 1947

## ACKNOWLEDGMENTS

I wish to thank Professors A. Y. Pope and G. K. Williams for their conscientious guidance and assistance in writing this paper. I also wish to thank Mr. J. E. Garrett for his cooperation in preparing the reproductions for Appendix I.

TABLE OF CONTENTS

# LIST OF FIGURES

PAGE

PAGE

PAGE

# APPARENT ADDITIONAL MASS

## INTRODUCTION

When a body moves through a perfect vacuum, there is nothing to hinder the motion once it has started. When the body is immersed in a perfect nonviscous, incompressible fluid, again there is nothing to hinder the motion once it has been started, but if the body should be accelerated, the force required would be that to accelerate the mass of the body plus a mass of air affected by the body. The apparent additional mass is a function of the affected mass.

Since each particle of fluid is not necessarily accelerated in the direction of motion, the apparent additional mass along the direction of motion need not be equal to the mass of the fluid displaced. For instance, theoretically the apparent additional mass of a sphere is only one-half of the mass of the displaced fluid.

It is the purpose of this paper to define the terms used, to present the basic theory, and to collect enough of the theoretical and experimental results so that the apparent additional effects for any body may be estimated.

These effects are not always small and should be considered for the following:

1. spinning of airplanes
2. maneuvering of airplanes
3. submarines

4. dirigibles
5. rockets
6. boats
7. pendulum tests
8. vibration tests
9. wind tunnel corrections where longitudinal static pressure gradient exists

## DEFINITION OF TERMS

Practically every paper written on apparent additional mass uses its own definitions and terms. This paper is no different. However, all of the definitions are basically the same. Each deals with a quantity that does not even exist but acts as though it does. This quantity has been called "virtual mass", "apparent mass", "entrained mass" and "additional mass". Probably the most descriptive term is "apparent additional mass", which will be used in this paper.

At this point it is well to dispense with "entrained mass". The apparent additional effect is not due to entrained fluid. This is an entirely different effect and is not connected with the apparent additional effect. Unfortunately, in experimental work it is impossible to completely separate the two effects as the entrained fluid effect is especially prevalent at the low velocities and accelerations at which most experimental work is conducted.

The term "apparent additional" may be used with any quantity based on a mass concept. This includes moment of inertia and momentum. The basic terms most commonly used are defined below:

$m_A$ = the apparent additional mass

$I_A$ = the apparent additional moment of inertia

$^1I_v$ = the virtual moment of inertia or the moment of inertia as measured in a fluid (not a vacuum)

$I_o = I_S$ = the true moment of inertia as measured in a vacuum

$k$ = the apparent additional mass coefficient and is equal to the apparent additional mass divided by the mass of the fluid displaced $(m_A/m_{D.F.})$

$k'$ = the apparent additional moment of inertia coefficient and is equal to the moment of inertia of the apparent additional mass divided by the moment of inertia of the displaced fluid $(I_A/I_{D.F.})$

$K$ = a special apparent additional mass coefficient. It is used in equations of the form $m_A = K \times C$, where C is a constant, dependent upon the body dimensions.

the mass density unless otherwise defined, slugs/ft$^3$

## THEORY

A solid in a perfect fluid moves like a solid in a vacuum except for one fundamental difference, this difference being due to the surrounding fluid that the solid affects. To determine the effect of this fluid, consider a solid moving through an infinite, motionless field of fluid particles. As the body moves, it pushes fluid particles out of its path, and since each particle has mass, work is done on each individual particle. As the body moves, the flow about it is created

---

[1] $I_v = I_o + I_A$

instantaneously as if created by impulse.[2] An impulse is applied by each increment of surface, and the direction of the impulse is normal to the surface increment.

The impulse is equal to the momentum imparted to each particle, whose kinetic energy is then proportional to the product of the velocity of the particle in the direction of motion (normal to the surface) and the impulse. The change of kinetic energy of the fluid due to the presence of the body is proportional to an impulse times the normal velocity or to the momentum of the fluid times the normal velocity. However, kinetic energy is equal to $1/2 mV^2$, where m is the mass and V is the velocity. If this kinetic energy is divided by $1/2 V^2$, where V is the velocity of the body in the direction of motion, the resulting number will have the units of mass. This is the apparent additional mass of the body in the direction of motion.

If the body moves with constant velocity, see Figure 1, momentum of the fluid is being constantly created at one point and annihilated at another, and in a perfect fluid the total momentum of the fluid remains zero. However, if the body is being uniformly accelerated, momentum of the flow is being built up and is stored in the fluid as kinetic energy.

It is now desirable to establish an equation for the calculation of this kinetic energy of the fluid which can then be used to compute

---

[2]The impulse of a constant force is defined as the product of the force and the time interval during which the force acts, where the time interval is extremely small.

the apparent additional mass and volume. As indicated above, the kinetic energy is dependent on the velocity normal to the surface and the impulse applied by each surface increment.

The normal velocity may be found from the velocity potential, $\phi$, which defines the flow. For a two-dimensional flow the velocity potential may be defined as $\phi = \int_c (udx + vdy)$, where u is the velocity in the x direction and v is the velocity in the y direction. Consider a flow in the x direction only where v is zero, then $\phi = \int_o^X udx = Xu$. From this it can be seen that the velocity potential is equal to a velocity times a distance, or in dimensional units

$$\phi = \frac{ft}{sec} \times ft = \frac{ft^2}{sec}$$

Also, from the above example it can be seen that the partial derivative of $\phi$ with respect to the direction is the velocity in that direction. Then the normal velocity is equal to the partial derivative of $\phi$ with respect to the normal direction or $\partial\phi/\partial m$.

Lamb[3] pointed out that any actual state of motion of a fluid could be produced instantaneously from rest by the application of a system of impulse pressures, provided a single valued velocity potential exists for the motion. The impulse pressure necessary to start the motion is $\rho\phi$, where $\rho$ is the mass density of the fluid. To show that $\rho\phi$ is an impulse pressure, or impulse per unit area, again consider the dimensional units:

---

[3] Lamb, Horace, Hydrodynamics, 5th ed., Cambridge: University Press, 1930. p. 16.

$$\rho\phi = \left[\frac{lb}{ft^3} \cdot \frac{sec^2}{ft}\right] \times \frac{ft^2}{sec} = \frac{lb\text{-}sec}{ft^2} = \frac{impulse}{unit\ area} = \text{impulse pressure}$$

The impulse may be found by multiplying the impulse pressure by an area. In this case, the surface increment area, $\Delta S$, is the area desired.

It is a proposition in dynamics that the work done by an impulse is equal to the impulse times one-half the sum of the initial and final velocities in the direction of the impulse. In this case, it is assumed that the fluid was motionless before it was displaced by the body; then the initial velocity is zero, and the average velocity is $\frac{1}{2}\frac{\partial\phi}{\partial m}$. Then the kinetic energy, $\Delta T$, of the fluid due to a surface increment is:

$$\Delta T = \rho\phi \cdot \frac{1}{2}\frac{\partial\phi}{\partial m}\Delta S$$

The most convenient way to summarize all the $\Delta T$'s is to take the surface integral of the quantity. Then

$$T = -\frac{\rho}{2}\iint_S \phi\frac{\partial\phi}{\partial m}\,dS \qquad (1)$$

To satisfy mathematical convention, the minus sign is used and indicates the inner normal.

The apparent additional mass may be computed by dividing T by $1/2\,V^2$, where V is the free stream velocity of the body.

$$m_A = \frac{2T}{V^2} \qquad (2)$$

The volume of the apparent additional mass is:

$$K = \frac{m_A}{\rho} \tag{3}$$

This volume can again be divided by the volume of the solid to give a non-dimensional coefficient which is dependent only on the shape of the body and its direction of motion. This coefficient is usually denoted by k and is called the inertia factor or the coefficient of apparent additional volume and equals K/volume displaced.

The same basic equation, as obtained above in Equation 1, may be developed from Green's theorem in space where one form of this theorem is:[4]

$$\iiint_V \left( \frac{\partial P}{\partial x} \cdot \frac{\partial Q}{\partial x} + \frac{\partial P}{\partial y} \cdot \frac{\partial Q}{\partial y} + \frac{\partial P}{\partial z} \cdot \frac{\partial Q}{\partial z} \right) dV = \iiint_V Q \left( \frac{\partial^2 P}{\partial x^2} + \frac{\partial^2 P}{\partial y^2} + \frac{\partial^2 P}{\partial z^2} \right) dV - \iint_S Q \frac{\partial P}{\partial m} dS \tag{4}$$

where $\frac{\partial P}{\partial m}$ is the directional derivative of P along the inner normal. Let $P = Q = \phi$, where $\phi$ is the velocity potential and is single-valued, finite, and differentiable over the entire region discussed. Since we are dealing with a perfect fluid, hence an incompressible fluid, the Laplacian of $\phi$ must be zero or:

$$\frac{\partial^2 \phi}{\partial x^2} + \frac{\partial^2 \phi}{\partial y^2} + \frac{\partial^2 \phi}{\partial z^2} = 0$$

---

[4] Woods, F. S., Advanced Calculus, Boston: Ginn and Company, 1932. p. 195.

Then it follows that

$$\iiint_V \left[\left(\frac{\partial\phi}{\partial x}\right)^2+\left(\frac{\partial\phi}{\partial y}\right)^2+\left(\frac{\partial\phi}{\partial z}\right)^2\right] dV = -\iint_S \phi\frac{\partial\phi}{\partial m}\,dS \qquad (5)$$

where the volume integral is taken over the entire region and the surface integral over the boundary of the region.

To interpret this physically, multiply both sides by $1/2\rho$:

$$\frac{\rho}{2}\iiint_V \left[\left(\frac{\partial\phi}{\partial x}\right)^2+\left(\frac{\partial\phi}{\partial y}\right)^2+\left(\frac{\partial\phi}{\partial z}\right)^2\right] dV = -\frac{1}{2}\iint \rho\phi\frac{\partial\phi}{\partial m}\,dS \qquad (6)$$

Then on the right-hand side of (6) $-\frac{\partial\phi}{\partial m}$ is the normal velocity of the fluid inwards and $\rho\phi$ is the impulse pressure necessary to cause the motion. Hence, the right-hand side is the work done by the impulsive pressures which, applied by the surface S, cause the motion of the fluid. In the left-hand side of the equation $\frac{\partial\phi}{\partial x}$, $\frac{\partial\phi}{\partial y}$, $\frac{\partial\phi}{\partial z}$ are the velocity components of the motion in the X, Y and Z direction or u, v, w. Then:

$$\frac{\rho}{2}\iiint\left[\left(\frac{\partial\phi}{\partial x}\right)^2+\left(\frac{\partial\phi}{\partial y}\right)^2+\left(\frac{\partial\phi}{\partial z}\right)^2\right] dV = (u^2+v^2+w^2)\frac{\rho}{2}\iiint_V dV$$

$$= \frac{\rho}{2}(\text{VOL.})(u^2+v^2+w^2) = \frac{1}{2}mV^2 = T$$

where T is the kinetic energy of the fluid. Therefore, from Equation 6 and identical to Equation 1

$$T = -\frac{\rho}{2}\iint_S \phi\frac{\partial\phi}{\partial m}\,dS$$

The above work has been developed for the case where the field of fluid is at rest and the body is moving through it. This establishes a flow about the body that is unstable relative to the surrounding fluid.

Another case would be where the body is at rest and the infinite field of fluid is moving past it. The same approach can not be used in both cases, although the apparent additional mass of the body is the same. For the field alone, moving at a constant velocity, the kinetic energy is infinite, but when the presence of the body is added, there is a change of kinetic energy. This change of energy may also be reduced to an apparent additional effect The infinite flow is again assumed to be built up from rest by constant acceleration. Since the surface of the body does not move, no energy passes through the surface during the creation of the flow; the fluid receives the energy by means of a pressure variation at a great distance. Then the basic integral of Equation 1 must be extended over a very large surface. A large sphere surrounding the solid may be used. This integral is usually indeterminate, and great care must be taken to approach the limit in keeping with the specified conditions, that is, with the external boundary, such as the sphere, moving like a solid.

The kinetic energies resulting from the application of Equation 1 to the finite solid surface and to the infinite surface are not the same. The difference consists of two parts. The first part is the infinite kinetic energy of the fluid due to the velocity of the fluid at a large distance relative to the body, and the second part is the energy of the fluid replaced by the solid. Upon elimination of the first part, there

will remain a volume of apparent additional mass greater than the one calculated by applying Equation 1 to the surface of the body. This difference is equal to the volume of the solid itself, so the difference between the apparent additional mass coefficients as obtained by Equation 1 is 1.0, the body fixed being larger.

These two cases should be kept in mind when computing the apparent additional effects from velocity potentials. All of the theoretical examples presented below are for the case where the fluid is at rest and the body is in motion.

Two-Dimensional Flow.

To illustrate the use of the basic equation, $2T = \rho \iint \phi \frac{\partial \phi}{\partial n} dS$, theoretical examples will be given. Consider first the case of a circular cylinder of infinite length moving through a motionless field of fluid with its axis perpendicular to the direction of motion as in Figure 1. This is not the case of the cylinder being at rest and the fluid moving past it. The velocity potential of the given situation is:[5]

$$\phi = \frac{Ua^2}{r} \cos \Theta \qquad (7)$$

where U is the velocity of the cylinder, a the radius of the cylinder and r the distance from the center of the cylinder to some point in the field. When determining the change in kinetic energy due to the presence

---

[5] Lamb, Horace, Hydrodynamics, 6th ed., Cambridge: University Press, 1932. p. 76.

of the moving body, the surface conditions only are of interest. Therefore, in this case r equals a. At the surface

$$\phi = Ur\cos\theta = Ua\cos\theta$$

The velocity normal to the cylinder is the velocity along the radii, or

$$\frac{\partial\phi}{\partial m} = \frac{\partial\phi}{\partial r} = \frac{\partial(Ur\cos\theta)}{\partial r} = U\cos\theta \qquad \text{AT } r = a$$

also

$$\iint_S dS = \int_0^{2\pi} \ell\, a\, d\theta \qquad \text{where } \ell = \text{length of cylinder}$$

then

$$\begin{aligned} 2T &= \iint \rho\phi \frac{\partial\phi}{\partial m} dS \\ &= \int_0^{2\pi} \rho U a\cos\theta \cdot U\cos\theta \cdot \ell\, a\, d\theta \\ &= \rho U^2 a^2 \ell \int_0^{2\pi} \cos^2\theta\, d\theta \\ &= \rho U^2 a^2 \ell \left[\frac{\theta}{2} - \frac{1}{4}\sin 2\theta\right]_0^{2\pi} \\ &= \pi a^2 \ell \rho U^2 \end{aligned}$$

but $m_A = \frac{2T}{U^2}$ apparent additional mass; therefore, for a circular cylinder

$$m_A = \frac{\pi a^2 \ell \rho U^2}{U^2} = \pi a^2 \ell \rho \qquad (8)$$

and the apparent additional volume is $K = \frac{m_A}{\rho}$

or

$$K = \frac{\pi a^2 \ell \rho}{\rho} = \pi a^2 \ell \qquad (9)$$

this is equal to the volume of a cylinder of length $\ell$ ; therefore, the volume of the apparent additional mass for a circular cylinder moving perpendicular to its axis is equal to the volume of the cylinder, and the coefficient of apparent additional volume k is 1.0.

The above example is a special case of the motion of an elliptic cylinder moving through motionless fluid. In two-dimensional flow, the stream lines are the same for all confocal elliptic forms of the cylinder, so that the above formulae hold even when the section reduces to a straight line joining the foci of the ellipse. This is an interesting result, because it indicates that the apparent additional mass of any two-dimensional elliptic body, including a straight line, is proportional to the maximum thickness or length perpendicular to the direction of motion. The apparent additional mass per unit length along the axis is then given by

$$m_A = \frac{\pi}{4} \rho t^2 \qquad (10)$$

where t is the maximum thickness perpendicular to the direction of motion.

Since the apparent additional mass is determined by the kinetic energy of the surrounding fluid, it is often advantageous to calculate

the kinetic energy from the left-hand member of Equation 5

$$2T = \rho \iiint_V \left[ \left(\frac{\partial \phi}{\partial x}\right)^2 + \left(\frac{\partial \phi}{\partial y}\right)^2 + \left(\frac{\partial \phi}{\partial z}\right)^2 \right] dV$$

This may be illustrated by considering a hollow elliptic cylinder with semi-axes a, b rotating about its longitudinal axis with the angular velocity $\omega$ (Figure 2). The velocity potential for the fluid contained within the hollow cylinder is:[6]

$$\phi = -\omega \frac{a^2-b^2}{a^2+b^2} xy$$

then

$$\left(\frac{\partial \phi}{\partial x}\right)^2 = \left[\omega \frac{a^2-b^2}{a^2+b^2}\right]^2 y^2$$

$$\left(\frac{\partial \phi}{\partial y}\right)^2 = \left[\omega \frac{a^2-b^2}{a^2+b^2}\right]^2 x^2$$

Substituting these in

$$2T = \rho \iint \left[ \left(\frac{\partial \phi}{\partial x}\right)^2 + \left(\frac{\partial \phi}{\partial y}\right)^2 \right] dx\,dy$$

to give

$$2T = 4\rho \int_0^b \int_0^{\frac{a}{b}\sqrt{b^2-y^2}} \left\{ \left[\omega \frac{a^2-b^2}{a^2+b^2}\right]^2 y^2 + \left[\omega \frac{a^2-b^2}{a^2+b^2}\right]^2 x^2 \right\} dx\,dy$$

---

[6] Ibid., p. 87.

or

$$2T = 4\rho\left[\omega\frac{a^2-b^2}{a^2+b^2}\right]^2\int_0^b\int_0^{\frac{a}{b}\sqrt{b^2-y^2}}(y^2+x^2)\,dx\,dy \qquad (11)$$

which upon integration, substituting limits, and clearing gives

$$2T = 4\rho\left[\omega\frac{a^2-b^2}{a^2+b^2}\right]^2\int_0^b\left[y^2\sqrt{b^2-y^2}\left(\frac{a}{b}-\frac{a^3}{3b^3}\right)+\frac{a^3}{3b}\sqrt{b^2-y^2}\right]dy$$

The second integration results in

$$2T = 4\rho\left[\omega\frac{a^2-b^2}{a^2+b^2}\right]^2\left\{\left(\frac{a}{b}-\frac{a^3}{3b^3}\right)\left(\frac{b^4}{8}\sin^{-1}1\right)+\frac{a^3}{6b}b^3\sin^{-1}1\right.$$
$$\left.-\left(\frac{a}{b}-\frac{a^3}{3b^3}\right)\left(\frac{b^4}{8}\sin^{-1}0\right)-\frac{a^3b^3}{6b}\sin^{-1}0\right\}$$

or

$$2T = 4\rho\left[\omega\frac{a^2-b^2}{a^2+b^2}\right]^2\left\{\left(\frac{a}{b}-\frac{a^3}{3b^3}\right)\frac{b^4}{8}\cdot\frac{\pi}{2}+\frac{a^3b}{6}\cdot\frac{\pi}{2}\right\}$$

upon clearing

$$2T = \rho\omega^2\frac{(a^2-b^2)^2}{(a^2+b^2)^2}\left[\frac{\pi ab}{4}(b^2+a^2)\right]$$

then

$$2T = \frac{\pi}{4}\omega^2 \frac{(a^2-b^2)^2}{a^2+b^2}\rho a b \quad \text{per unit length} \qquad (12)$$

Then for a hollow elliptic cylinder rotating about its longitudinal axis, the apparent additional moment of inertia of the internal fluid per unit cylinder length is

$$I_A = \frac{\pi}{4}\rho a b \frac{(a^2-b^2)}{a^2+b^2} \qquad (13)$$

Considering the same conditions, the kinetic energy of the external fluid per unit cylinder length is[7]

$$2T = \frac{\pi}{8}\rho\omega^2(a^2-b^2)^2 \qquad (14)$$

and the apparent additional moment of inertia for the external fluid per unit length is given by

$$I_A = \frac{\pi}{8}\rho(a^2-b^2)^2 \qquad (15)$$

This result is valid for all confocal elliptic cylinders.

Notice that in the last two illustrations it was necessary to use the concept of apparent additional moment of inertia rather than

---

[7] Ibid., p. 88.

apparent additional mass. The best way to see the reason for this is to again revert to the use of dimensional analysis. Consider the dimensional quantities in the above equation for kinetic energy. Multiplying by a length factor $\ell$ gives

$$T \cong \rho \omega^2 (a^2 - b^2) \ell$$

which in dimensional units is

$$T = \left( \frac{\text{lb}}{\text{ft}^3} \cdot \frac{\text{sec}^2}{\text{ft}} \right) \left( \frac{\text{rad}^2}{\text{sec}^2} \right) \text{ft}^4 \cdot \text{ft} = \text{lb-ft}$$

or the units of kinetic energy. Dividing by the units of the square of the angular velocity gives

$$\frac{T}{\omega^2} = \left( \frac{\text{lb}}{\text{ft}^3} \cdot \frac{\text{sec}^2}{\text{ft}} \right) \text{ft}^4 \cdot \text{ft} = \text{lb-ft sec}$$

These are the units for moment of inertia. Thus, whenever considering the apparent additional effects due to rotation, it becomes necessary to employ a moment of inertia concept. An apparent additional moment of inertia coefficient, $k'$, may be obtained by dividing the apparent moment of inertia by the moment of inertia of the displaced fluid, both being determined about the same axis.

Three-Dimensional Flow.

Even though the development of the apparent additional mass coefficients for three-dimensional potential flow is beyond the scope of this paper, some of the results are interesting and worthy of discussion.

Green[8] developed the necessary equations for the apparent additional mass coefficients of ellipsoids of revolution in the paper presented here in Appendix III, and Lamb simplified the solution. Both derived equations of the form

$$k = \frac{A}{2-A} \tag{16}$$

For prolate ellipsoids, Lamb[9] gives equations and tabulated values for three types of motion in Reference 8 and makes use of the following notation:

$$e = \sqrt{1 - \frac{a^2}{c^2}} = \tanh u, \quad c = a \cosh u$$

where c is the semi-major axis and a is the semi-minor axis. Then for end-on motion parallel to the x axis, the coefficient is

$$k_1 = \frac{\gamma}{2-\gamma}$$

where

$$\gamma = \frac{2}{\sinh^2 u} (u \coth u - 1) \tag{17}$$

---

[8] Green, George, "Researches on the Vibration of Pendulums in Fluid Media," Transactions of the Royal Society of Edinburgh, Vol. 13, 1836. pp. 54-62.

[9] Lamb, Horace, "The Inertia-Coefficients of an Ellipsoid Moving in Fluid," Advisory Committee for Aeronautics Reports and Memoranda No. 623, Vol. 1, 1918-1919. pp. 128-129.

or

$$\gamma = \frac{2(1-e^2)}{e^3}\left(\frac{1}{2}\ln\frac{1+e}{1-e} - e\right) \tag{18}$$

For the same prolate ellipsoid moving broadside to the x axis, the coefficient is

$$k_2 = \frac{\alpha}{2-\alpha} \tag{19}$$

where

$$\alpha = \frac{1}{\tanh^2 u}\left(1 - \frac{2u}{\sinh 2u}\right)$$

or

$$\alpha = \frac{1}{e^2} - \frac{1-e^2}{2e^3}\ln\frac{1+e}{1-e} \tag{20}$$

Using the above notation, the apparent additional moment of inertia coefficient for rotation about the minor axis of the ellipsoid is

$$k' = \frac{e^4(\alpha-\gamma)}{(2-e^2)[2e^2-(2-e^2)(\alpha-\gamma)]} \tag{21}$$

Making use of the conventional notation of semi-axis; i.e., a:x, b:y, c:z, the following equations are developed from Green's paper.[10]

---

[10] Green, loc. cit.

The equations for A refer to

$$k = \frac{A}{2-A}$$

To aid in the calculation of the apparent additional mass coefficient for any ellipsoid of revolution in rectilinear motion parallel to the x axis, equations are presented as functions of the ratios of the semi-axes. These equations are indeterminate for the special case of the sphere where a = b = c, but this development will be presented later. The prolate ellipsoid is generated by revolving the ellipse about its major axis, while the oblate ellipsoid is generated by revolving the ellipse about its minor axis.

For the prolate ellipsoid moving end-on

$$b = c < a, \quad \text{let } P = \frac{a}{b} > 1$$

then

$$A = ab^2 (a^2-b^2)^{-3/2} \ln \frac{a+\sqrt{a^2-b^2}}{a-\sqrt{a^2-b^2}} - \frac{2b^2}{(a^2-b^2)} \qquad (22)$$

and

$$k_1 = \frac{\left( P \ln \frac{P+\sqrt{P^2-1}}{P-\sqrt{P^2-1}} - 2\sqrt{P^2-1} \right)}{2(P^2-1)^{3/2} - \left( P \ln \frac{P+\sqrt{P^2-1}}{P-\sqrt{P^2-1}} - 2\sqrt{P^2-1} \right)} \qquad (23)$$

For the prolate moving broadside, a = c < b, let $N = \frac{b}{a} > 1$

then

$$A = -\frac{1}{2}a^2 b(b^2-a^2)^{-3/2} \ln \frac{b+\sqrt{b^2-a^2}}{b-\sqrt{b^2-a^2}} + \frac{b^2}{(b^2-a^2)} \qquad (24)$$

and

$$k_2 = \frac{-N \ln \frac{N+\sqrt{N^2-1}}{N-\sqrt{N^2-1}} + 2N^2\sqrt{N^2-1}}{4(N^2-1)^{3/2} - \left(-N \ln \frac{N+\sqrt{N^2-1}}{N-\sqrt{N^2-1}} + 2N^2\sqrt{N^2-1}\right)} \qquad (25)$$

For the oblate moving lengthwise, $a = c > b$, let $M = \frac{a}{b} > 1$

then

$$A = a^2 b(a^2-b^2)^{-3/2}\left(\frac{\pi}{2} - \text{TAN}^{-1}\frac{b}{\sqrt{a^2-b^2}}\right) - \frac{b^2}{(a^2-b^2)} \qquad (26)$$

and

$$k_3 = \frac{\frac{\pi}{2} - \text{TAN}^{-1}\frac{1}{\sqrt{M^2-1}} - \frac{\sqrt{M^2-1}}{M^2}}{\frac{2(M^2-1)^{3/2}}{M^2} - \left(\frac{\pi}{2} - \text{TAN}^{-1}\frac{1}{\sqrt{M^2-1}} - \frac{\sqrt{M^2-1}}{M^2}\right)} \qquad (27)$$

For the oblate moving broadside, $b = c > a$, let $Q = \frac{b}{a} > 1$

then

$$A = 2ab^2(b^2-a^2)^{-3/2}\left(\text{TAN}^{-1}\frac{a}{\sqrt{b^2-a^2}} - \frac{\pi}{2}\right) + \frac{2b^2}{(b^2-a^2)} \qquad (28)$$

and

$$k_4 = \frac{\text{TAN}^{-1}\frac{1}{\sqrt{Q^2-1}} - \frac{\pi}{2} + \sqrt{Q^2-1}}{\frac{1}{Q^2}(Q^2-1)^{3/2} - \left(\text{TAN}^{-1}\frac{1}{\sqrt{Q^2-1}} - \frac{\pi}{2} + \sqrt{Q^2-1}\right)} \qquad (29)$$

Tabulated values and curves for the above equations are presented in Appendix I. The values calculated from the above equations for the prolate ellipsoids are equal to those Lamb presented in Reference 8. For comparison, all four curves are plotted together in Figure 5. Remembering that k is the apparent mass coefficient, that is, the apparent additional volume divided by the actual displaced volume, the results are as would be expected.

As the ratio of the major axis to the minor axis approaches infinity, the oblate ellipsoid approaches a circular disk of zero thickness. There would be an apparent volume for motion perpendicular (broadside) to this disk, but no actual volume would be displaced; hence, the coefficient k would approach infinity. For motion parallel (lengthwise) to this disk, there is no surface present, not even a theoretical one of zero thickness, to cause a change of kinetic energy of the surrounding fluid, so the coefficient naturally approaches zero.

A prolate ellipsoid under the same conditions would approach a circular cylinder of infinite length. It has already been pointed out that for such a cylinder moving broadside the apparent additional mass coefficient is one.[11] This is borne out by the curve. For end-on

---

[11] Cf. ante, p. 12.

motion of an infinite cylinder, the surrounding fluid would be set in motion only by viscous forces between the body and the fluid. Such viscous forces are nonexistent in a perfect fluid, so the apparent additional volume would be zero.

For the motion of a sphere in the x direction through an infinite mass of fluid at rest, Lamb[12] gives the three-dimensional velocity potential to be

$$\phi = \frac{1}{2} U \frac{a^3}{r^2} \cos\eta \tag{30}$$

where $\eta$ is the space angle between the x axis and the radius vector, r. Then

$$\frac{\partial\phi}{\partial m} = \frac{\partial\phi}{\partial r} = \frac{1}{2} U a^3 \left(\frac{-2}{r^3}\right) \cos\eta$$

$$= -U\cos\eta \quad \text{AT } r = a \tag{31}$$

and

$$\phi \frac{\partial\phi}{\partial m} = -\frac{1}{2} U^2 \frac{a^6}{r^5} \cos^2\eta$$

$$= -\frac{1}{2} U^2 a \cos^2\eta \quad \text{AT } r = a \tag{32}$$

From Equation 1

$$2T = -\rho \iint_S \phi \frac{\partial\phi}{\partial m} dS = \frac{\rho}{2} U^2 a \iint_S \cos^2\eta \, dS$$

---

[12] Lamb, Hydrodynamics, 6th ed., p. 123.

but[13]

$$\iint_S dS = 2\int_0^{2\pi}\int_0^{\pi} a^2 \sin\psi \, d\psi \, d\theta \tag{33}$$

where $\psi$ is the angle between the radius vector, r, and the positive axis, and $\theta$ is the angle between the projection of the radius vector on the xy plane and the x axis. Also $x = r \cos\theta \sin\psi$. Then

$$\frac{x}{r} = \cos\eta = \cos\theta \sin\psi$$

and

$$\cos^2\eta = \cos^2\theta \sin^2\psi$$

which gives

$$2T = \frac{\rho}{2} U^2 a \int_0^{2\pi}\int_0^{\pi} 2a^2 \sin^3\psi \cos^2\theta \, d\psi \, d\theta \tag{34}$$

$$= \rho U^2 a^3 \int_0^{2\pi} \left[-\frac{1}{3}\cos\psi(\sin^2\psi + 2)\right]_0^{\pi} \cos^2\theta \, d\theta$$

$$= \rho U^2 a^3 \int_0^{2\pi} \frac{2}{3}\cos^2\theta \, d\theta$$

$$= \frac{2}{3}\rho U^2 a^3 \left[\frac{\theta}{2} + \frac{1}{4}\sin 2\theta\right]_0^{2\pi}$$

$$= \frac{2}{3}\rho\pi a^3 U^2 \tag{35}$$

The apparent additional mass is $\frac{2}{3}\pi a^3\rho$, and since the displaced mass is $\frac{4}{3}\pi a^3\rho$, it is evident that the apparent additional mass is half the displaced mass. The apparent additional mass coefficient k is 0.5.

---

[13] Woods, op. cit., p. 190.

## EXPERIMENTAL

Experimental determinations of the apparent additional mass effect have been presented by various papers published in the United States, England, Russia and Germany. It is fortunate that, since many of the original papers are now unavailable, most of the results have been incorporated into papers that are available. Since the apparent additional mass effect is due to the motion of the fluid about the body and to the density of this fluid, experimental results are usually obtained by studying the motion of the body in fluids of various densities. The results can then be extrapolated to an absolute vacuum or zero density and the apparent additional mass determined.

The motion of a body may be studied in one of three ways. The body may be dropped vertically, towed in rectilinear motion, or oscillated as a pendulum. There are many disadvantages and few advantages to all three methods. Both the accelerations and the Reynolds numbers obtainable with the first two systems are very low, and both systems require elaborate laboratory equipment, the size of which more or less determines the range and value of the experimental results. The major disadvantage of the pendulum method is that the pendulum moves in disturbed fluid. This difficulty may be overcome by moving the center of rotation of the pendulum rectilinearly, but this again requires elaborate laboratory equipment, and the resulting motion is difficult to analyze. In all three cases, the surrounding fluid is seldom unbounded, and it is also impossible to separate out the viscous effects. The

latter may not be a disadvantage in that in practical applications it is necessary to deal with fluids which are to some extent viscous.

Reference 1 discusses the results of an experiment where a small streamlined body with a fineness ratio of 4:1 was dropped into a vertical tank of water.[14] The purpose of this experiment was to determine the effect of acceleration on the resistance of a body. The range of acceleration was from 0 to 0.2g. It was concluded that for a good streamlined body the acceleration effect was not greater than the order of error of the experiment. The curves, Figure 15, do indicate that the resistance or drag does increase with acceleration. The slopes of these curves are proportional to what may be considered apparent additional masses in that the increased drag is equal to an apparent additional mass times the acceleration. The increase of drag with acceleration and the experimental set-up used are the only points of interest in this report because the range of velocities and accelerations covered were so low that the quantitative results are of little practical usage.

Figure 15 also shows a diagram of the body used in this experiment. This body was hollow and filled with various amounts of mercury to weight it. Light from an arc was projected by a lens on a mirror, from which it was reflected down into the vertical water tank, where the body was held suspended by an electromagnet. A motor rotated a cardboard disk from which a sector had been cut out so that the light illuminated

---

[14] Cowley, W. L., and H. Levy, "On the Effect of Acceleration on the Resistance of a Body," Advisory Committee for Aeronautics Reports and Memoranda No. 612, Vol. 1, 1918-1919. pp. 95-101.

the tank at regular intervals. One side of the tank was glass in order that a photograph of the motion could be made. Each model configuration was tested several times to confirm the accuracy of the tests.

By plotting distance traveled versus time and differentiating, the velocity was obtained. The velocity was then plotted against distance traveled, and the curve was differentiated and multiplied by velocity to give the acceleration. The equation of motion used to find the resistance was:

$$ma = (m-m_1)g - R \qquad (36)$$

where $m$ = mass

$m_1$ = buoyancy

$a$ = acceleration

$g$ = gravity

$R$ = resistance

Both masses, $m$ and $m_1$, were determined by weighing the body in air and water.

The work discussed above was continued in a more thorough manner in experiments reported in Reference 2.[15] Here a streamlined body 18.82 inches long with a fineness ratio of 4:1 and a 6 inch diameter sphere were towed rectilinearly by known applied forces under water, and time-displacement curves were recorded chronographically.

---

[15] Frazer, R. A., and L. F. G. Simmons, "The Dependence of the Resistance of Bodies Upon Acceleration, as Determined by Chronograph Analysis," Advisory Committee for Aeronautics Reports and Memoranda No. 590, Vol. 1, 1918-1919. pp. 102-121.

The tests were conducted in a 65 foot experimental tank of the William Froude Tank Department. Of the over-all length, 22 feet were used for the preliminary run and 15 feet for braking, leaving a working section of 28 feet. This section was 5 feet wide and 3 feet deep. The streamlined body was towed 12 inches below the free surface and the sphere 15 inches below. It was considered that with clearances of this order, interference effects due to the boundaries of the tank and the surface of the water were not appreciable.

The model was mounted on a light aluminum carriage, motivated by a system of weights and pulleys similar to an Attwood machine. Complete calibration and tare runs were made, and small frictional effects were compensated for by applying for each test an excess "dead" driving load just sufficient to initiate motion of the system. The velocity and acceleration were determined in a manner similar to that discussed above.

Relatively low velocities were used throughout this experiment in that the velocities of the body moving through the water ranged from 0.6 to 5 feet per second. For the same Reynolds numbers[16] in air these velocities would correspond to approximately 7.7 and 64 feet per second. For the sphere used, these velocities correspond to Reynolds numbers of two to seven thousand. There is little appreciable change of resistance with Reynolds number for the range covered.

The tabulated results for both the streamlined body and the sphere were presented. These data were plotted, faired, cross-plotted and

---

[16] For equal Reynolds numbers and standard conditions the velocity in air is equal to 12.8 times the velocity in water.

cross-faired for presentation in this paper, and a slightly different interpretation of the data is discussed below.

The resistance was plotted versus acceleration for constant velocities, and then versus velocity for constant accelerations. These two curves were then cross-faired. The slope of the resistance versus acceleration curve at a point is equal to the apparent mass for that velocity and acceleration, because the resistance as plotted is that due to only the fluid motion about the body and not due to the actual mass of the model. Then the increase of resistance from zero acceleration is equal to the apparent additional mass times the acceleration. The apparent additional mass was divided by the mass of water displaced to give the apparent additional mass coefficient, k, which in turn was plotted versus velocity.

Figures 16, 17 and 18 are for the streamlined body of fineness ratio 4:1. Apparently the resistance increases more rapidly with acceleration than a simple linear variation, although the increase is relatively small. This would indicate that the apparent additional mass increases with acceleration, especially accelerations of a higher order. Due to the small slope of the resistance versus acceleration curve, the apparent additional mass was difficult to determine accurately, and as might be expected, there is serious scatter when the apparent additional mass coefficient was plotted versus velocity for the various constant values of acceleration (Figure 17). However, the trend of these linear curves does seem to indicate that the apparent additional mass increases with velocity. This increase is of the order of 2 percent of the mass displaced

per foot per second velocity. For the velocity and acceleration range covered, the apparent additional mass ranged from 5 to about 49 percent of the mass of fluid displaced. As the authors of this reference pointed out, the mean value of the apparent additional mass coefficient seems to be about 19 percent.

It would be expected that a body as aerodynamically inefficient as a sphere would have very marked apparent additional mass effects, as the apparent additional mass is a function of the velocity increment over the body. A study of Figures 19, 20 and 21 substantiates this, as well as giving evidence to some rather amazing phenomena. The resistance versus acceleration curve, Figure 19, was faired somewhat differently than the original in order that it would cross-fair with the resistance versus velocity curve. There seems to be a linear variation of resistance with acceleration for constant velocity after a certain acceleration has been reached. In this experiment that acceleration is 0.3 $ft/sec^2$. The curves of resistance versus velocity for constant values of acceleration, Figure 21, seem to converge to a single point. It would be interesting to determine in the laboratory whether or not such a condition does exist, and if so, at what point.

Remembering that the theoretical value of the apparent mass of a sphere is 50 percent of the mass of the fluid displaced for any velocity, the values of this quantity and its variation with velocity as shown on Figure 20 are indeed amazing. Since for a velocity of 0.6 ft/sec, there is a linear variation of resistance with acceleration, the two curves intersect at this velocity at a value of the apparent

additional mass of 85 percent of the mass of fluid displaced. For an acceleration of 0.1 ft/sec$^2$ the rate of change of the apparent additional mass coefficient with velocity is 155 percent of the mass of fluid displaced per one ft/sec water velocity, and for accelerations from 0.3 to 0.8 ft/sec$^2$, the rate of change is 275 percent per one ft/sec water velocity. Both rates of change are apparently constant for their particular acceleration range. These values seem extremely large, especially for such low velocity, and theory does not indicate any such variation.

In conclusion, the apparent additional mass coefficients for both the streamlined and the bluff body do increase with velocity and acceleration, the effects being more pronounced for the sphere. An explanation of this increase is that since the bodies were tested in a viscous fluid, there was a boundary layer about them and, no doubt, separation did occur. The increase would be less evident for the streamlined body, because the flow about this body would approximate more closely the theoretical potential flow than would the flow about the sphere; hence, the pressure recovery would be more complete, and a greater percent of the energy would be regained. As mentioned above, theory does not predict variation of the apparent additional effects with either velocity or acceleration; hence, it is obvious that there is serious need for additional experimental studies to be made in an effort to determine the validity of the above results, as well as to determine the extent of such effects. Such experiments would require equipment similar to that used in the experiment discussed here because pendular oscillations would at best tend to average any such effects.

In the two experiments discussed above, the basic law of motion (Force is equal to mass times acceleration.) has been used where there was no change in the direction of the moving body.

Next to be considered is the case where there is a periodic change in direction of the moving body. Experimental oscillatory tests may be of two general classifications: One is where the system oscillates freely at a natural or resonance frequency, and the other is where the system has an arbitrary frequency caused by forced oscillations. Pendulum testing is more popular than towing or free-falling bodies because of the simplicity of the equipment and the wealth of theoretical background available for pendulums. The various types of pendulums and their pertinent equations are discussed below before any tests are described. The following notation will be used throughout:

$$I_v = I_s + I_E + I_A \tag{37}$$

$$I_{eA} = I_A + m_A \times L^2 \tag{38}$$

where $I_v$ = virtual moment of inertia (measured in the fluid)

$I_s$ = true moment of inertia (measured in vacuum)

$I_E$ = moment of inertia of entrapped fluid

$I_A$ = moment of inertia of apparent additional mass

$I_e$ = effective moment of inertia (moment of inertia about some line not through center of gravity of the mass)

$m_A$ = apparent additional mass

L = distance from center of gravity of mass to line about which moment of inertia is taken (The center of gravity of the apparent additional mass is assumed to be at the center of gravity of the displaced mass.)

For a simple pendulum, the undamped period of oscillation of small amplitude is of the form:

$$T = 2\pi\sqrt{I/b} \tag{39}$$

so that

$$I = T^2 b/4\pi^2 \tag{40}$$

where T = period, time of one complete oscillation

I = moment of inertia of pendulum about the axis of oscillation

b = a constant depending upon the weight and dimensions of the pendulum

Equation 39 is valid, not only for the simple pendulum, but also for any freely oscillating system where the constant b varies with the type of pendulum, as well as its weight and dimensions.

For either a simple or compound pendulum $b = WL$ and $I = \frac{T^2 WL}{4\pi^2}$, where L is the distance between the center of gravity and the axis of oscillation. For determining the moments of inertia for a body such as an airplane, the compound pendulum is used for oscillation about the x and y axes. A diagram of such an arrangement is shown in Figure 23. For a compound pendulum such as illustrated, the axis of oscillation is horizontal and passes through the points of support but not through the center of gravity of the pendulum. For the moment of inertia about an axis through the center of gravity, it is necessary to use an equation of the form:

$$I_{cg} = \frac{T^2 WL}{4\pi^2} - ML^2 \tag{41}$$

where M is the mass of the pendulum.

A simple torsion pendulum is illustrated in Figure 22. Here, the constant b is equal to K, the torsional constant of the wire expressed in dyne centimeters. Then

$$T = 2\pi\sqrt{I/K} \tag{42}$$

and

$$I = \frac{T^2K}{4\pi^2} \tag{43}$$

Again an equation similar to Equation 41 is used to transfer the moment of inertia to about a line through the center of gravity of the body. A bifilar torsion pendulum, such as is shown in Figure 24, is used to determine the moment of inertia about the z axis of an airplane. The axis of oscillation is vertical, lies midway between the two filaments and passes through the center of gravity of the system. For this pendulum:

$$b = \frac{WA^2}{4\ell} \tag{44}$$

and consequently,

$$I = \frac{T^2WA^2}{16\pi^2\ell} \tag{45}$$

where W = the weight of the pendulum

A = the distance between the vertical filaments

$\ell$ = the length of the filaments

The above equations are those for systems in an absolute vacuum where there is no damping; whereas, in any practical case, the motion of the pendulum will be damped by friction. Damping has the effect of increasing the period over the theoretical value. Observations made during swinging tests of airplanes at the N.A.C.A. have shown that the decrease of amplitude during the first oscillation never exceeds one tenth the original amplitude. For this amount of damping the error in the moment of inertia is less than 0.02 percent and, hence, is negligible. Naturally, the effect of damping would become greater with increasing density of the surrounding fluid. However, an example cited for an experiment[17] conducted with circular disks mounted on a simple torsion pendulum in water indicates that here, too, the damping may be neglected. The period for a damped torsion pendulum is given by:

$$T = 2\pi \Big/ \left( \frac{K}{I} - \frac{f^2}{4I^2} \right)^{1/2} \qquad (46)$$

where K = the torsional constant of the wire

I = the effective moment of inertia of the cross-arm and attached parts

f = the damping factor

For this particular case, T was found to be 1.705 seconds and $f^2/4I^2$ was 0.012. Using Equation 46, K/I is approximately 13.6 or over one thousand times as large as $f^2/4I^2$. If the damping factor was

---

[17] Yee-Tak Yu, "Virtual Masses and Moments of Inertia of Disks and Cylinders in Various Liquids," Journal of Applied Physics, Vol. 13, 1942. p. 67.

neglected in this case, the error would be less than 0.1 percent, which is certainly less than the over-all experimental accuracy obtainable.

Since it is permissible to neglect the effects of damping in this work, the Equations 40, 43 and 45, although derived for the motion of a pendulum in vacuum, apply to the case of the pendulum oscillating in any relatively nonviscous fluid. However, in these equations I, W and M refer to virtual values of moment of inertia, weight and mass of the pendulum immersed in a real fluid. The differences between the virtual values of I, W and M and the true values arise from three effects: the buoyancy of the structure, the air entrapped within the structure and the apparent additional mass effect.

The true mass of the body may be computed from:

$$M_s = \frac{W_v}{g} - V_s \rho \qquad (47)$$

where $M_s$ = true mass of body

$W_v$ = virtual weight of body

$V_s$ = volume of body

$\rho$ = mass density of surrounding fluid

Practically the total volume enclosed within the external coverings of an airplane, for instance, is filled with air of the same density as the surrounding air. This mass of air should be considered as part of the airplane, because the major portion of it moves with the airplane, even though there is always some leakage. Thus, the true mass of the airplane is:

$$M = \frac{W_v}{g} + V_s \rho + (V - V_s)\rho$$

or

$$M = \frac{W}{g} + V\rho \tag{48}$$

where V is the total volume of the airplane. Similarly, the true moment of inertia of the pendulum is made up of two parts: a constant part equal to the moment of inertia of the structure, and a part $I_E$ representing the moment of inertia of the entrapped air. The term $I_E$ varies with density of the air. Then:

$$I = I_s - I_E \tag{49}$$

and the moment of inertia as measured in the fluid, the virtual moment of inertia, is:

$$I_v = I_s + I_E + I_A \tag{50}$$

Presenting this equation serves two purposes. First, it illustrates the need for evaluating the apparent additional moment of inertia, and second, it can lead to the determination of the apparent additional moment of inertia. If the virtual moment of inertia, $I_v$, and the true moment of inertia, $I_s$, are known, assuming there is no entrapped fluid, then the apparent additional moment of inertia is the difference. That is:

$$I_A = I_v - I_s \tag{51}$$

The solution of this equation offers three experimental possibilities. If $I_v$ can be measured and $I_s$ calculated, $I_A$ can be determined.

As will be shown later, the apparent additional mass and, hence, the apparent additional moment of inertia varies directly with density; so the virtual quantities may be measured for several different densities, plotted versus the density and the curve faired to $\rho = 0$. Since there is a linear variation between the density and the apparent additional mass, the apparent additional mass will be some constant times the density. This constant will be the slope of the above curve.

The third experimental possibility is actually an approximation that may be used when the fluid normally surrounding the body is dense, as in the case of water. Here it is assumed that the moment of inertia as measured in air is equal to the true moment of inertia, and the apparent additional moment of inertia is equal to the difference between that measured in air and measured in water. This method is the one that is generally used in actual experimental work with pendulums.

The equations for the apparent additional mass will now be developed for the various pendulum arrangements, assuming that the moment of inertia as measured in air is the true moment of inertia. While these equations are not exact, they will indicate the general method to be used, and the actual equations may be developed to suit the particular experiment. The subscripts "L" and "a" will be used and refer to liquid and air, respectively, while the subscript "A" refers to the apparent additional quantity. Then the basic equation is:

$$I_A = I_L - I_a$$

For a simple pendulum where

$$I = \frac{T^2 WL}{4\pi^2}$$

then

$$I_A = \frac{L}{4\pi^2}\left(T_L^2 W_L - T_a^2 W_a\right) \qquad (52)$$

and

$$m_A = \frac{1}{4\pi^2 L}\left(T_L^2 W_L - T_a^2 W_a\right) \qquad (53)$$

This makes use of the assumption used throughout this work, that the center of gravity of the apparent additional mass is at the center of gravity of the mass of the displaced fluid and that $I_A = m_A L^2$. This latter assumption is accurate to a fair degree, since the moment of inertia of the apparent additional mass about its gravity axis is usually small. A relatively small L will increase the accuracy of this assumption.

Equations for a compound pendulum are similar, except that the effect of the supporting structure must be subtracted out. As illustrated in Figure 23, the distances from the axis of oscillation to the various centers of gravity are designated as follows:

L = distance to the c.g. of supported body

$L_1$ = distance to the c.g. of the complete pendulum

$L_2$ = distance to the c.g. of the supporting structure, or the swinging gear

To determine the apparent additional mass of the body alone, it is necessary to first find the apparent additional moment of inertia of the body alone about the axis of oscillation. This may be accomplished by subtracting from the moment of inertia of the complete pendulum the apparent additional moment of inertia of the swinging gear. From Equation 52, it can be seen that this latter quantity is:

$$I_{A_s} = \frac{L_2}{4\pi^2}\left(T_L^2 W_L - T_a^2 W_a\right)_s \qquad (54)$$

where the subscript "s" refers to the swinging gear.

In a similar manner, the apparent additional moment of inertia of the complete pendulum is:

$$I_{A_p} = \frac{L_1}{4\pi^2}\left(T_L^2 W_L - T_a^2 W_a\right)_p \qquad (55)$$

Then the apparent additional moment of inertia of the body alone about the same axis of oscillation is the difference between Equations 55 and 54, or:

$$I_{A_B} = I_{A_P} - I_{A_s} \qquad (56)$$

Since

$$I_{A_B} = m_A L^2$$

then

$$m_A = \frac{I_{A_P} - I_{A_s}}{L^2} \qquad (57)$$

For a simple torsion pendulum as shown in Figure 22, the moment of inertia was given in Equation 43 as $I = T^2K/4\pi^2$. Then the apparent additional moment of inertia of the entire system is:

$$I_{A_P} = I_L - I_a = \frac{K}{4\pi^2}\left(T_L - T_a\right)_P \qquad (58)$$

Here again, it is necessary to subtract the apparent additional moment of inertia of the system without the bodies attached at each end of the cross-arm. For this arrangement:

$$I_{A_s} = \frac{K}{4\pi^2}\left(T_L^2 - T_a^2\right)_s \qquad (59)$$

and since there are two bodies, the apparent additional moment of inertia of one body is:

$$I_{A_B} = \frac{1}{2}\left(I_{A_P} - I_{A_s}\right) \qquad (60)$$

The apparent additional mass of one body is:

$$m_A = \frac{I_{A_P} - I_{A_s}}{2L^2} \qquad (61)$$

where L is the distance from the wire to the center of gravity of the body.

For the apparent additional moment of inertia about the z axis of a body like an airplane, the bifilar torsion pendulum shown in Figure 24 may be used. Here again, it is necessary to use a concept of apparent additional moment of inertia rather than apparent additional mass, since the radius of gyration is unknown. A general procedure quite similar

to the above is also used in this case, where the basic moment of inertia is given by Equation 45:

$$I = \frac{T^2 W A^2}{16 \pi^2 \ell}$$

The swinging gear must be designed so that its center of gravity coincides with the axis of oscillation, and the body is so mounted that its center of gravity is also at this same location.

Then the apparent additional moment of inertia of the swinging gear is:

$$I_{A_s} = \frac{A^2}{16 \pi^2 \ell} \left( T_L^2 W_L - T_a^2 W_a \right)_s \qquad (62)$$

and the apparent additional moment of inertia of the complete pendulum is:

$$I_{A_p} = \frac{A^2}{16 \pi^2 \ell} \left( T_L^2 W_L - T_a^2 W_a \right)_p \qquad (63)$$

The apparent moment of inertia of the body alone is then the difference between Equations 63 and 62, or:

$$I_A = I_{A_p} - I_{A_s} \qquad (64)$$

If the apparent additional mass for motion along the z axis is desired, rather than the apparent additional moment of inertia about the z axis, it is necessary to swing the body as a simple pendulum.

It should be remembered that in all oscillation tests the displacement angle should be small enough that the sine of the angle can be considered to be equal to the angle. Another reason for keeping the amplitude small is that for small amplitude and high frequency the actual flow about an oscillating body approaches potential flow, provided that the motion is assumed to be translational.

The first such experiment to be discussed was reported in Reference 11.[18] Small one inch diameter models were oscillated in air and in water. Each model was suspended by a bifilar arrangement with two long parallel wires attached near the nose and tail. Such a suspension will allow the model to oscillate along or perpendicular to its axis, or to oscillate in yaw about a point near its center of length.

Models of various fineness ratios were tested for both the longitudinal and the lateral effect. The models were equipped with either pointed or hemispherical ends and cylindrical center portions of various lengths. A drawing of the model and the test results are shown in Figure 25.

As would be expected, the models with the hemispherical ends had larger apparent additional mass coefficients for the same fineness ratio than did the models with the pointed ends, since the hemispherical ends would cause a greater disturbance of the surrounding fluid as well as

---

[18] Relf, E. F., and R. Jones, "Measurement of the Effect of Accelerations on the Longitudinal and Lateral Motion of an Airship Model," Advisory Committee for Aeronautics Reports and Memoranda No. 613, Vol. 1, 1918-1919. pp. 121-127.

suffer more from viscosity effects. The minimum longitudinal apparent additional mass coefficient was in the neighborhood of a fineness ratio of 6:1, while the lateral apparent additional mass coefficient increased with increasing fineness ratio. An indication of the experimental accuracy is the different values of k for the 1:1 fineness ratio hemispherical model. The lateral and the longitudinal coefficients should have been equal, since the model was a sphere. An average value of $k = 0.75$ agrees rather well with other experimental data, but not with the theoretical value of 0.5. For an infinite cylinder the lateral k is 1.0, so the results of this experiment give at least a general indication of end effect.

One objection to oscillation tests of this type has been that the model was always moving through fluid previously disturbed by itself. To check this effect, several of the experiments were repeated with the axis of oscillation moving at a uniform velocity. Unfortunately, it was not possible to run a sufficient number of tests to completely bracket the effect because the models of higher fineness ratios could not be made to swing with enough steadiness to enable readings to be taken. There is sufficient evidence that the uniform velocity through the surrounding fluid does not appreciably change the longitudinal effect. Increased velocity does seem to decrease the lateral effect, but as demonstrated by Figure 27, this can not be definitely concluded.

Effects of acceleration on yawing motion were investigated only in still water, because with the bifilar suspension the model could not execute a pure oscillation in yaw when in a moving stream. As usual,

the measured effect is expressed as apparent additional moment of inertia, and the results are presented in Figure 26. The quantities obtained appear to be of the same order as the previously discussed lateral effect.

The authors of this report commented that the experiments were quickly and easily made and that, even though there were certain objections to the method used, the experimental errors were not likely to be greater than 10 percent of the apparent additional mass measured. While the original report used the terminology "virtual mass", it has been referred to here as "apparent additional effect", because it is not the same as the "virtual effect" previously defined as the true plus the apparent additional.

Reference 4[19] presents a resumé of test procedures which make use of free vibration pendulums and results of experimental determinations of the apparent additional mass effects of flat plates. In addition to the resumé, the effect of taper ratio on the apparent additional moments of inertia was investigated, and some previously reported results were checked.

The various tests and experiments will be referred to in the following manner:

| | |
|---|---|
| 1940 N.A.C.A. tests | 1930 German tests |
| 1933 N.A.C.A. tests | British tests |
| 1937 German tests | Russian tests |

---

[19] Gracey, William, "The Additional-Mass Effect of Plates as Determined by Experiments," U. S. National Advisory Committee for Aeronautics Technical Report No. 707, 1941. 10 pp.

In the 1930 German tests small plates were attached to one end of a vertical tube normal to the plane of the plates, and the other end of the tube was secured to two flat steel springs in such a manner that the complete system vibrated in a vertical plane. The apparent additional mass of translation was determined as the difference between the total mass as measured in air and in water. Four plates of various aspect ratios were tested. One curve of Figure 34 is from the report of these German tests and was presented in Reference 4. The apparent additional mass curve was extrapolated to aspect ratio (AR) 10 by means of the empirical relationship:

$$K = \ell - \frac{0.537}{AR} \tag{65}$$

and

$$I_A = \frac{\rho\pi}{48} c^2 b^3 K' \tag{66}$$

$$m_A = \frac{\rho\pi c^2 b}{4} K \tag{67}$$

where c is the chord and b the span.

The original purpose of the British test was to determine the apparent additional mass of a Bristol fighter, but the experiment was extended in an attempt to determine the effect of model construction accuracy and the affect of different pendulum lengths upon the apparent additional mass determination of a flat plate.

Two 1/20-scale balsa wood models of a Bristol fighter were constructed. One was a close replica of the actual airplane, and the other one approximated the airplane only in over-all dimensions and relative

positions of the component parts, all of which were rectangular. The apparent additional moments of inertia of the crude model were as much as 150 percent greater than those of the other model. This indicates that the apparent moments do not depend mainly on the over-all dimensions of the body but are largely affected by such details as sharp edges. Hence, a moderately accurate model should be used for apparent additional mass effects.

A 2 foot balsa plate of aspect ratio 7 was swung as a compound pendulum with the axis of rotation parallel to the chord in the plane of the plate, parallel to the chord in the plane of symmetry and parallel to the span in the plane of symmetry. The apparent additional moments of inertia were found by deducting the computed moment of the structure from the virtual moment. For the plate vertical, the additional moment of inertia about the axis of rotation is plotted in Figure 28 against $\left(\frac{\ell}{b/2}\right)^2$. By extrapolating this curve to $\ell = 0$, the apparent additional moment of inertia about the midchord is determined. This value is compared in Figure 29 with the data obtained by swinging the plate with its plane horizontal. A bifilar suspension was used to obtain a value of $I_A$ for $\ell = 0$ for this curve.

The Russian experiments were conducted to obtain experimental confirmation of theoretically derived formulae for the additional effects of elliptic plates. For elliptic plates of fineness ratio 1.0 (circular plates), the theoretical formulae are:[20]

---

[20] Cf. post, p. 68-69.

$$m_{A_z} = \frac{8}{3}\rho r^3 \tag{68}$$

$$I_{A_x} = I_{A_y} = \frac{16}{45}\rho r^5 \tag{69}$$

Where $m_{A_z}$ is the apparent additional mass along the z axis, perpendicular to the plate, $I_{A_x}$ and $I_{A_y}$ are the apparent additional moments of inertia, and r is the radius of the plate. These formulae may be used for elliptic plates by substituting for r the semi-major axis and applying the appropriate correction factor of Figure 30. The above equations then become:

$$m_{A_z} = \frac{8}{3}\rho a^3 c_z \tag{70}$$

$$I_{A_x} = \frac{16}{45}\rho a^5 c_x \tag{71}$$

$$I_{A_y} = \frac{16}{45}\rho a^5 c_y \tag{72}$$

For plates of nonelliptic shape, the assumption is made that the moment of inertia would be that of an elliptic plate with the same axes increased in the ratio of the areas. This ratio would be $16/3\pi$ or 1.7 for a rectangle.

The Russian tests were conducted on small cardboard frames covered with paper. Moments of inertia about the two axes of the plate were found by swinging the models in air with a bifilar suspension. Homogeneous and constant density material were assumed when the moments of inertia of the structure were computed.

The 1933 N.A.C.A. tests were conducted with four light wooden frameworks covered with paper. These plates had a 4 foot span, one quarter-inch thickness, and the span-chord ratio was varied from 2 to 8. The apparent additional moments of inertia were found by deducting the computed moments of inertia of the structure and entrapped air from the virtual quantity measured in normal density air.

The German investigation of 1937 tested two rectangular frameworks 0.75 by 3.0 meters, one made of steel tubing and the other of aluminum tubing. These were swung as compound pendulums. The span-chord ratio was varied from 0.25 to 8 by partially covering the frames. They were then tested in normal density air with and without covering.

For the 1940 N.A.C.A. tests, a 54 inch diameter vacuum tank was constructed so that the absolute pressures could be varied from 27 to 4 inches of mercury. Tests of the apparent additional moment of inertia were conducted on rectangular plates of span-chord ratios 2, 4, 6 and 8 and on two tapered plates of aspect ratio 4 and taper ratios of 2.5:1 and 5:1. Apparent additional mass was determined for two rectangular plates of aspect ratios 4 and 6. All plates had a span of 20 inches and were built of aluminum tubing covered with aluminum foil. Diagrams of the suspension methods used are shown in Figures 31 and 32. The thickness, t, is not to scale.

Comparison curves of the apparent additional effects of rectangular plates from the various tests are presented in Figures 33 and 34. The Russian results shown in Figure 33 fall below all the other curves. This may be due to assuming uniform density for the paper covered

cardboard plates. Results of the 1937 German tests are considerably higher than both the 1930 German tests and the 1933 N.A.C.A. tests, while the 1940 N.A.C.A. test results seem to agree reasonably well with both.

According to Reference 4, the additional moment of inertia theoretically should be independent of the distance between the center of oscillation and the plate, because displacement of the axis should result only in an additional component of motion to the plate. However, if the concept of apparent additional mass is used, it seems that the measured apparent additional moment should be a function of the pendulum length, $\ell$, because of the relationship

$$I_A = I_{A_o} + m_A \ell^2 \qquad (73)$$

where $I_A$ is the apparent additional moment of inertia about the oscillation axis, $I_{A_o}$ the apparent additional moment of inertia about the gravity axis, $m_A$ the apparent additional mass and $\ell$ is, in this case, the pendulum length. Results of the British and 1937 German tests shown in Figures 28, 29 and 35 substantiate the conclusion that the measured apparent additional moment of inertia does increase with suspension length.

The effect on the apparent additional moment of inertia due to the mutual interference of two parallel plates with no stagger was investigated in the 1937 German and 1933 N.A.C.A. tests. Results of these two experiments are shown in Figure 36 and are in excellent agreement. It may be concluded that for a gap-chord ratio greater than one the two plates may be considered separately.

The effect of dihedral angle on the apparent additional moment of inertia was examined during the 1933 N.A.C.A. tests using a single plate of aspect ratio 4. The results of these tests are shown in Figure 37.

Taper ratio results in a decrease of the apparent additional moment of inertia, as is illustrated by Figure 38. The results are from the 1940 N.A.C.A. tests and are presented as the ratio of the apparent additional moment of inertia of a tapered plate to that of an equivalent rectangular plate. The "equivalent rectangular plate" is one of span and area equal to the given tapered plate. This correction is of particular importance for obtaining the true apparent additional moment of inertia about the longitudinal axis of airplanes with tapered wings.

Reference 14[21] and 15[22] report the results of tests on circular disks, cylinders, rectangular plates and rectangular parallelepipeds. A simple torsion pendulum that could be submerged in liquid was used. Two of the above series of tests were conducted, using water, gasoline and carbon tetrachloride as the liquid. These liquids are relatively non-viscous and have a wide range of densities. The assumptions made were that the difference between the moment of inertia measured in air and liquid is the apparent additional moment of inertia, that damping is negligible and that $I_A = m_A \ell^2$.

---

[21] Yee-Tak Yu, loc. cit.

[22] _____, "Virtual Masses of Rectangular Plates and Parallelepipeds in Water," Journal of Applied Physics, Vol. 16, 1945. pp. 724-729.

Some of the data presented for these tests have been presented in a different form in this paper. Wherever possible, the coefficients of apparent additional mass or moment of inertia have been calculated from the physical data given. In the case of the rectangular parallelepipeds, the results were cross-plotted and faired in order to estimate the apparent additional mass coefficients for bodies of varying fineness ratio, but with a square, rather than rectangular, surface normal to the direction of motion.

Thin lead disks, 3.4 mm thick and of various radii, were tested in water. The coefficient and the apparent additional mass presented in Figure 39 are for motion normal to the plane of the disk. Where $\rho$ is the density of the fluid and is equal to 1.0 for water, the empirical relation between apparent additional mass and radius, as indicated by this test, is:

$$m_A = 3.41\ r^3 \rho \qquad (74)$$

For the same configuration, theory[23] gives:

$$m_A = \frac{8}{3}\ r^3 \rho \qquad (75)$$

Then the experimental result is about 1.28 times as great as the theoretical.

For the experiments on cylinders, thin-walled brass tubing was used. A thin metal disk was soldered at the center of each tube to give

---

[23] *Cf. post*, p. 68.

the equivalent of two cups, base to base. The purpose of such a model configuration is not understood. Figure 40 shows the variation of the apparent additional moment of inertia and mass for motion parallel to the longitudinal axis of the cylinder. The apparent additional mass may be represented by:

$$m_A = (7.1 + 5.1\ h)\rho \qquad (76)$$

where h is the length of the cylinder. Equation 76 may be written in the form:

$$m_A = (3.41\ r^3 + \pi r^2 h)\rho \qquad (77)$$

where r is the radius of the cylinder. The first term is the apparent additional mass of a circular disk, and the second term is just the mass of the water contained in the cylinder.

Results are also presented in Figure 40 for the longitudinal axis normal to the direction of motion. This straight line may be approximated by:

$$m_A = (9.8\ h - 10.1)\rho \qquad (78)$$

The above experiments were repeated in gasoline ($\rho = 0.734$) and in carbon tetrachloride ($\rho = 1.574$). In each case, the experimental values were found to be the same as those in water when multiplied by the density of the corresponding liquid. Hence, the apparent additional effect depends directly on the density of the surrounding liquid.

Three groups of rectangular parallelepipeds were tested. The cross-section areas normal to the direction of motion were 8 x 5, 6 x 5 and 4 x 5 $cm^2$, and the thickness varied from 0.15 to 8 cm. Apparent additional mass in grams for the three groups has been plotted versus thickness in Figure 41. The apparent additional mass coefficients computed from these data were plotted with a large scale, faired, and extrapolated to a thickness of 16 cm. The faired values were then cross-plotted for constant thickness. It was then possible to estimate the apparent additional mass for a rectangular parallelepiped whose face normal to the surface was 5 x 5 $cm^2$. Apparent additional mass coefficients were calculated by dividing the above apparent additional masses by the mass of the water displaced. The estimated values are presented in Figure 43 plotted against fineness ratio. For the mutual range of fineness ratios, this curve compares very well with coefficients of apparent additional mass for the longitudinal effect of a circular cylinder with hemispherical ends shown in Figure 25.

The apparent additional mass may be represented by the empirical relationship:

$$m_A = \rho\left[\frac{6.3a^2b^2}{(a^2+b^2)^{1/2}} + 3.5\ abc^{\frac{1}{2}}\right] \qquad (79)$$

where 2a, 2b and 2c represent the dimensions of the block. The dimension parallel to the direction of motion is 2c.

Rectangular plates with cross-section areas of 4 x 4, 4 x 6, 4 x 7, 4 x 8 and 4 x 12 $cm^2$ were tested with the angle, $\theta$, between the direction

of motion and the normal to the plane of the plate varying from 0 to 90 degrees. The apparent additional mass in grams for these plates are plotted in Figure 42, and the coefficients are plotted in Figure 44. This latter figure also presents a plot of the apparent additional mass against maximum plate dimension for zero $\Theta$. This experiment proves conclusively that the apparent additional mass does depend upon the direction of motion of a body. Except for angles near 90 degrees, the empirical relationship shown below compares reasonably well with the experimental results:

$$m_A = \rho \left[ \frac{6.3\ a^2 b^2}{(a^2 + b^2)^{1/2}} \right] \cos^2 \Theta \qquad (80)$$

## APPLICATION

The concept of apparent additional mass has a practical application whenever a body is moving with accelerated motion through any real fluid. Perhaps the two most important applications, certainly the most obvious, are finding the true moments of inertia from swinging tests of bodies and using the virtual (true plus apparent additional) mass in vibration studies. These two applications are of opposite types in that, in one case, the apparent additional effects must be removed, and in the other case, they must be added. In either case, the apparent additional effects must be estimated or experimentally determined. It is hoped that there is a sufficient amount of information in this paper to enable at least a crude estimate to be made of the apparent additional effects for any body.

Usually, it is sufficiently accurate to consider the body as consisting of flat plates and ellipsoids. Malvestuto[24] discovered that more accurate estimates could be made for fuselages of airplanes if an equivalent ellipsoid was used rather than the projected area which was previously used.

The equivalent ellipsoid has approximately the same volume and length as the fuselage. That is, the maximum depth and maximum width of the equivalent ellipsoid are equal to $\sqrt{\frac{6}{\pi}}\,d$ and $\sqrt{\frac{6}{\pi}}\,w$ of the fuselage, where d and w are the average values of fuselage depth and width, respectively.

Theory and experiment show that the values of the apparent additional effects for motion along and rotation about the x principal (longitudinal) axis are relatively small and so were not considered in this reference. However, the coefficient of Figure 7 may be used as an estimate if the apparent additional mass along the x axis is desired.

For motion along the y and z axes, the apparent additional mass of the fuselage is given in terms of the average depth, d, and width, w, by:

$$m_{A_y} = \rho K_y L_f wd \tag{81}$$

and

$$m_{A_z} = \rho K_z L_f wd \tag{82}$$

---

[24] Malvestuto, F. S., Jr., and L. J. Gale, "Formulas for Additional Mass Corrections to the Moments of Inertia of Airplanes," U. S. National Advisory Committee for Aeronautics, Technical Note No. 1187, Feb. 1947. 28 pp.

where $L_f$ is the fuselage length. The coefficients $K_y$ and $K_z$ are presented in Figure 45 for several d/w ratios and are plotted against the plan view fineness ratio of the equivalent ellipsoid.

For rotation about the y and z axes, the apparent additional moments of inertia may be determined from:

$$I_{A_y} = \frac{\rho}{5} K'_y L_f w d \left( \frac{L_f^2}{4} + \frac{3d^2}{2\pi} \right) \tag{83}$$

and

$$I_{A_z} = \frac{\rho}{5} K'_z L_f w d \left( \frac{L_f^2}{4} + \frac{3w^2}{2\pi} \right) \tag{84}$$

where the coefficients $K'_y$ and $K'_z$ are presented in Figure 46 as functions of the plan view fineness ratio $\left( \frac{L_f}{W} \sqrt{\frac{\pi}{6}} \right)$ for several d/w ratios.

It was assumed that the flat plate coefficients were approximately correct for surfaces such as wings and tails. For translatory motion, the apparent additional mass may be calculated from:

$$m_A = \frac{\pi \rho}{4} K \frac{S}{b} \tag{85}$$

where S is the planform area, b is the span and K is the coefficient from Figure 47.

For rotation of a flat surface about its chord at the midspan, the apparent additional moment of inertia is:

$$I_A = \frac{\pi \rho}{48} F_D F_T K' S^2 b \tag{86}$$

where

$F_D$ = dihedral correction factor (Figure 37)

$F_T$ = taper correction factor (Figure 38)

K' = coefficient (Figure 48)

For rotation about a spanwise axis through the centroid of the area, the apparent additional moment of inertia is:

$$I_A = \frac{\pi\rho}{48} K' s^2 b \qquad (87)$$

where K' is also taken from Figure 48, but at an aspect ratio of 1/AR.

For the apparent additional moment of inertia about an axis displaced from the centroid of the area, the general moment of inertia equation below was used:

$$I'_A = I_A + m_A \ell^2 \qquad (88)$$

where $\ell$ is now the distance from the axis of rotation to the centroid of the area. This notation should not be confused with that previously used where $\ell$ was always measured to the center of gravity of the displaced volume.

It was found that for airplanes many of the terms were negligible and that approximate equations of the apparent additional moment of inertia could be used without sacrificing accuracy. These equations for the three swinging axes are given below:

$$I'_{A_x} = \frac{\pi\rho}{48}\left(K' F_D F_T S^2 b\right)_W + \rho\left(K_y L_f w d \ell_{f_x}^2\right)_{FUS} \tag{89}$$

$$I'_{A_y} = \left[\frac{\rho}{5} K'_y L_f w d \left(\frac{L_f^2}{4} + \frac{3d^2}{2\pi}\right)\right]_{FUS}$$

$$+\rho\left(K_z L_f w d\, \ell_{f_y}^2\right)_{FUS} + \frac{\pi\rho}{4}\left(K \frac{S^2}{b} \ell_{t_y}^2\right)_{HT} \tag{90}$$

$$I'_{A_z} = \left[\frac{\rho}{5} K'_z L_f w d \left(\frac{L_f^2}{4} + \frac{3w^2}{2\pi}\right)\right]_{FUS}$$

$$+\rho\left(K_y L_f w d \ell_{f_z}^2\right)_{FUS} + \frac{\pi\rho}{4}\left(K \frac{S^2}{b} \ell_{t_z}^2\right)_{VT} \tag{91}$$

where the subscripts are:

FUS = fuselage

HT = horizontal tail

VT = vertical tail

and where

$\ell_{f_y}$ = component in the x-y plane of the perpendicular distance between the centroid of the fuselage "plan" area and the axis of rotation parallel to and in the plane of the y axis

$\ell_{f_z}$ = distance from centroid of side area of fuselage to axis of rotation parallel to and in the plane of the z axis

$l_{t_y}$ = component in the x-y plane of fuselage of the perpendicular distance between the centroid of the horizontal tail area and the axis of rotation parallel to and in the plane of the y axis

$l_{t_z}$ = distance from centroid of vertical tail area to axis of rotation for z swinging.

These last equations were checked for 40 airplane models by testing the models in the N.A.C.A. vacuum tank previously described. The agreement was found to be good. Upon comparing the results of these tests, it was found that in the majority of cases the apparent additional moments of inertia did not exceed 25 percent of the true moments of inertia, both moments being taken about the body axes.

# BIBLIOGRAPHY


1. Cowley, W. L., and H. Levy, "On the Effect of Acceleration on the Resistance of a Body," Advisory Committee for Aeronautics Reports and Memoranda No. 612, Vol. 1, 1918-1919. pp. 95-101.

2. Frazer, R. A., and L. F. G. Simmons, "The Dependence of the Resistance of Bodies Upon Acceleration, as Determined by Chronograph Analysis," Advisory Committee for Aeronautics Reports and Memoranda No. 590, Vol. 1, 1918-1919. pp. 102-121.

3. Glauert, Hermann, Wind Tunnel Interference on Wings, Bodies and Airscrews, London: His Majesty's Stationery Office, 1933. (Aeronautical Research Committee Reports and Memoranda No. 1566). 102 pp.

4. Gracey, William, "The Additional-Mass Effect of Plates as Determined by Experiments," U. S. National Advisory Committee for Aeronautics Technical Report No. 707, 1941. 10 pp.

5. Green, George, "Researches on the Vibration of Pendulums in Fluid Media," Transactions of the Royal Society of Edinburgh, Vol. 13, 1836. pp. 54-62.

6. Lamb, Horace, Hydrodynamics, 5th ed., Cambridge: University Press, 1930. 687 pp.

7. _____, Hydrodynamics, 6th ed., Cambridge: University Press, 1932. 738 pp.

8. _____, "The Inertia-Coefficients of an Ellipsoid Moving in Fluid," Advisory Committee for Aeronautics Reports and Memoranda No. 623, Vol. 1, 1918-1919. pp. 128-129.

9. Malvestuto, F. S., Jr., and L. J. Gale, "Formulas for Additional Mass Corrections to the Moments of Inertia of Airplanes," U. S. National Advisory Committee for Aeronautics Technical Note No. 1187, Feb., 1947. 28 pp.

10. Munk, Max M., "Some Tables of the Factor of Apparent Additional Mass," U. S. National Advisory Committee for Aeronautics Technical Note No. 197, July, 1924. 7 pp.

11. Relf, E. F., and R. Jones, "Measurement of the Effect of Accelerations on the Longitudinal and Lateral Motion of an Airship Model," Advisory Committee for Aeronautics Reports and Memoranda No. 613, Vol. 1, 1918-1919. pp. 121-127.

12. Soulé, Hartley A., and M. P. Miller, "The Experimental Determination of the Moments of Inertia of Airplanes," U. S. National Advisory Committee for Aeronautics Technical Report No. 467, 1933. 15 pp.

13. Woods, F. S., Advanced Calculus, Boston: Ginn and Company, 1932. 397 pp.

14. Yee-Tak Yu, "Virtual Masses and Moments of Inertia of Disks and Cylinders in Various Liquids," Journal of Applied Physics, Vol. 13, 1942. pp. 66-69.

15. _____, "Virtual Masses of Rectangular Plates and Parallelepipeds in Water," Journal of Applied Physics, Vol. 16, 1945. pp. 724-729.

# APPENDIX I

## Formulae, Tables and Curves

The first portion of this appendix is a collection of theoretical apparent additional mass factors. For two-dimensional flows, the apparent additional mass is given as $m_A$, while for three-dimensional flows, the apparent additional mass coefficient k is used. The apparent additional mass may be found by multiplying k by the displaced volume times the density of the fluid, $\rho$. All tubular data are plotted in curves immediately following the factors. Wherever it seemed advisable, comparison curves have also been plotted.

The second portion of this appendix presents results of various experiments and, in some cases, diagrams of the equipment used. Figures 45 to 48 present the most important apparent additional constants for estimating the apparent additional effects for various bodies.

## Two-Dimensional Flows.

1. Straight line, length = a

$$m_A = \frac{\pi}{4} \rho a^2$$


Reference 10.

2. Straight line, length = a, rotating about its center

$$I_A = \frac{\pi}{8} \rho a^4$$

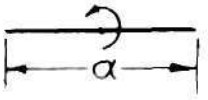


Reference: See 6(a) when b = 0

3. Circle, diameter a

$$m_A = \frac{\pi}{4} \rho a^2$$

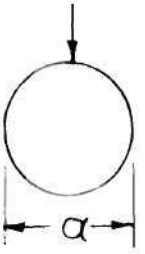


Reference 10.

4. Ellipse, moving at right angles to its major axis, a

$$m_A = \frac{\pi}{4} \rho a^2$$

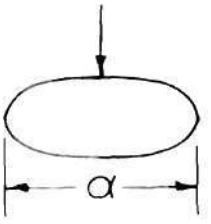


Reference 10.

5. Ellipse moving at right angles to its minor axis, a

$$m_A = \frac{\pi}{4} \rho a^2$$


---

Arrows indicate direction of motion of body.

6. Ellipse, rotating about its center

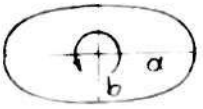


a = semi-major axis
b = semi-minor axis

(a) Apparent additional moment of inertia of fluid outside of ellipse

$$I_A = \frac{\pi}{8}\rho(a^2-b^2)^2$$

(b) Apparent additional moment of inertia of fluid inside ellipse

$$I_A = \frac{\pi}{4}\rho ab\frac{(a^2-b^2)^2}{a^2+b^2}$$

7. Pair of straight parallel lines

(No Stagger)

length = a  distance = h

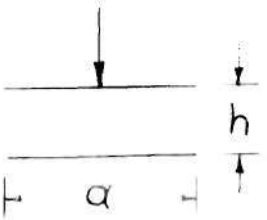


$$m_A = \frac{\pi}{4}\rho a^2 C$$

Reference 10.

Table I

| | | | | | | | |
|---|---|---|---|---|---|---|---|
| h/a = 0<br>C = 1 | 0.05<br>1.123 | 0.10<br>1.212 | 0.15<br>1.289 | 0.20<br>1.353 | 0.30<br>1.462 | 0.40<br>1.55 | 0.50<br>1.63 |
| h/a = 0.39<br>C = 1.55 | 0.46<br>1.60 | 0.56<br>1.67 | 0.64<br>1.71 | 0.79<br>1.77 | 0.98<br>1.83 | 1.11<br>1.86 | |
| h/a = 1.46<br>C = 1.91 | 2.02<br>1.91 | 2.87<br>1.94 | 5.76<br>1.94 | 13.88<br>1.99 | 57.7<br>1.99 | 2.00 | |

See Figure 3 for plot of C versus h/a.

8. Rectangle moving at right angles to its major side

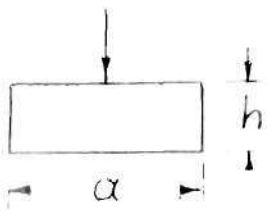


$$m_A = \frac{\pi}{4}\rho a^2 C - ah\rho$$

Reference 10.

Table II

| h/a - 0 | 0.05 | 0.10 | 0.15 | 0.20 | 0.30 | 0.40 | 0.50 |
|---|---|---|---|---|---|---|---|
| C - 1 | 1.156 | 1.271 | 1.371 | 1.471 | 1.664 | 1.835 | 2.00 |

See Figure 4 for plot of C versus h/a.

9. Rankin Oval )
   Ellipse ) moving parallel to
   Joukowski Section ) major axis
   Modified Joukowski Section )

$$m_A = \frac{\pi}{2} \lambda_2 t^2 \rho - A\rho$$

where t = maximum thickness of section
A = area of section

See Figure 14 for drawing of the sections and Figure 12 for plot of $\lambda_2$ versus fineness ratio.

Reference 3.

All of the above equations for apparent additional mass or moment of inertia may be considered to be the apparent additional mass or moment of inertia per unit length for cylinders of infinite aspect ratio. To determine the actual apparent additional mass or moment of inertia, multiply each above equation by the length of the infinite aspect ratio cylinder and change to the appropriate density, $\rho$.

Three-Dimensional Flows.

1. Prolate ellipsoid, motion parallel to axis of revolution (end-on)

$b = c < a$ $\qquad\qquad$ $a/b = P > 1$

$$m_A = \rho \text{ Volume } k_1$$

See Table III for tabulated values of $k_1$.

2. Prolate ellipsoid, motion perpendicular to axis of revolution (broadside)

$$a = c < b \qquad b/a = M > 1$$

$$m_A = \rho \text{ Volume } k_2.$$

See Table III for tabulated values of $k_2$.

3. Oblate ellipsoid, motion perpendicular to axis of revolution (lengthwise)

$$a = c > b \qquad a/b = M > 1$$

$$m_A = \rho \text{ Volume } k_3.$$

See Table III for tabulated values of $k_3$.

4. Oblate ellipsoid, motion parallel to axis of revolution (broadside)

$$b = c > a \qquad b/a = Q > 1$$

$$m_A = \rho \text{ Volume } k_4.$$

See Table III for tabulated values of $k_4$.

The prolate ellipsoid is generated by revolving the ellipse about its major axis, and the oblate ellipsoid is generated by revolving the ellipse about its minor axis. The letters a, b, and c refer to the conventional semi-axes in the x, y, and z directions, respectively, and the letters P,N,M, and Q refer to the ratio of the major axis to the minor axis. Equations 23, 25, 27, and 29 were used to calculate the apparent additional mass coefficients.

Table III

| Major Axis / Minor Axis | $k_1$ | $k_2$ | $k_3$ | $k_4$ |
|---|---|---|---|---|
| 1.5 | 0.304 | 0.622 | 0.383 | 0.804 |
| 2 | 0.209 | 0.705 | 0.310 | 1.114 |
| 3 | 0.122 | 0.804 | 0.223 | 1.743 |
| 4 | 0.082 | 0.860 | 0.174 | 2.374 |
| 5 | 0.059 | 0.894 | 0.143 | 3.008 |
| 6 | 0.045 | 0.917 | 0.121 | 3.642 |
| 7 | 0.036 | 0.933 | 0.105 | 4.277 |
| 8 | 0.029 | 0.945 | 0.092 | 4.912 |
| 9 | 0.024 | 0.954 | 0.083 | 5.548 |
| 10 | 0.021 | 0.960 | 0.075 | 6.184 |
| $\infty$ | 0.000 | 1.000 | 0.000 | $\infty$ |
| See Figure | 6 | 7 | 8 | 9 |

5. Prolate ellipsoid rotating about its minor axis

$I_A$ = $k'$ times moment of inertia of displaced fluid

$k'$ = coefficient of apparent additional moment of inertia
R = major axis/minor axis

Table IV

| $R_1$ = 1<br>$k'$ = 0 | 1.50<br>.094 | 2.00<br>.240 | 2.51<br>.367 | 2.99<br>.465 | 3.99<br>.608 | 4.99<br>.701 |
|---|---|---|---|---|---|---|
| R<br>$k'$ | 6.01<br>.764 | 6.97<br>.805 | 8.01<br>.840 | 9.02<br>.865 | 9.99<br>.883 | <br>1.00 |

See Figure 10 for plot of $k'$

Reference 10.

6. Circular disk, radius = a, moving perpendicular to its plane

$$m_A = \frac{8}{3} \rho a^3$$

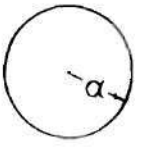


Reference 7.

7. Circular disk, radius = a, rotating about its diameter

$$I_A = \frac{16}{45} \rho a^5$$


Reference 7.

8. Elliptic disk moving perpendicular to its plane

(a) $m_A = \rho ab^2 \frac{4}{3} \pi C$

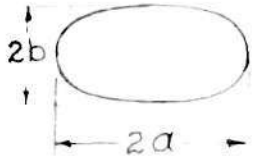


major axis = 2a
minor axis = 2b

Table V

| | | | | | |
|---|---|---|---|---|---|
| b/a | 1.00 | .899 | .799 | .695 | .602 |
| C | .637 | .671 | .704 | .746 | .781 |
| b/a | .500 | .399 | .301 | .250 | .199 |
| C | .826 | .870 | .912 | .933 | .952 |
| b/a | .167 | .125 | .101 | 0000 | |
| C | .964 | .978 | .984 | 1.00 | |

See Figure 11 for plot of C versus b/a

Reference 10.

(b) $m_{A_z} = \frac{8}{3} \rho a^3 C_z$

$I_{A_x} = \frac{16}{45} \rho a^5 C_x$

$I_{A_y} = \frac{16}{45} \rho a^5 C_y$

major axis = 2a

See Figure 30 for plot of $C_z$, $C_x$, and $C_y$ versus fineness ratio.

Reference 4.

9. Rankine ovoid and prolate ellipsoid moving parallel to their major axes

$$m_A = \frac{\pi}{4}\rho\lambda_3 t^3 - A\rho$$

where t = maximum thickness of body
A = volume of body

See Figure 14 for drawings of sections and Figure 13 for plot of $\lambda_3$ versus fineness ratio.

Reference 3.

Figure 1. Streamlines About a Circular Cylinder Moving Through Motionless Fluid. (Reference 6)

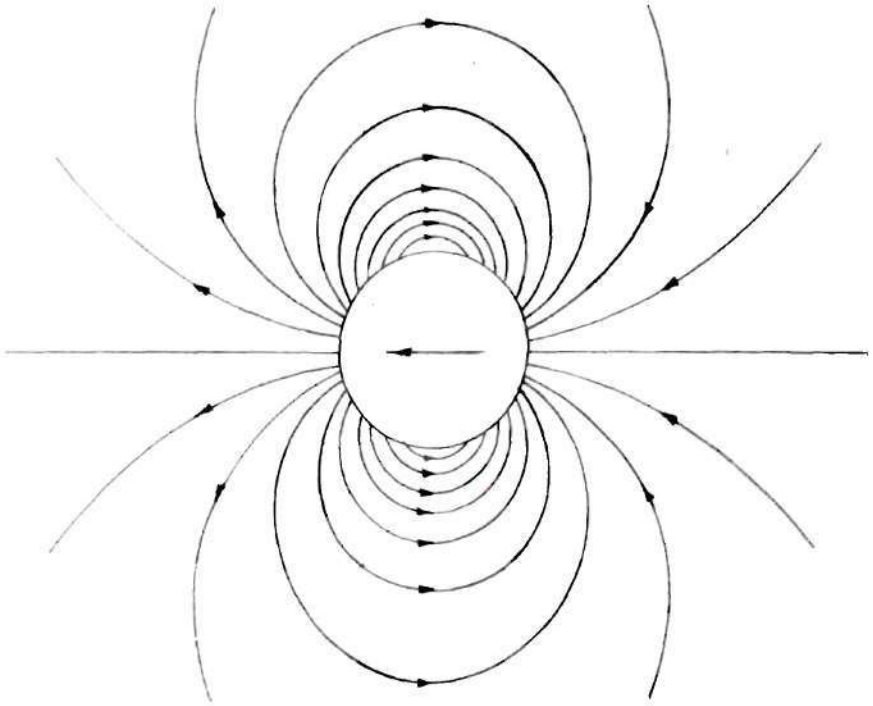

Figure 2. Hollow Infinite Elliptic Cylinder Rotating About its Longitudinal Axis. (Reference 6)

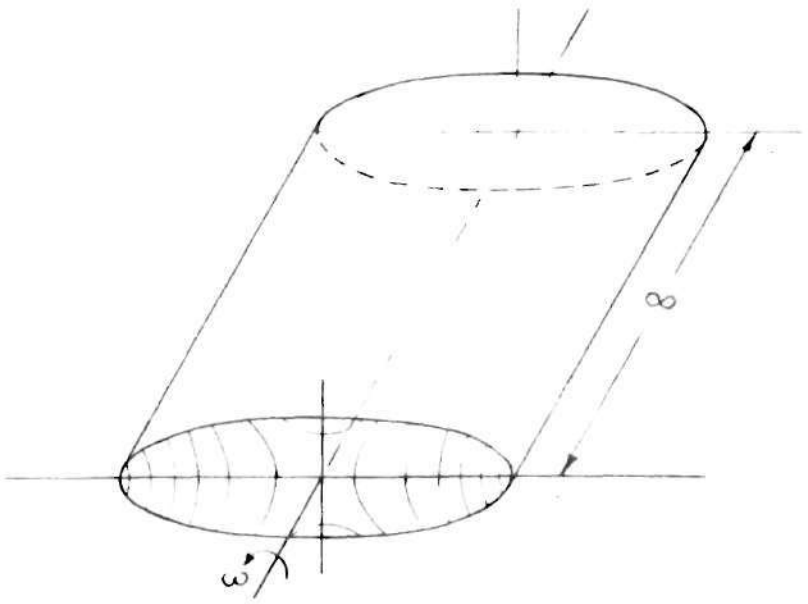

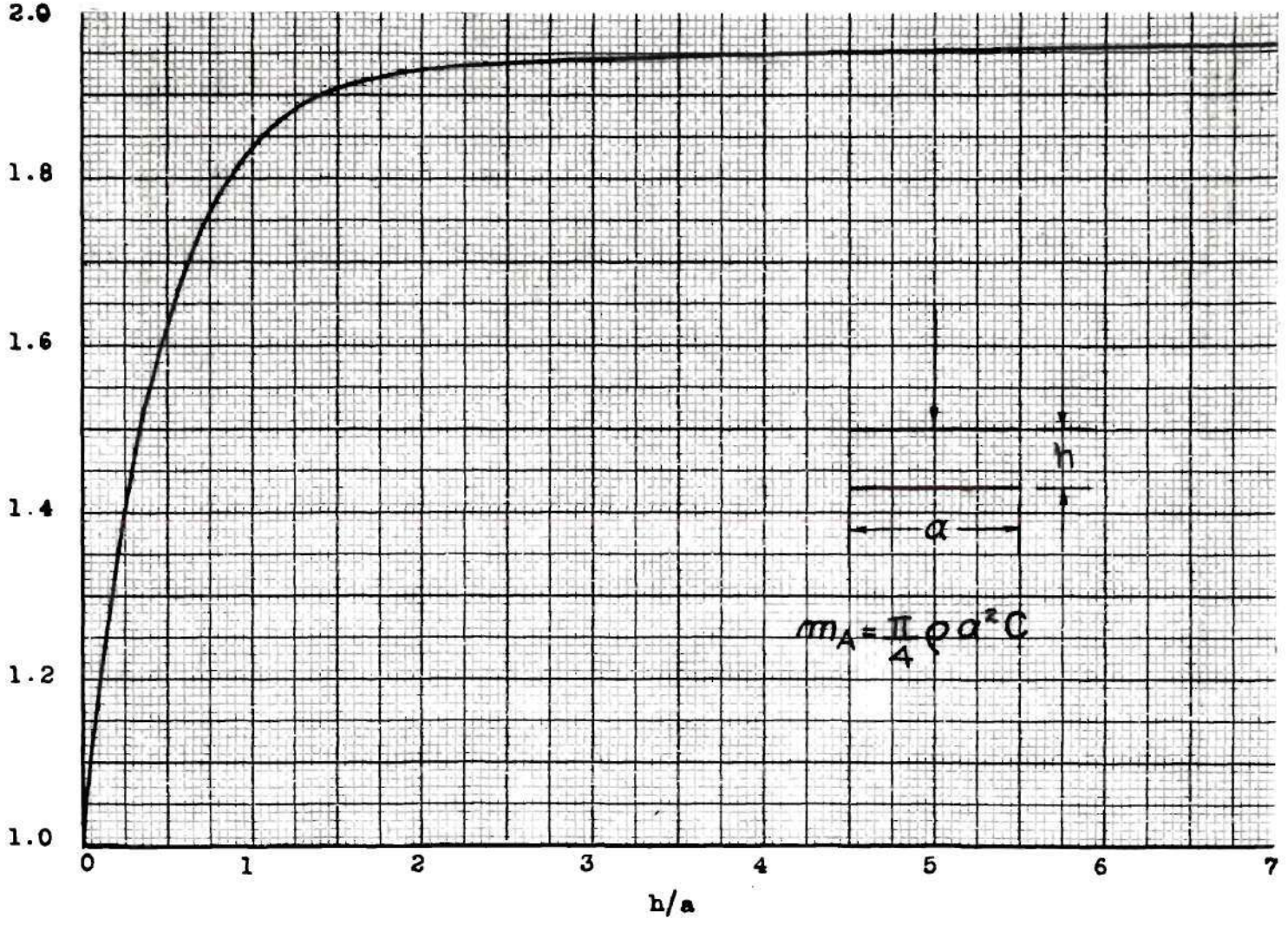


Figure 3. Apparent Additional Mass Constant for Pair of Straight Parallel Lines. (Reference 10)

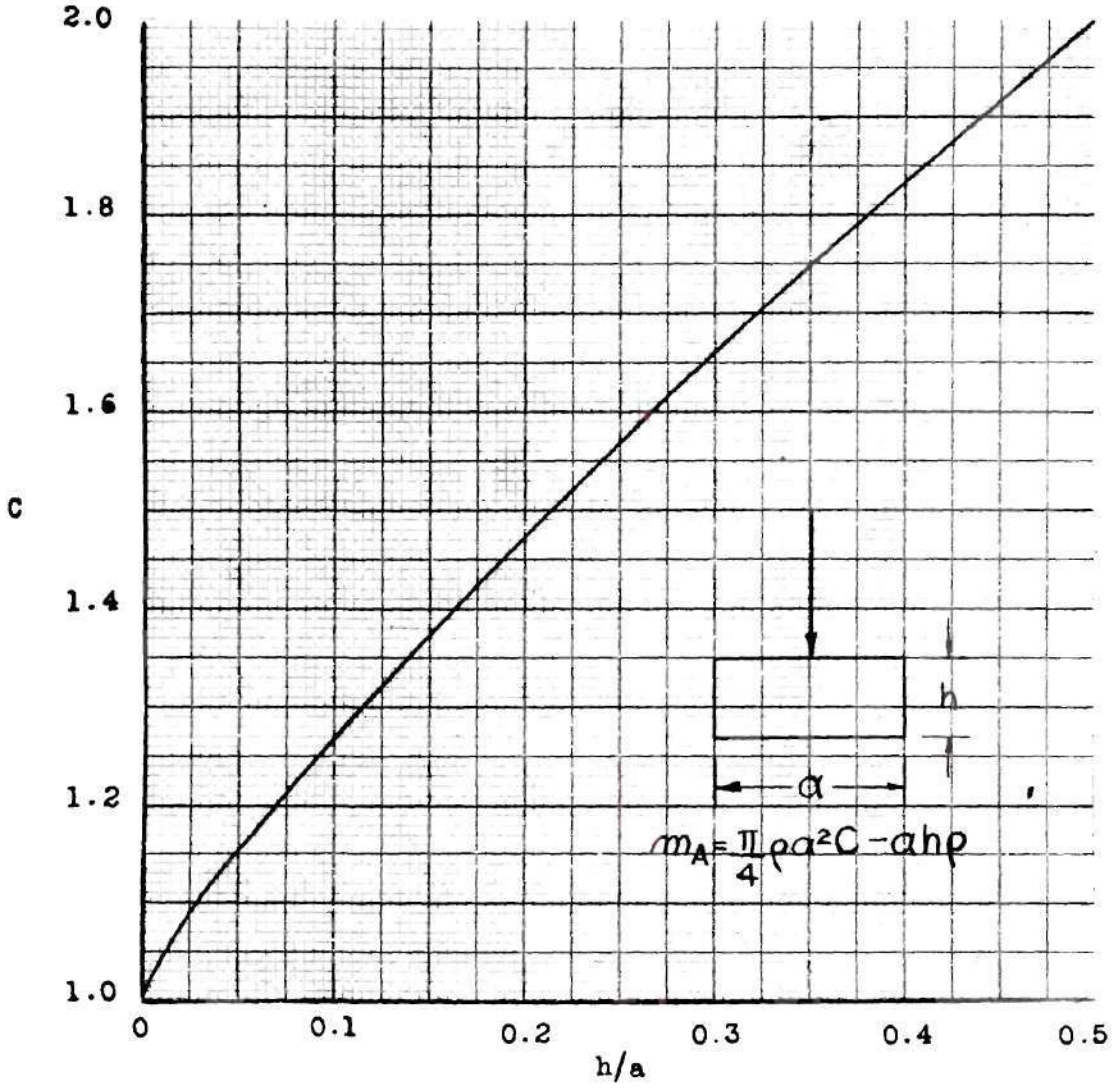


Figure 4. Apparent Additional Mass Constant for Rectangle Moving Perpendicular to its Major Side. (Reference 10)

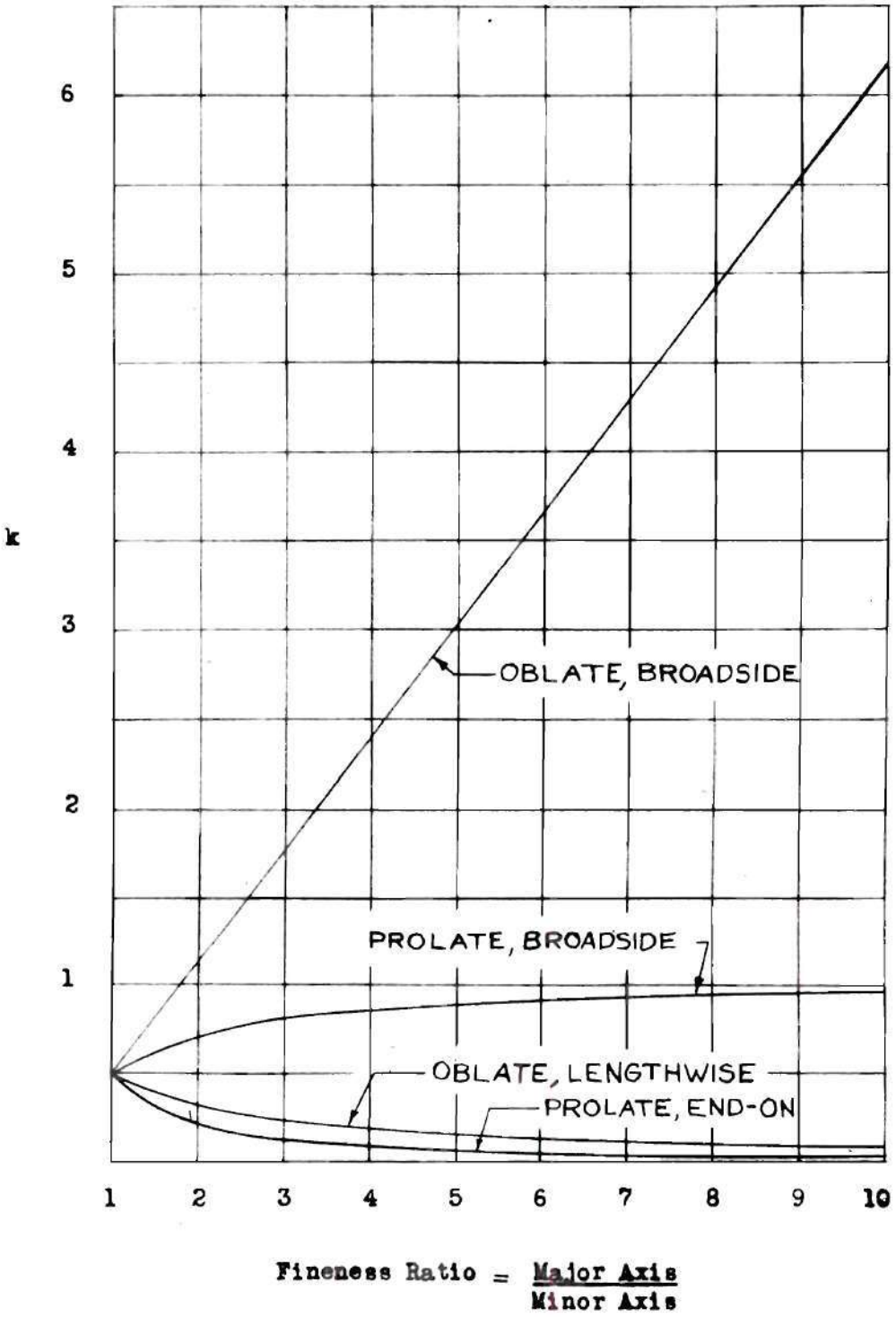


Figure 5. Comparison of Ellipsoid Apparent Additional Mass Coefficients.

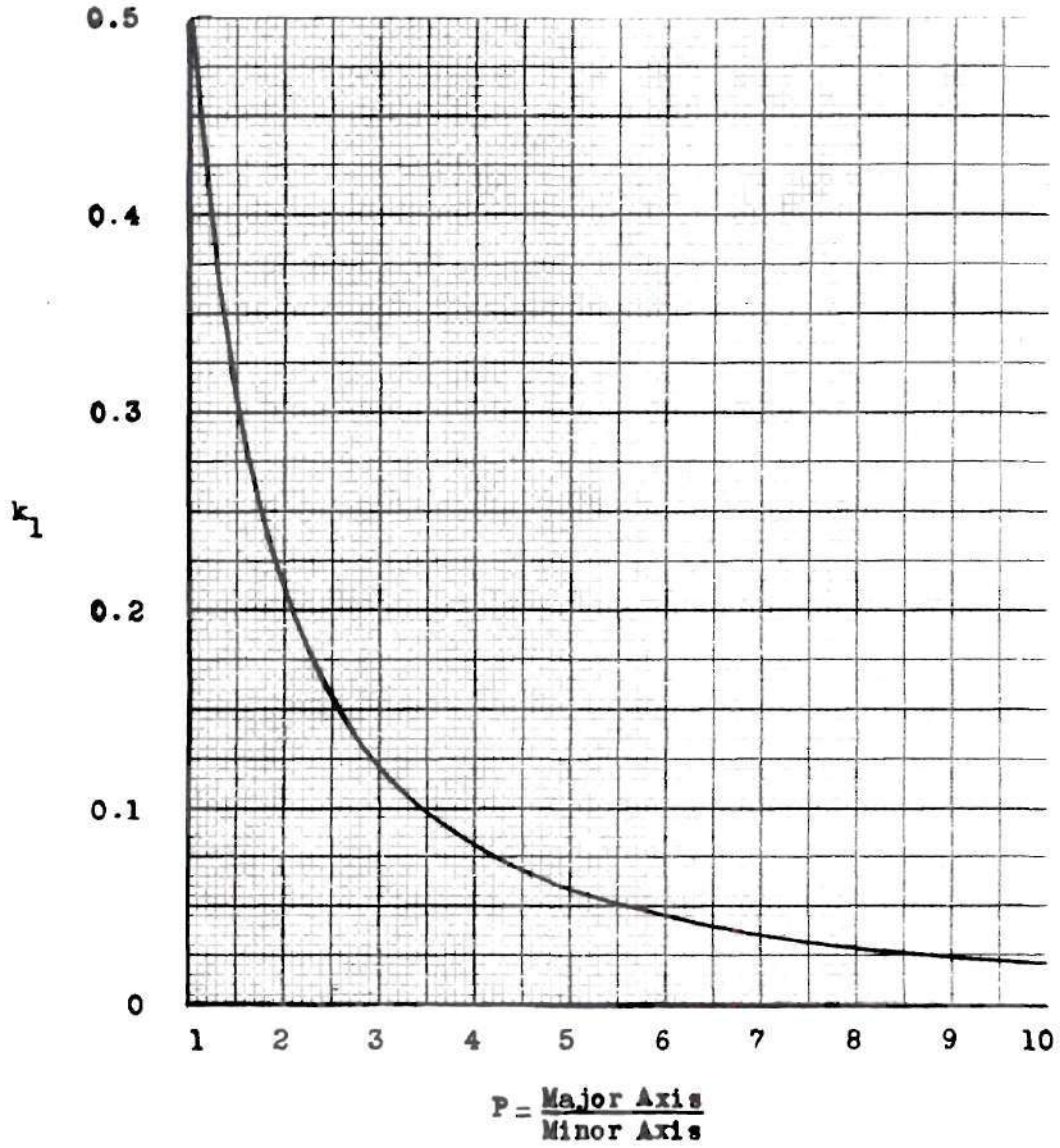


**Figure 6.** Apparent Additional Mass Coefficient for Prolate Ellipsoid, Motion Parallel to Axis of Revolution (End-on).

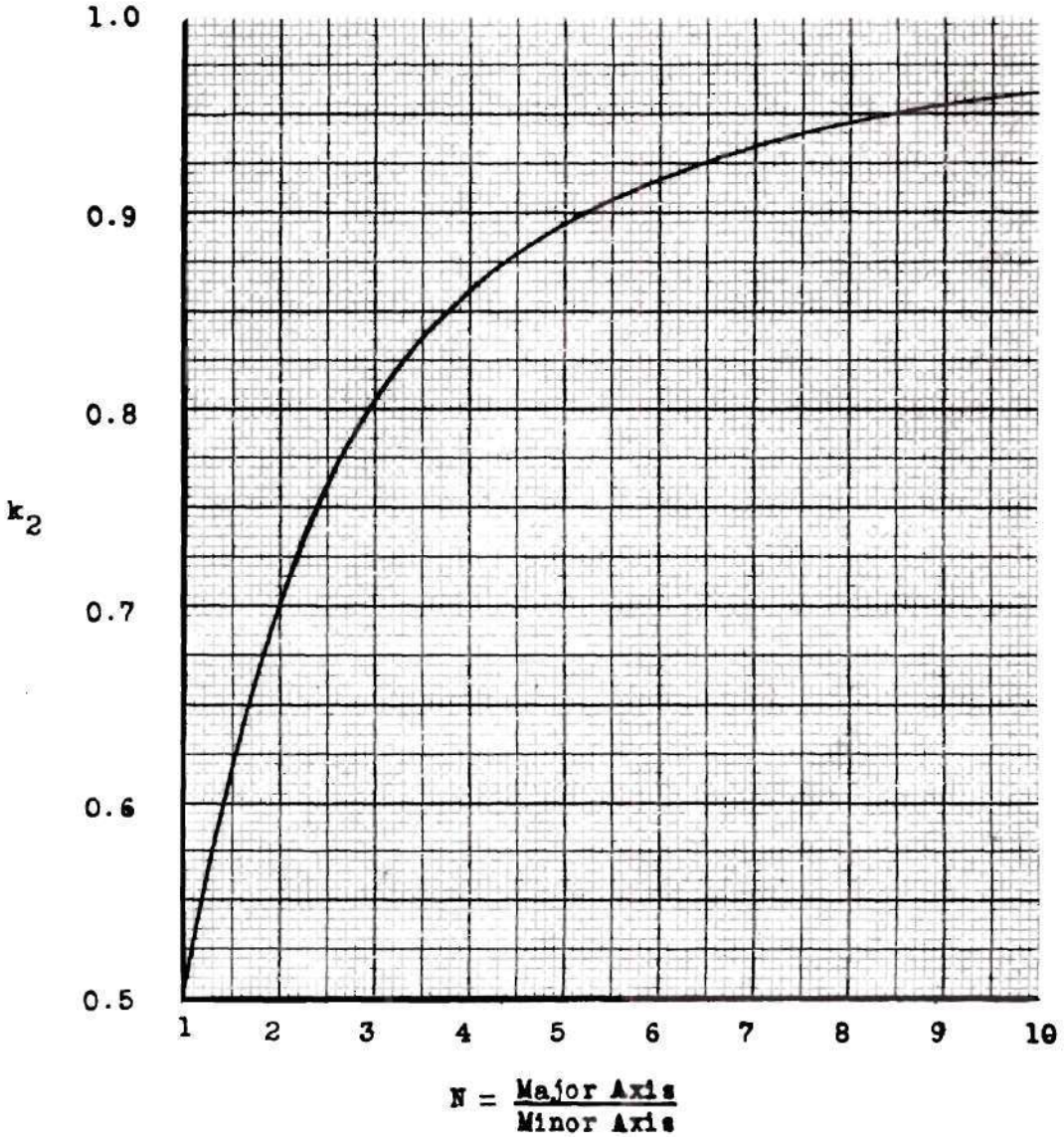


Figure 7. Apparent Additional Mass Coefficient for Prolate Ellipsoid, Motion Perpendicular to Axis of Revolution (Broadside).

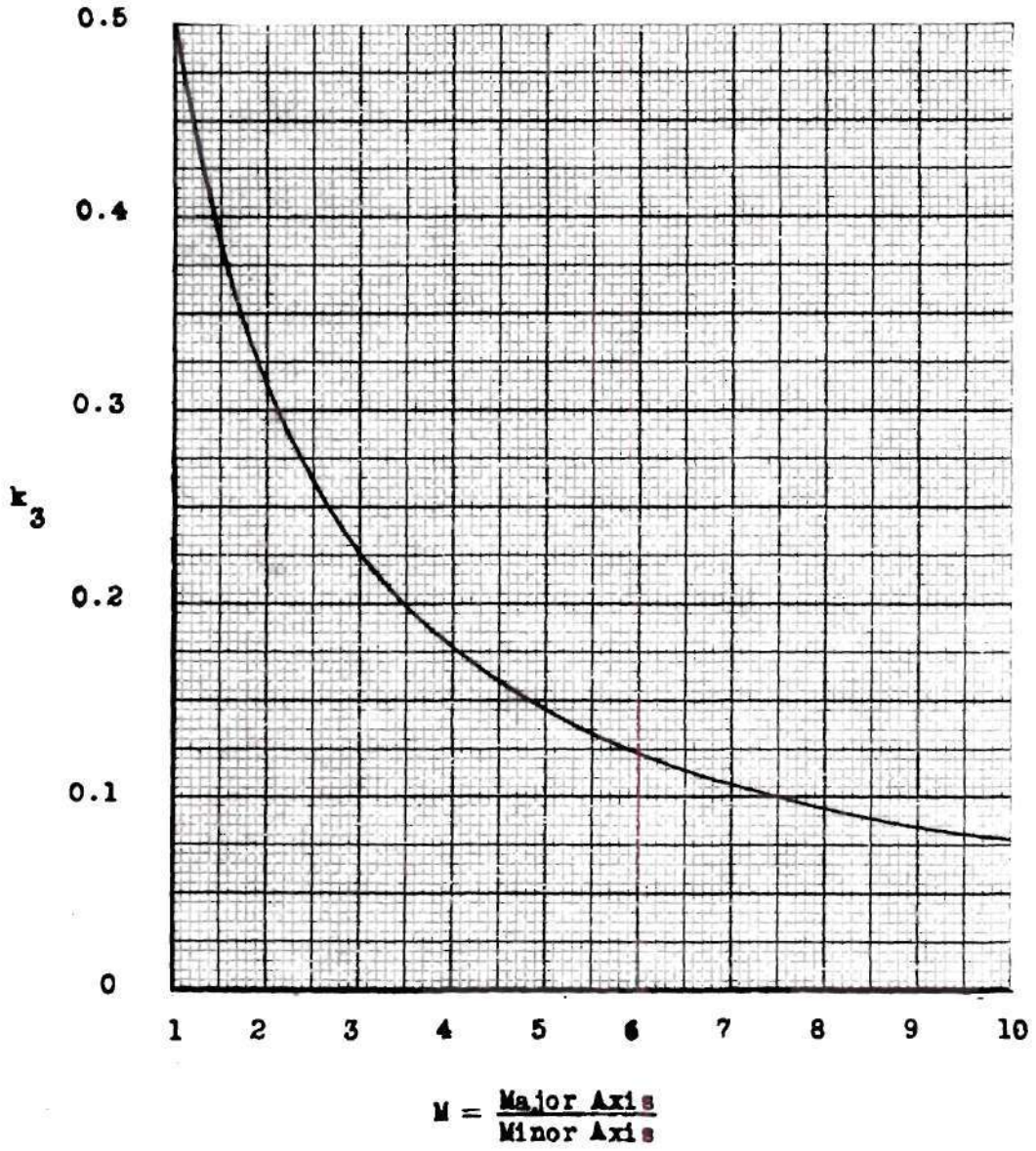


Figure 8. Apparent Additional Mass Coefficient for Oblate Ellipsoid, Motion Perpendicular to Axis of Revolution (Lengthwise).

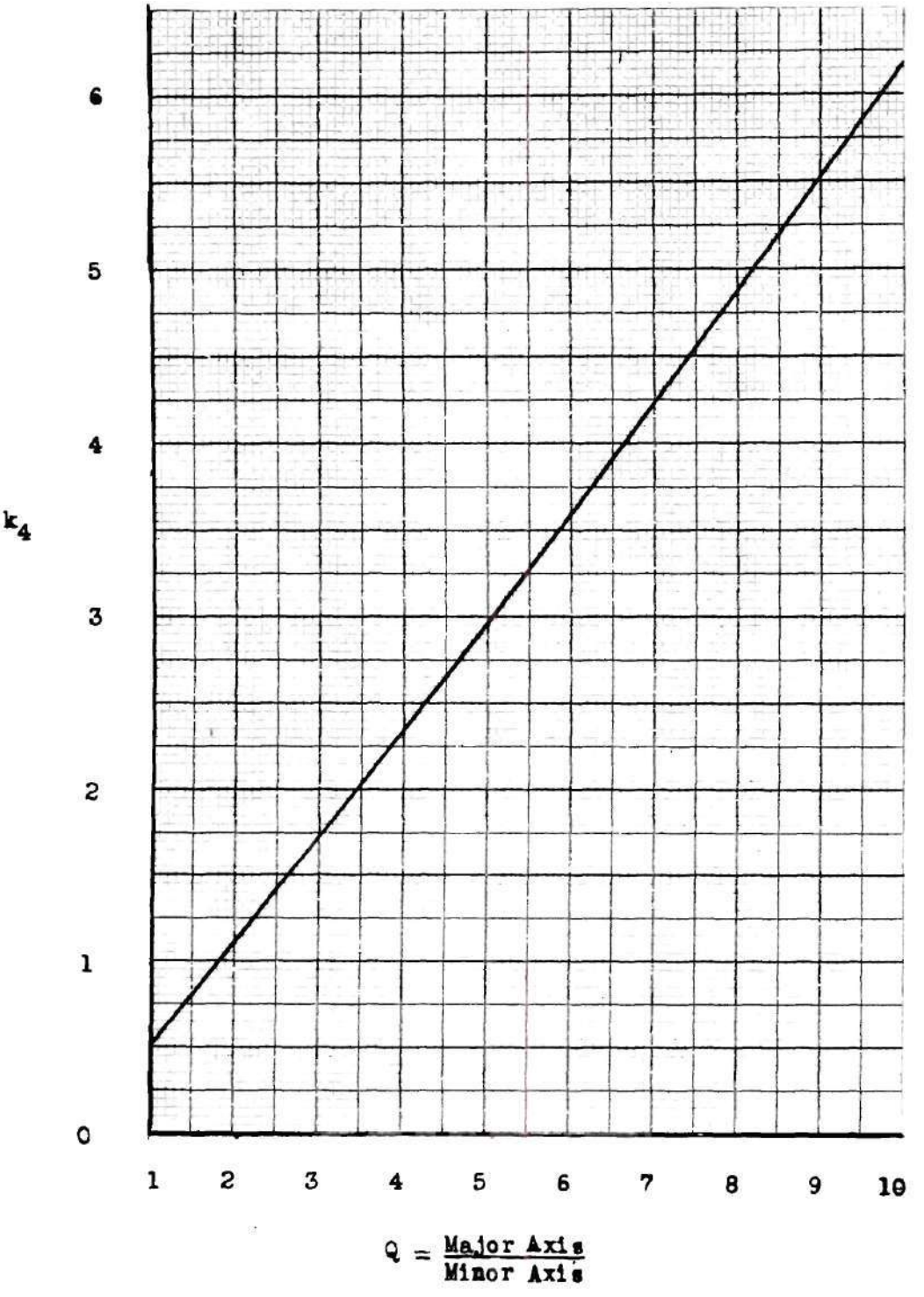


Figure 9. Apparent Additional Mass Coefficient for Oblate Ellipsoid, Motion Parallel to Axis of Revolution (Broadside).

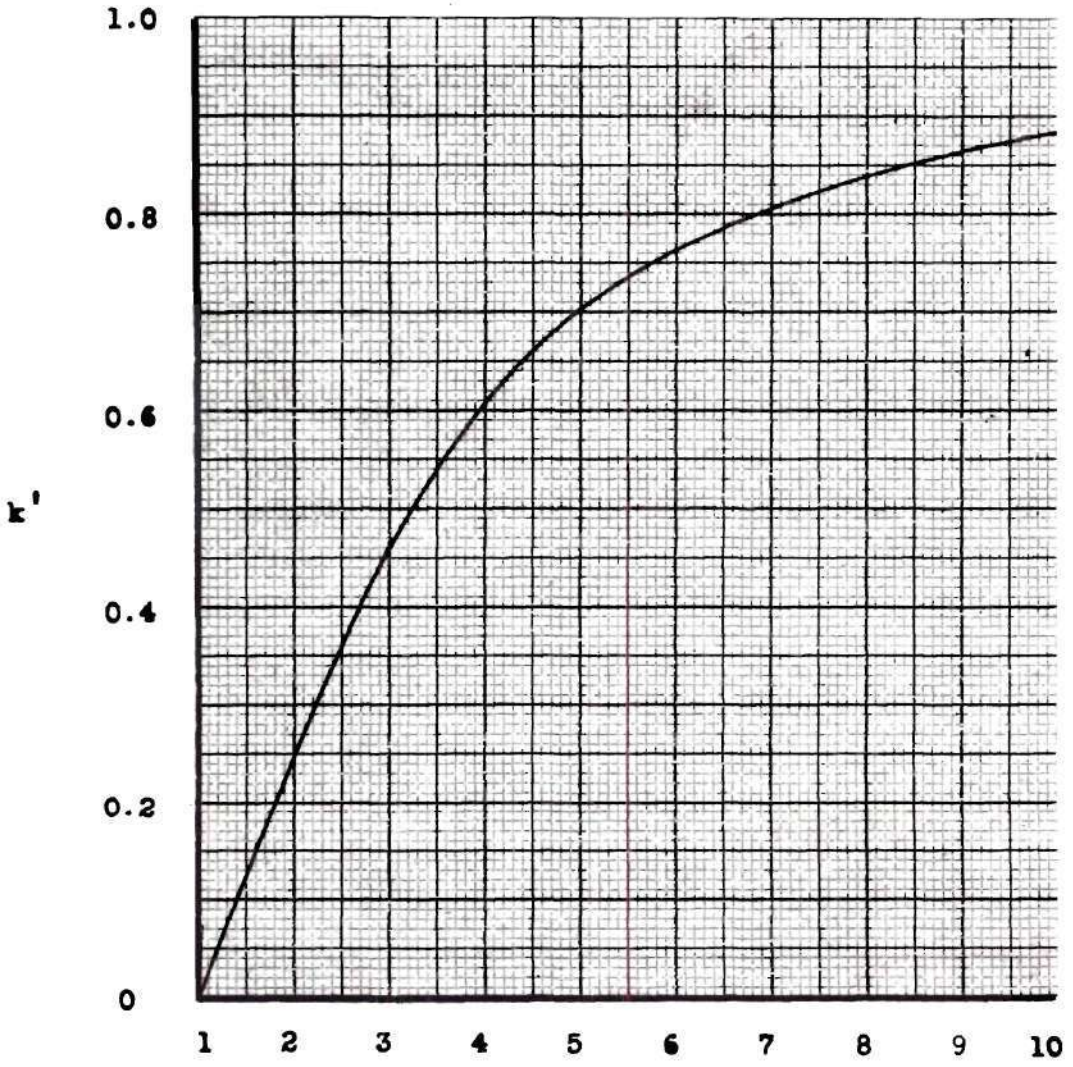


**Figure 10. Apparent Additional Moment of Inertia Coefficient for Prolate Ellipsoid Rotating About its Minor Axis.**

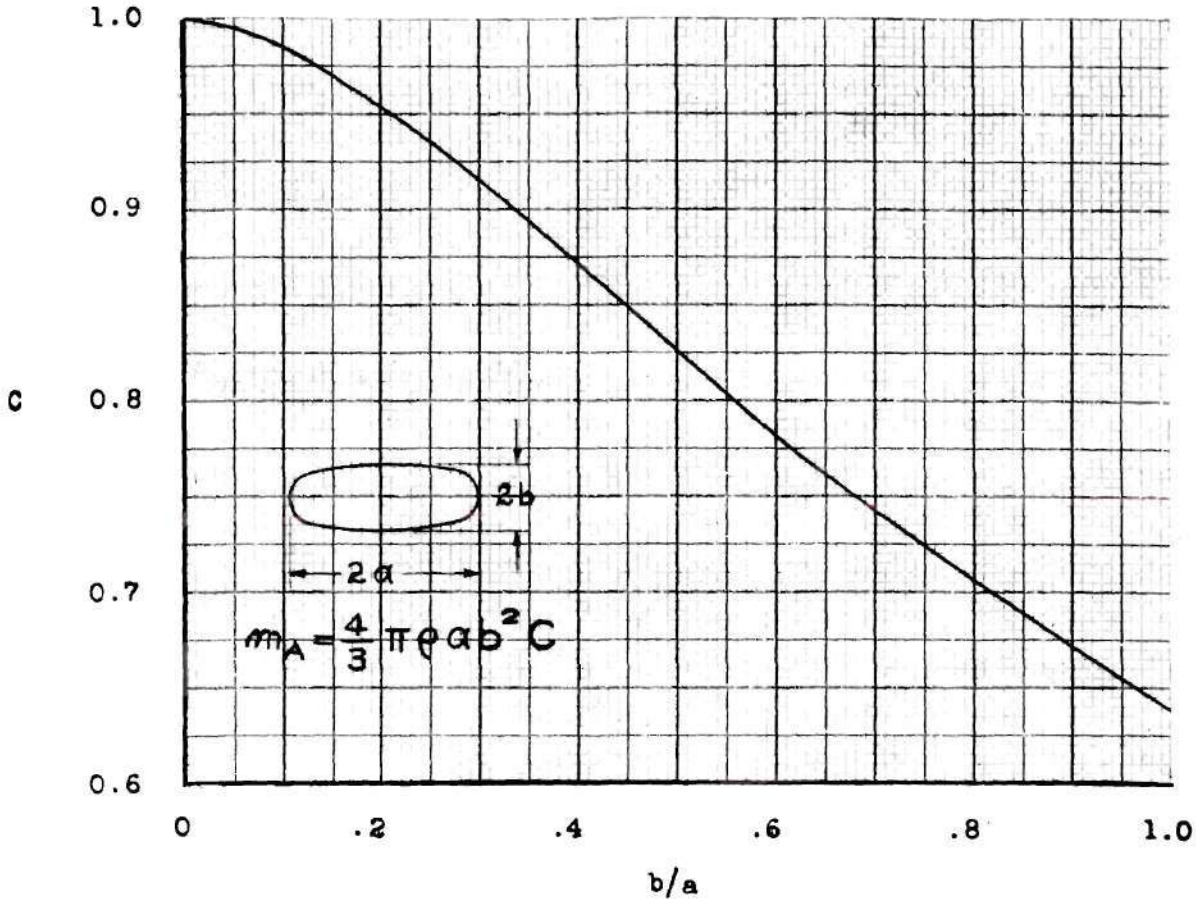


Figure 11. Apparent Additional Mass Constant for Elliptic Disk Moving at Right Angles to its Plane.

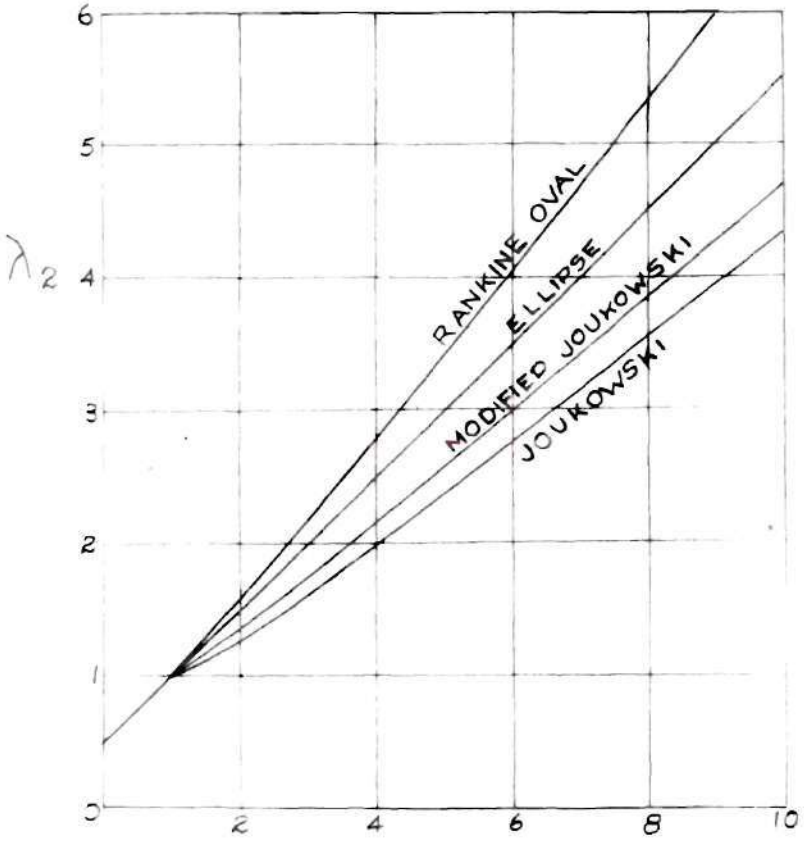


Figure 12. Two-Dimensional Apparent Additional Mass Coefficients. (Reference 3)

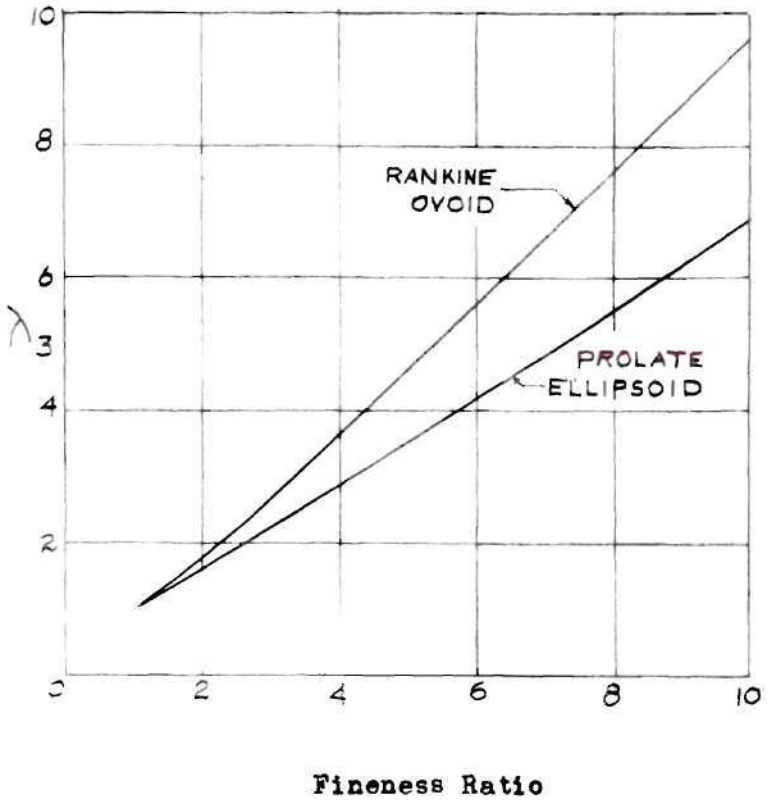


Figure 13. Three-Dimensional Apparent Additional Mass Coefficients. (Reference 3)

(See Figure 14 for Two-Dimensional Sections)

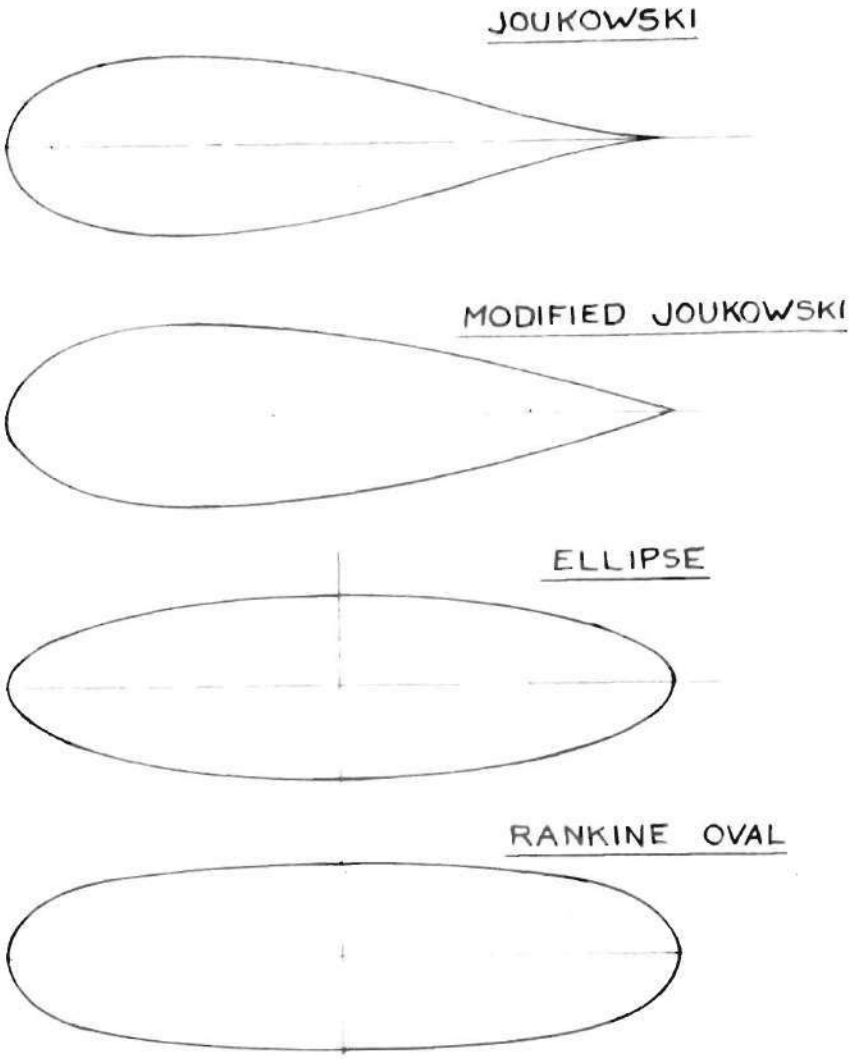


**Figure 14. Two-Dimensional Sections for Figures 12 & 13. (Reference 3)**

Diagram of Body Tested.

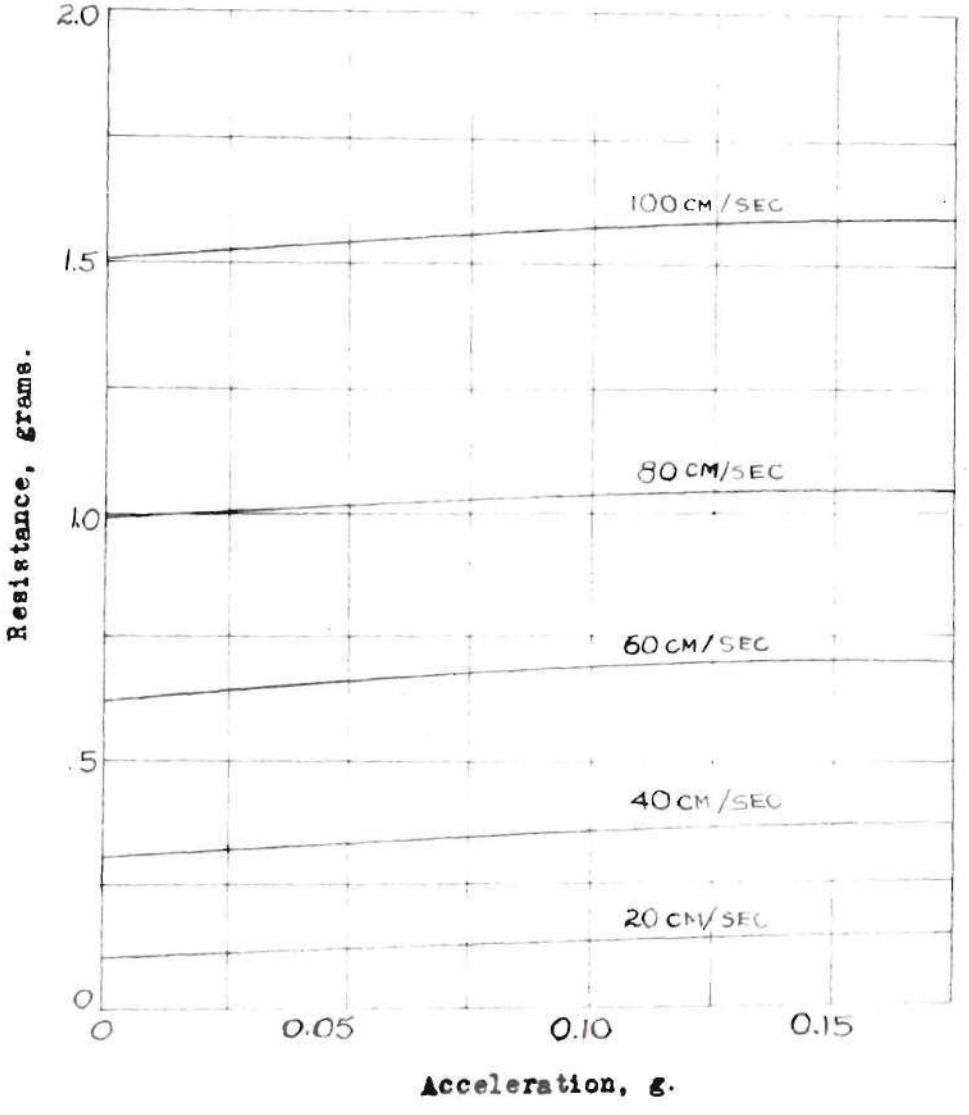


Figure 15. Effect of Acceleration on Resistance from Drop Tests. (Reference 1)

**Figure 16. Effect of Acceleration on Resistance of Streamlined Body. (Reference 5)**

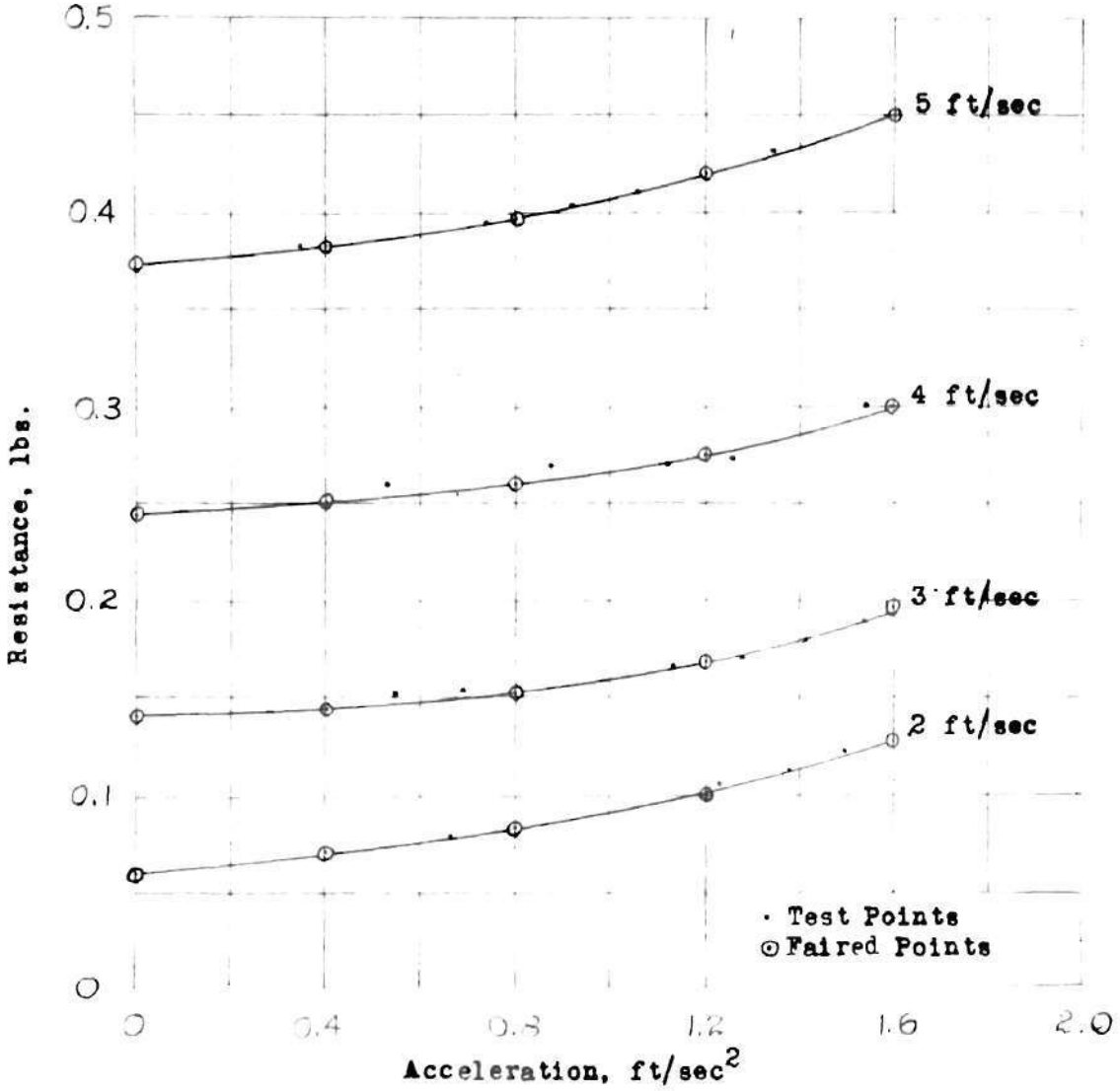


**Figure 17. Effect of Velocity on Apparent Additional Mass Coefficient of Streamlined Body. (Reference 5)**

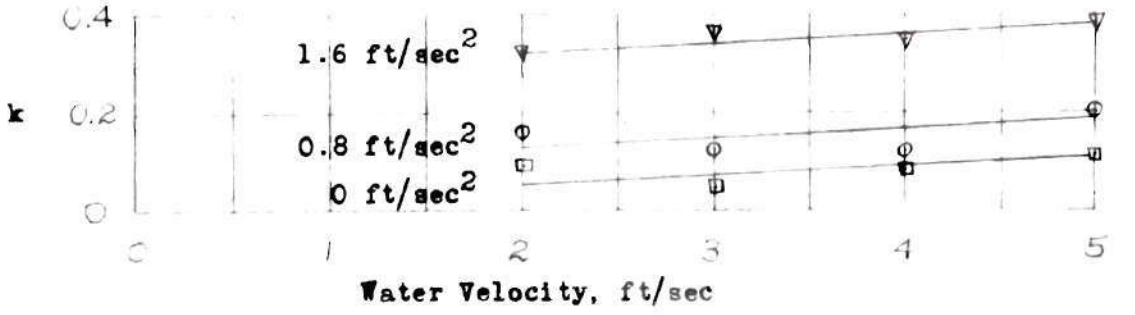

**Figure 18. Variation of Resistance with Velocity for Constant Acceleration of Streamlined Body. (Reference 5)**

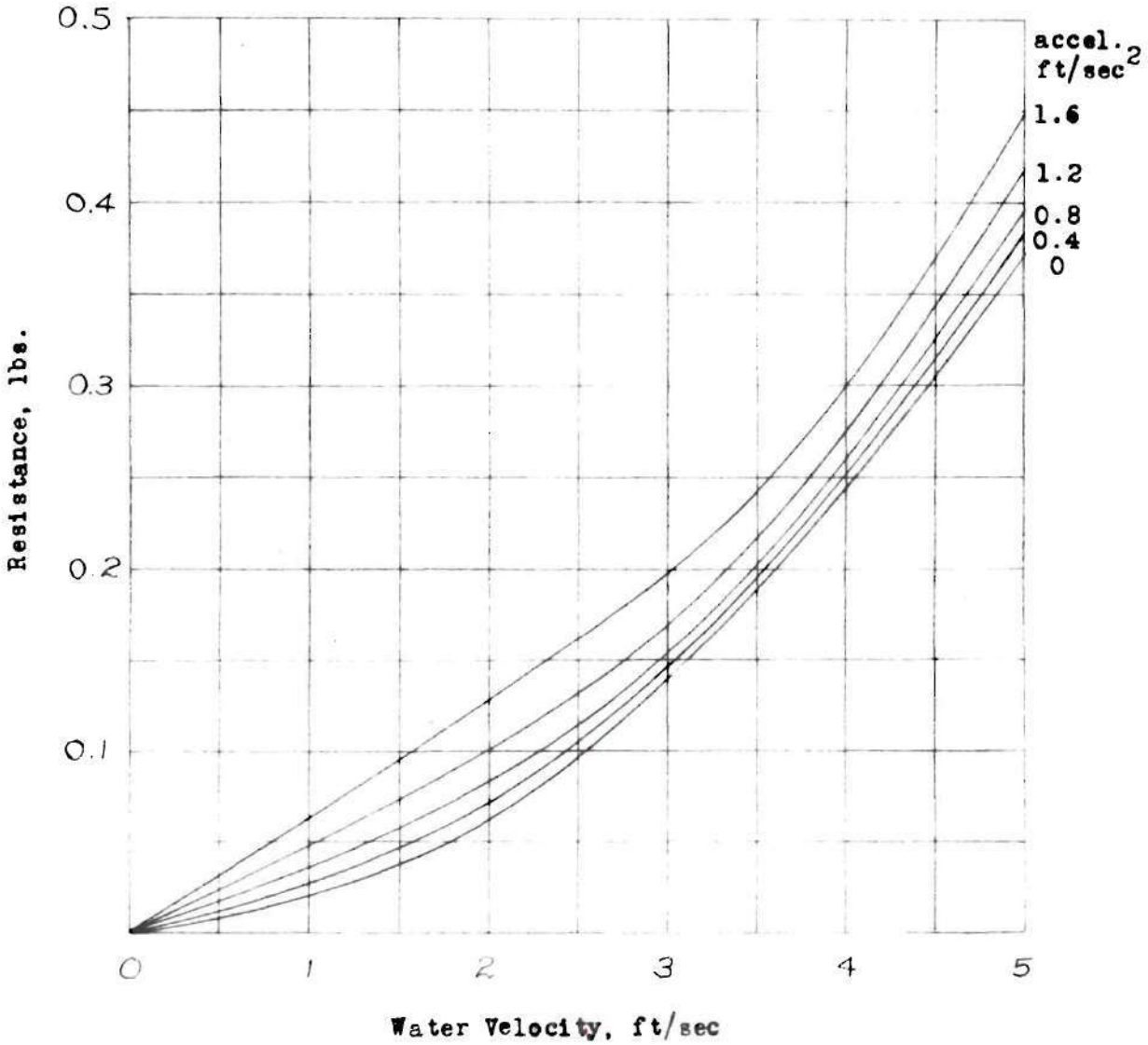

**Figure 19. Variation of Resistance with Acceleration at Constant Velocity of a Sphere. (Reference 5)**

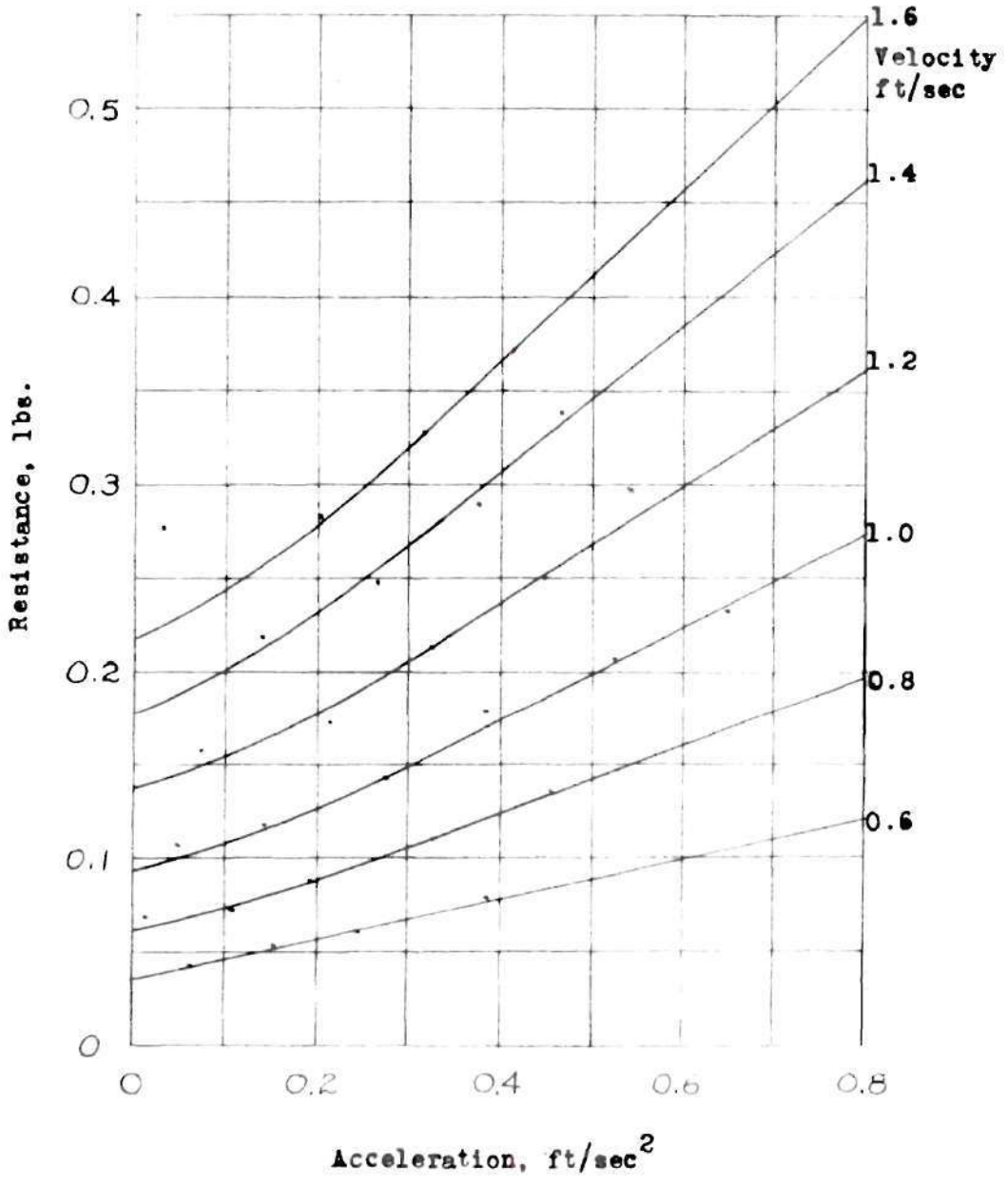

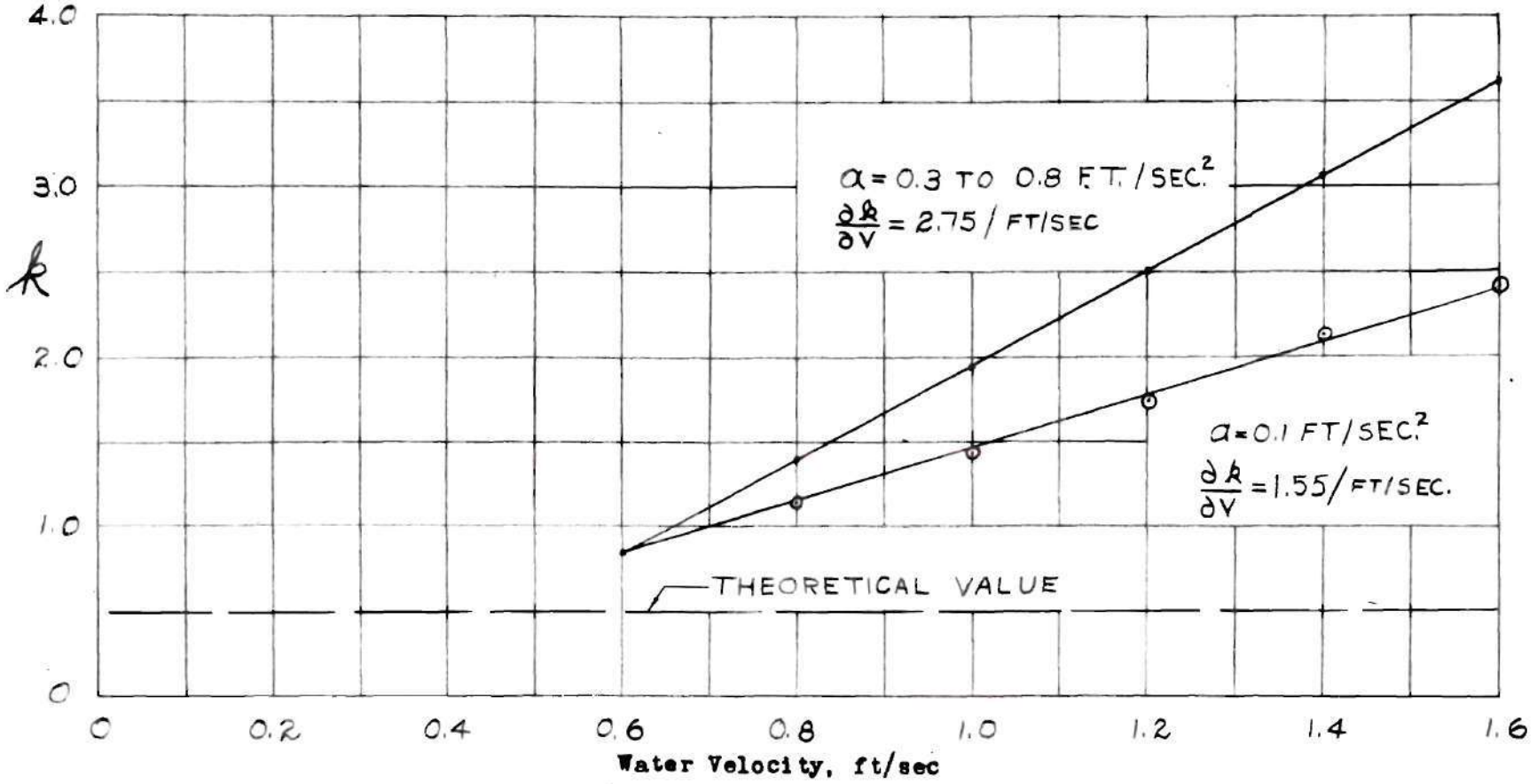


**Figure 20. Variation of Apparent Mass Coefficient of Sphere with Velocity. (Reference 5)**

Figure 21. Variation of Resistance with Velocity for Constant Acceleration of a Sphere. (Reference 5)

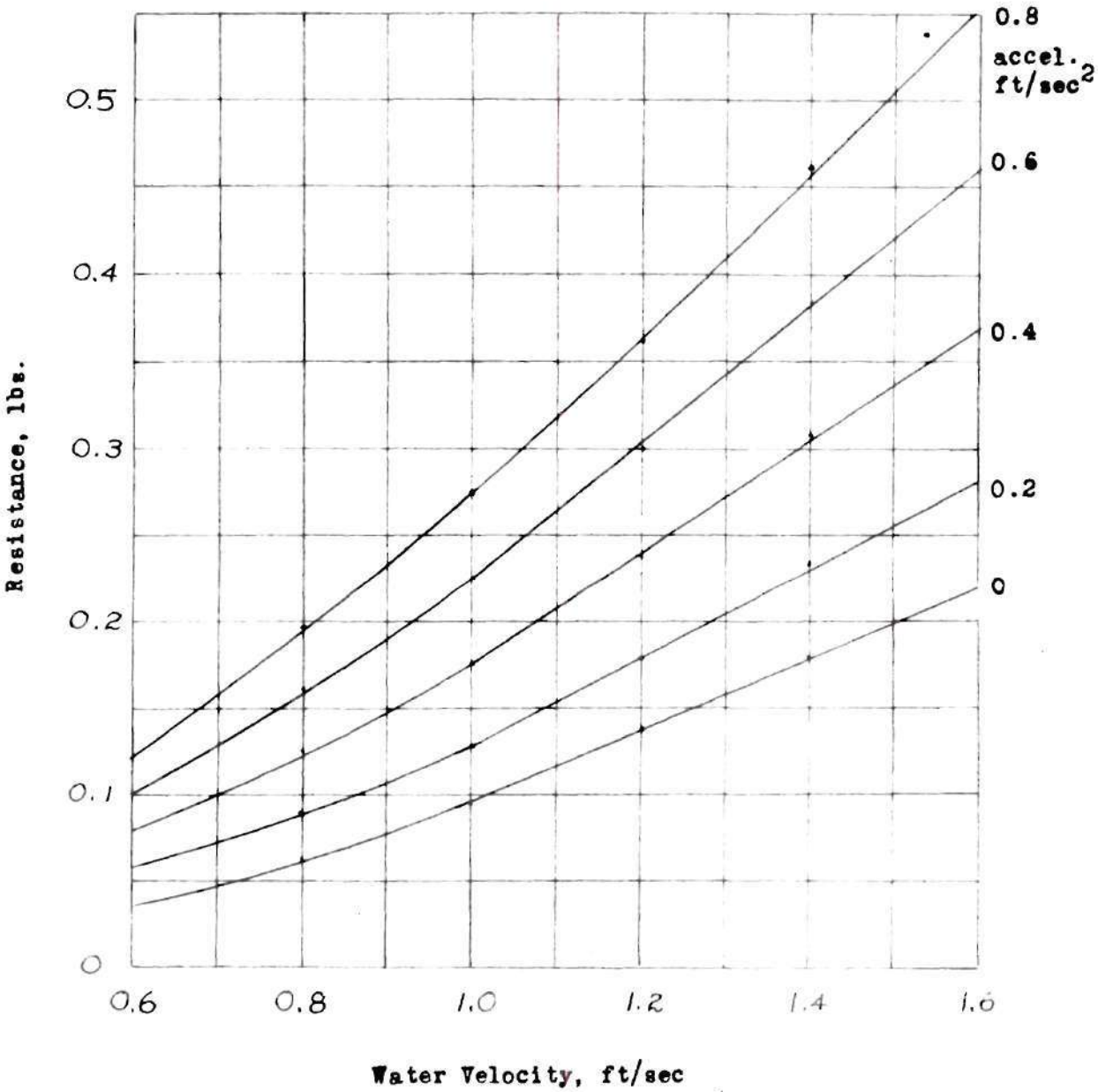

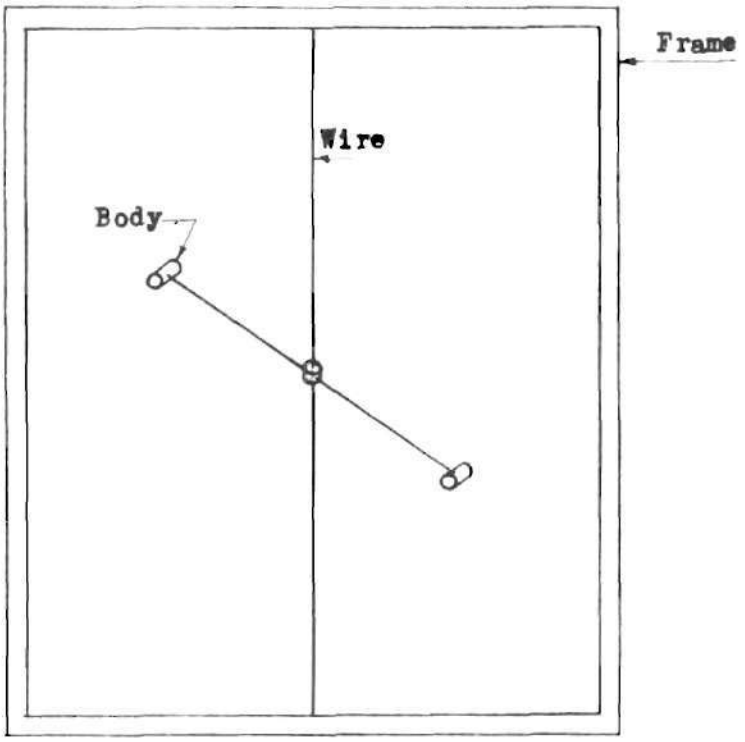


Figure 22. Simple Torsion Pendulum.

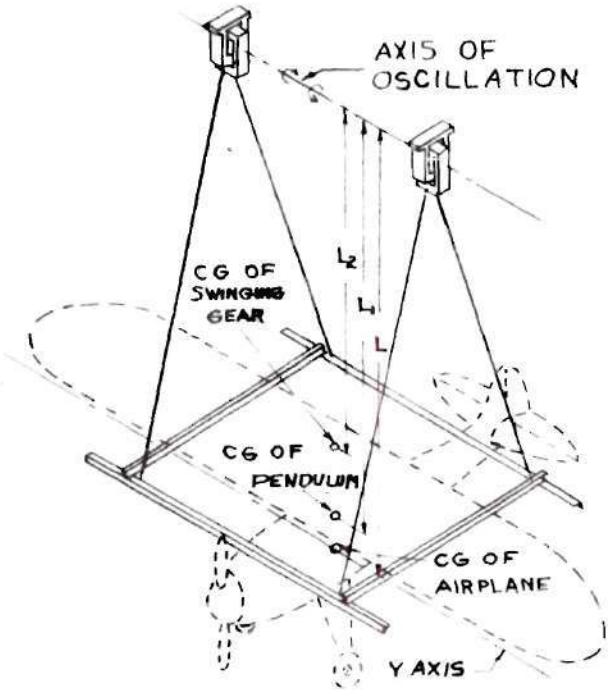


**Figure 23.** Compound-Pendulum Method of Swinging an Airplane. (Reference 12)

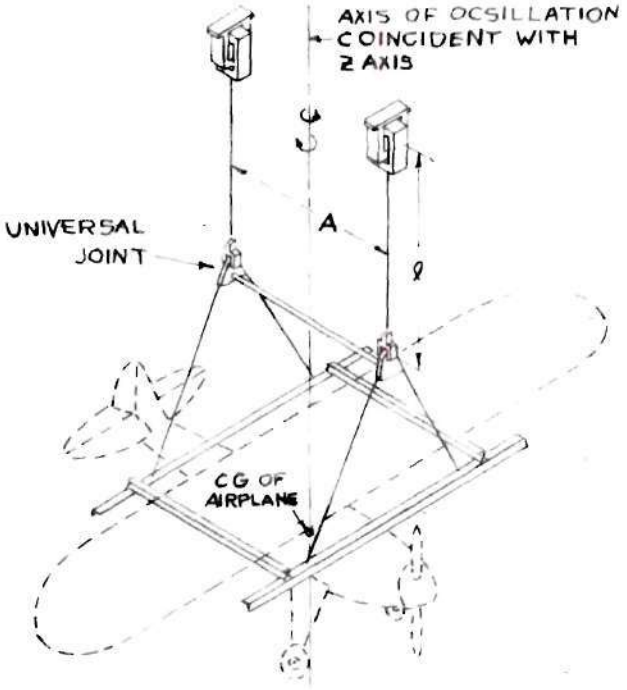


**Figure 24.** Bifilar Torsion Pendulum Method of Swinging an Airplane. (Reference 12)

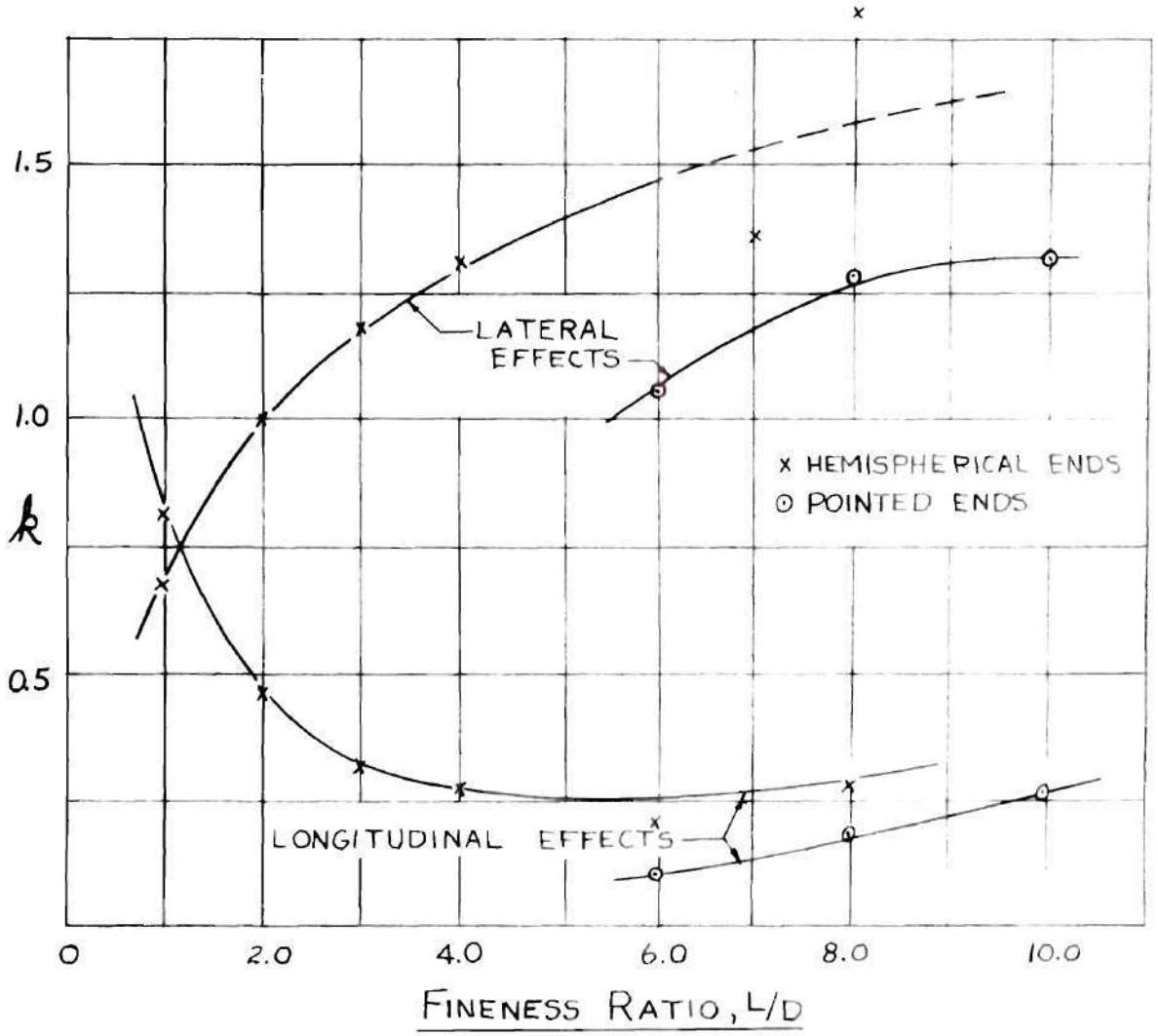


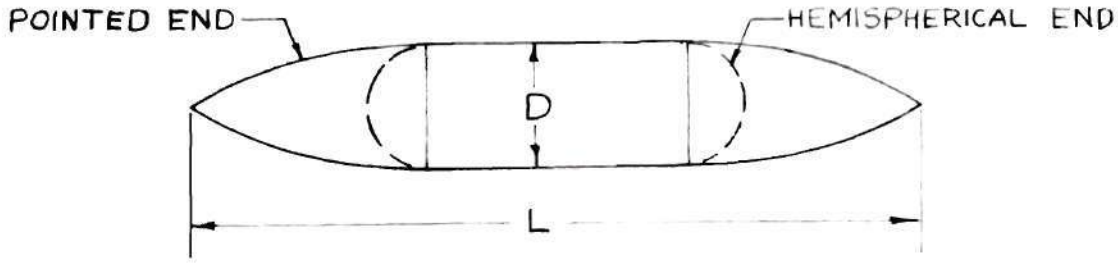


**Figure 25 Effect of Fineness Ratio on Apparent Additional Mass Coefficients. (Reference 11)**

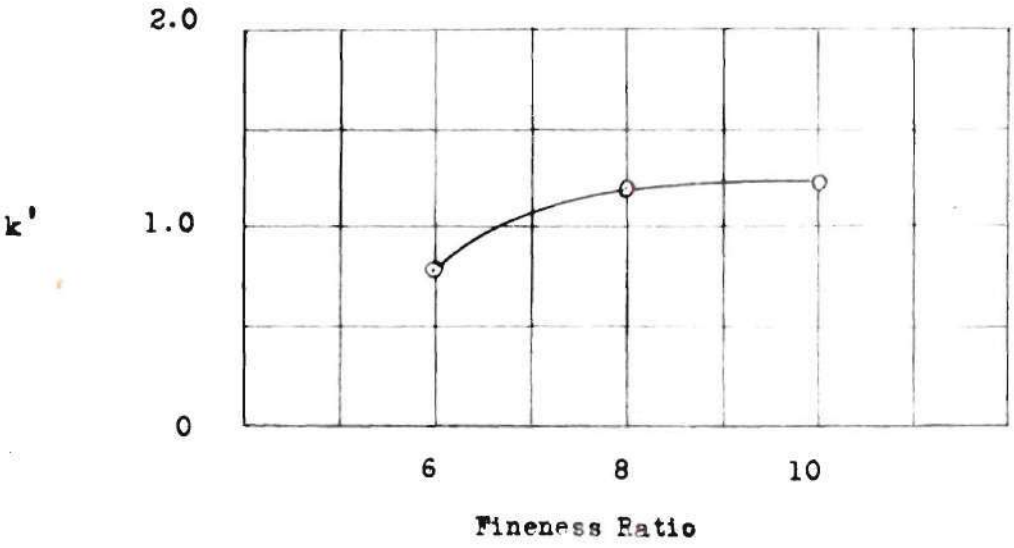


**Figure 26.** Apparent Additional Moment of Inertia About Transverse Axis of Pointed Models. (Reference 11)

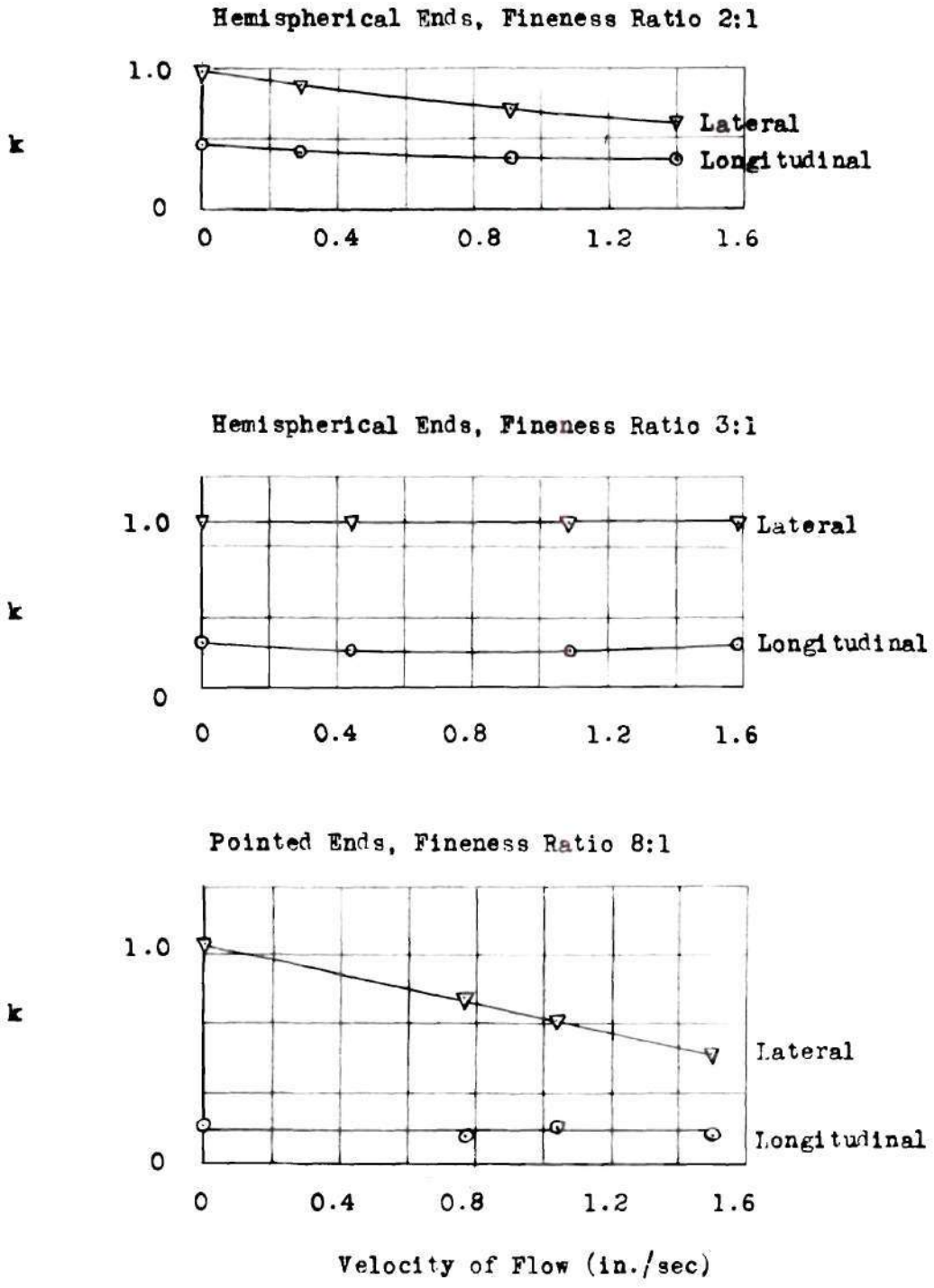


Figure 27. Effect of Uniform Velocity of Surrounding Fluid on Apparent Additional Mass Coefficients as Determined by Free Vibration Tests. (Reference 11)

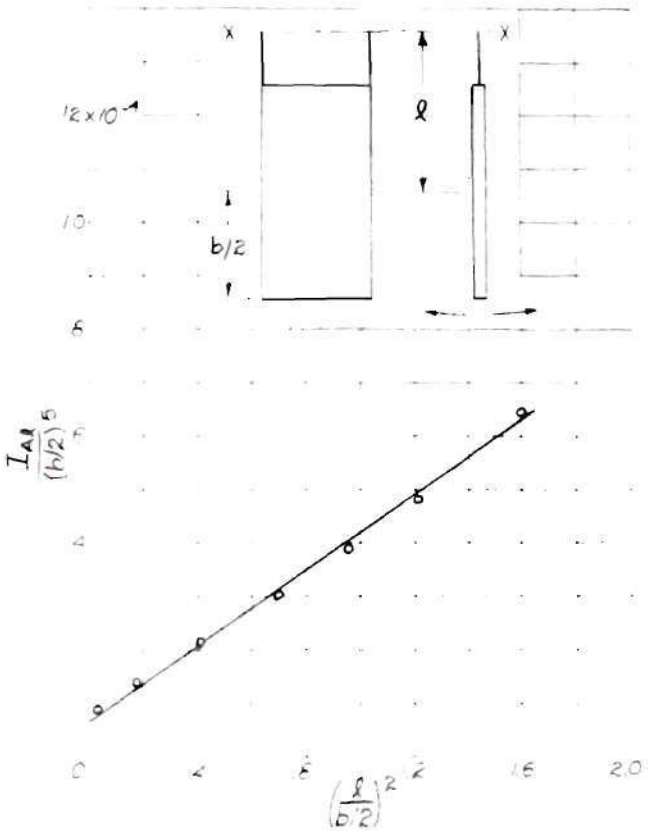


Figure 28. Variation of Apparent Additional Moment of Inertia with Suspension Length. (Reference 4)

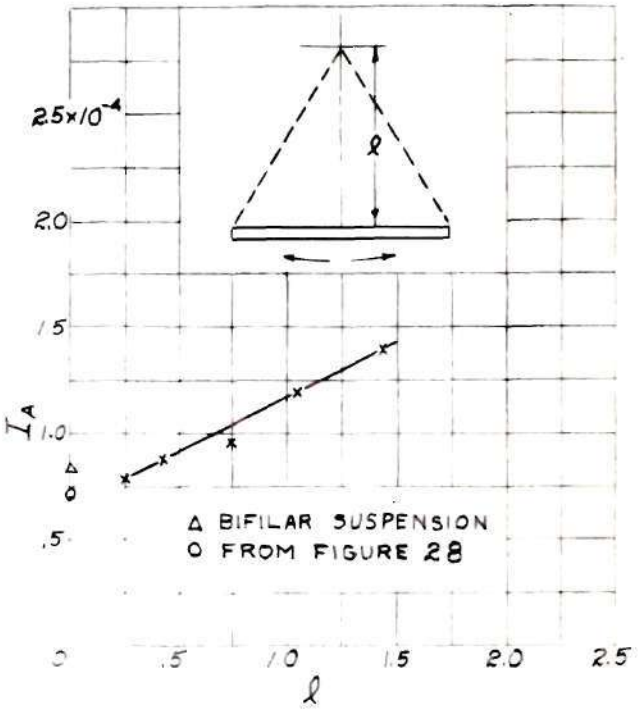


Figure 29. Variation of Apparent Additional Moment of Inertia with Suspension Length. (Reference 4)

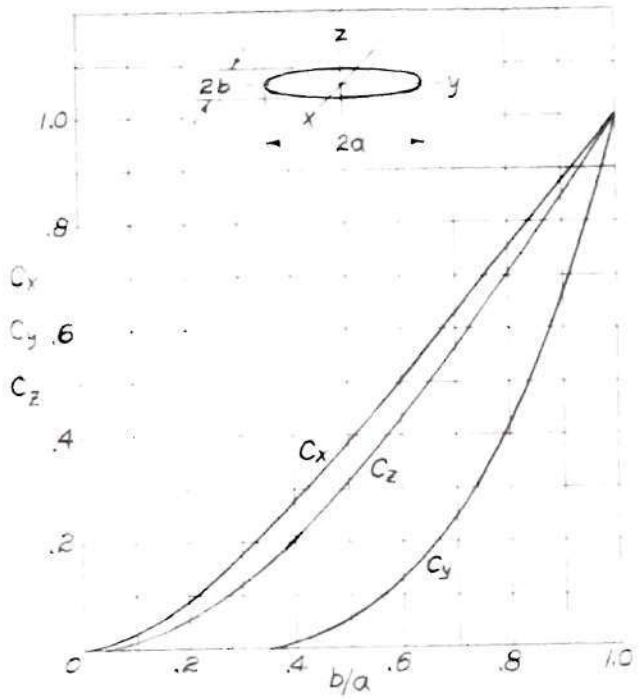


Figure 30. Coefficients of Apparent Additional Mass and Moment of Inertia for Elliptic Plates. (Reference 4)

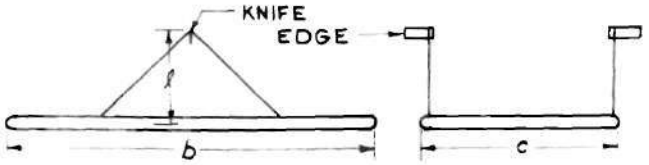


Figure 31. Suspension Method for Apparent Additional Moment of Inertia Tests of Plates. (Reference 4)

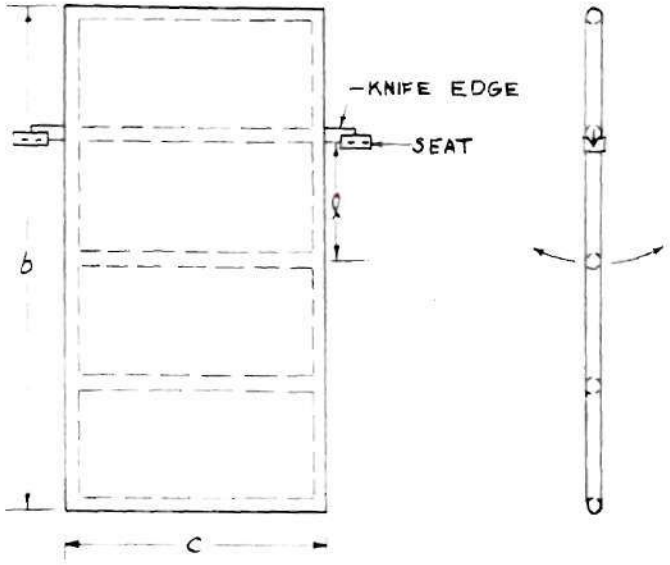


Figure 32. Suspension Method for Apparent Additional Mass Tests of Plates. (Reference 4)

Figure 33. Apparent Additional Moment of Inertia Coefficients for Rectangular Plates. (Reference 4)

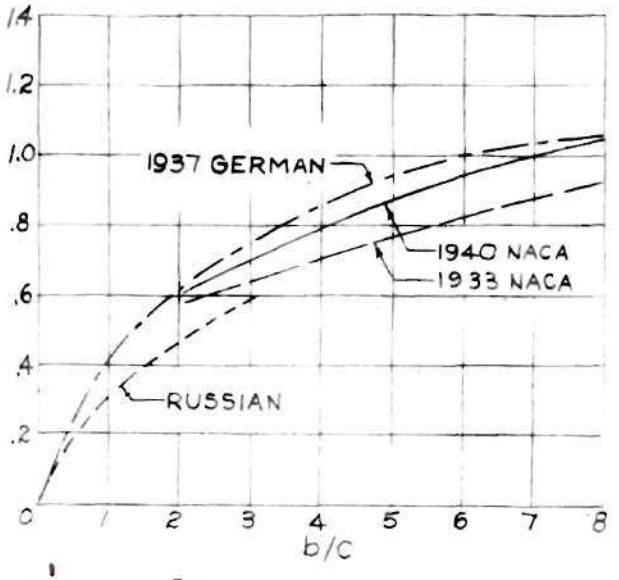


$$K' = \frac{48\, I_A}{\pi \rho c^2 b^2}$$

Figure 34. Apparent Additional Mass Coefficients for Elliptic and Rectangular Plates. (Reference 4)

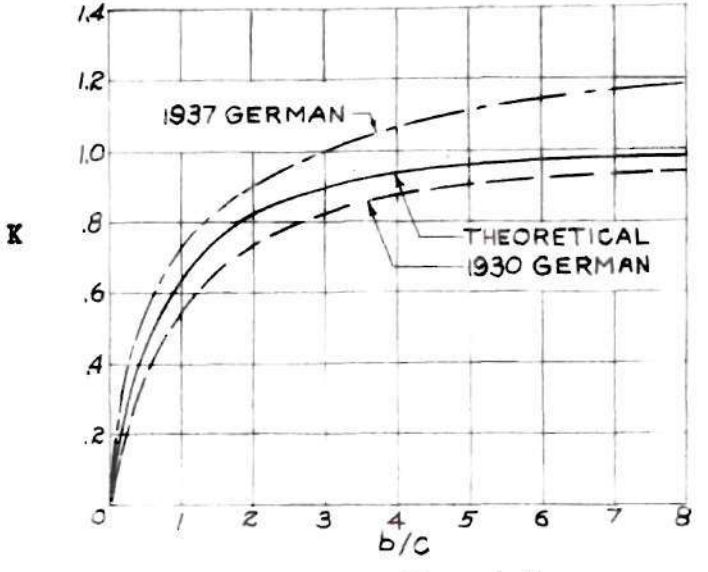


$$K = \frac{4\, m_A}{\pi \rho c^2 b}$$

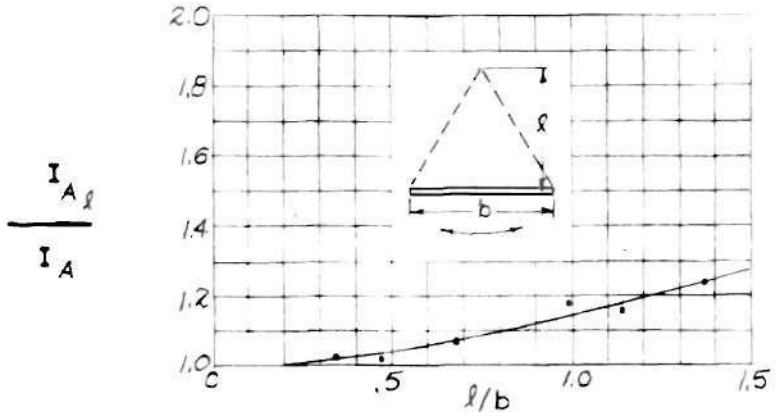


Figure 35 Variation of Apparent Additional Moment of Inertia with Suspension Length. (Reference 4)

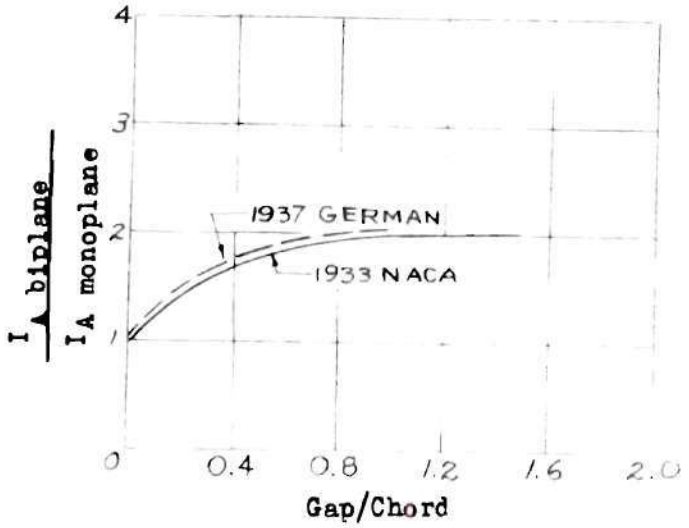


Figure 36. Variation of Apparent Additional Moment of Inertia with Biplane Gap-Chord Ratio. (Reference 4)

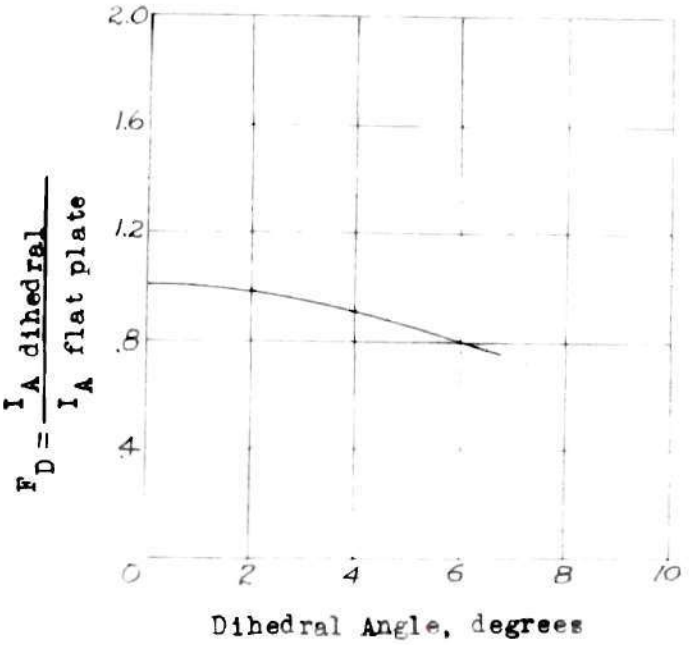


Figure 37. Variation of Apparent Additional Moment of Inertia with Dihedral Angle. (Reference 4)

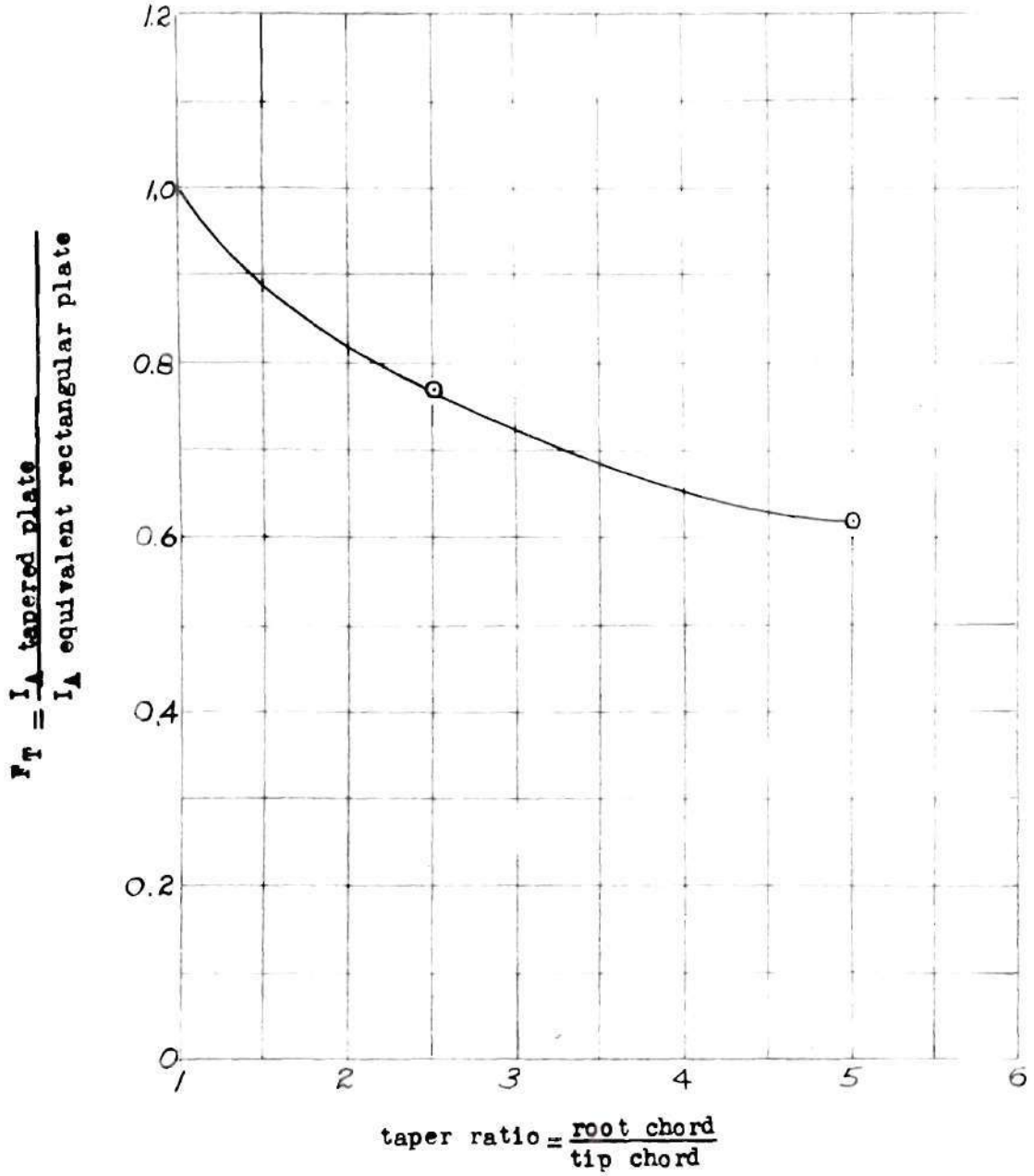


Figure 38. Effect of Taper Ratio on Apparent Additional Moment of Inertia of Plates. (Reference 4)

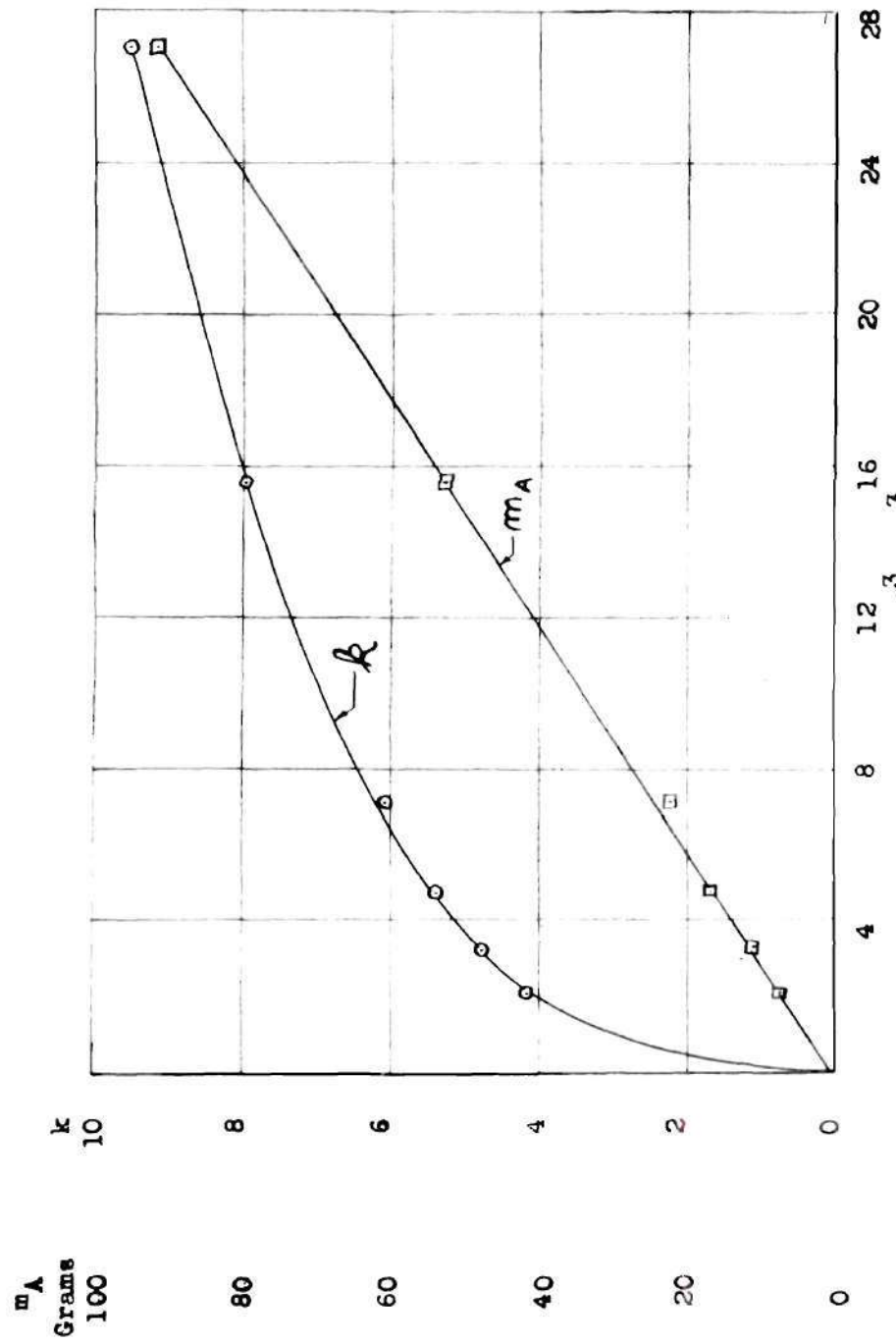


Figure 39. Apparent Additional Mass and Apparent Additional Mass Coefficient of Circular Disk. (Reference 14)

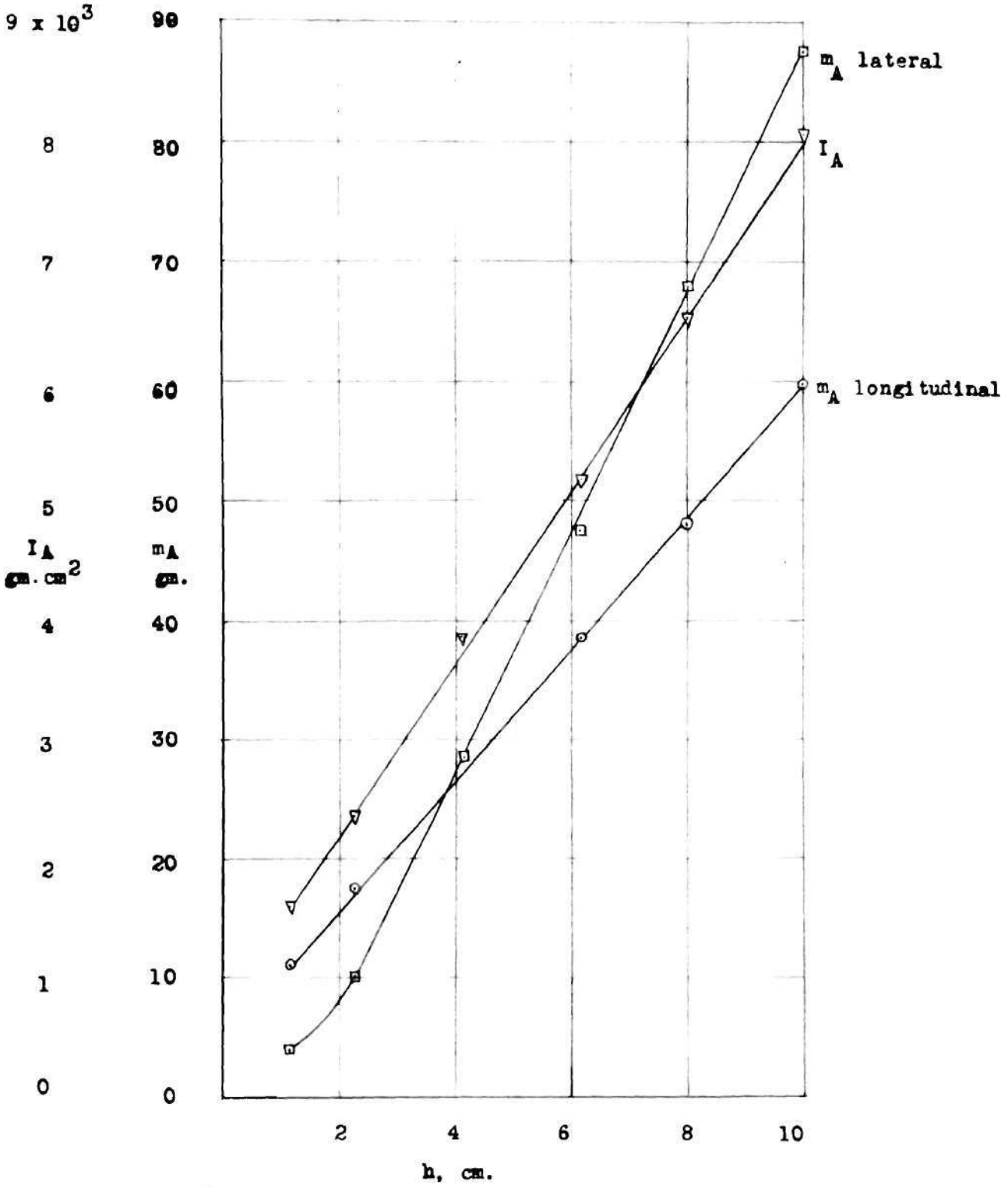


Figure 40. Apparent Additional Moment of Inertia and Mass of Circular Cylinder. (Reference 14)

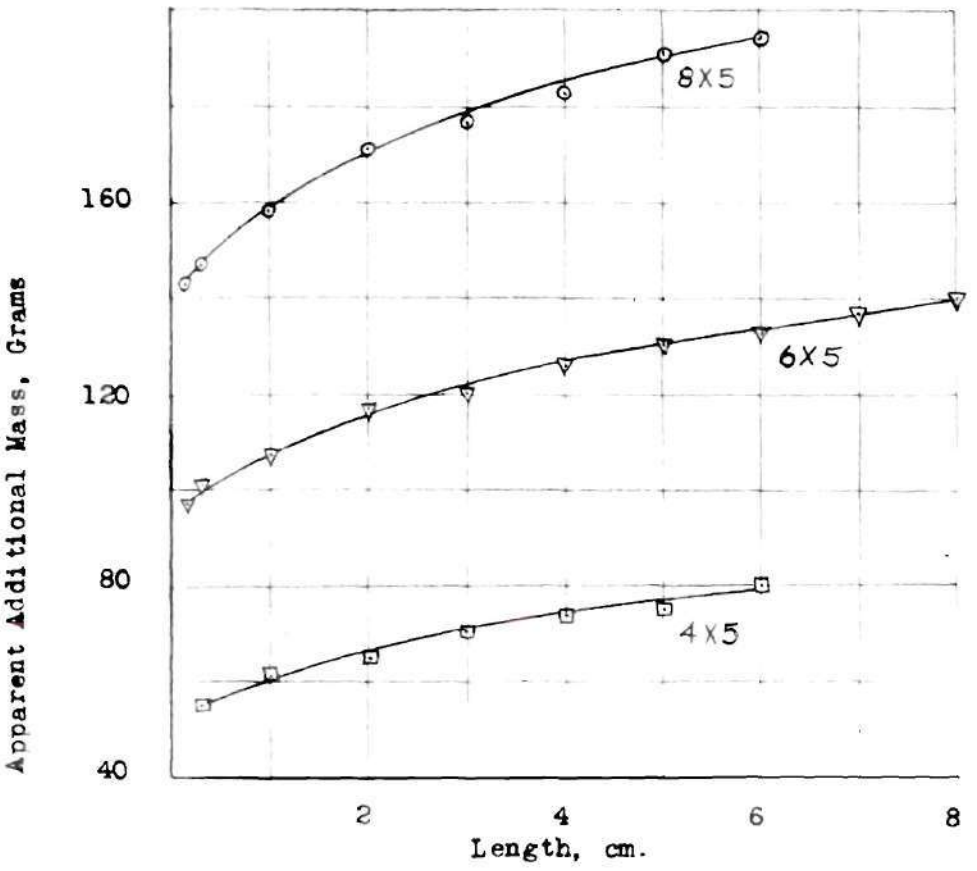


Figure 41. Apparent Additional Mass of Rectangular Parallelepipeds.

(Dimensions under curves refer to area in square centimeters of face normal to direction of motion.) Reference 4.

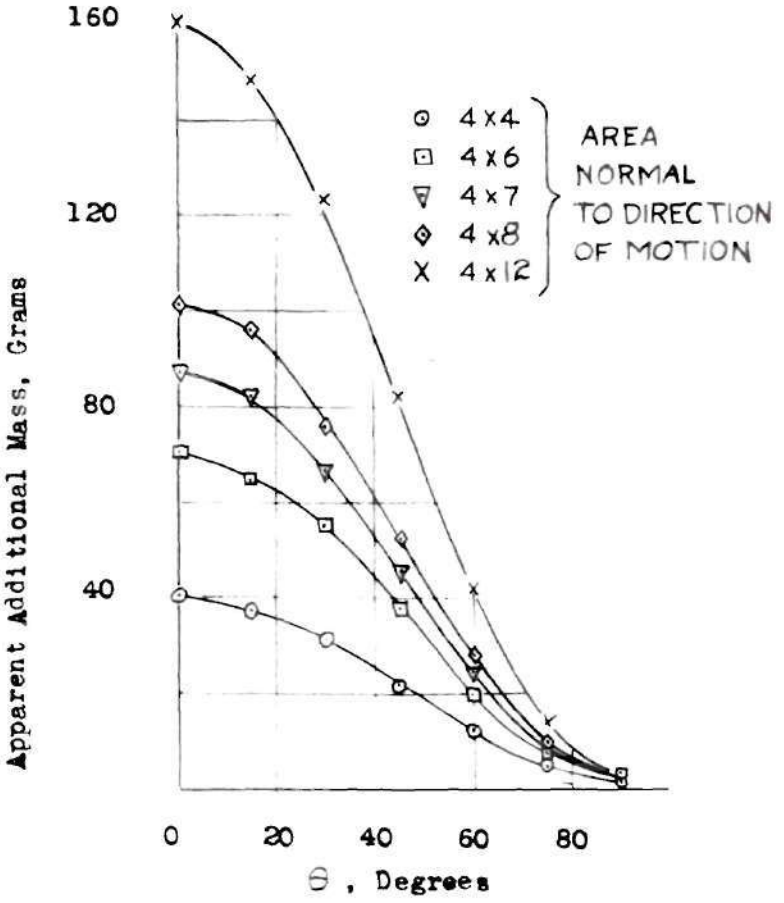


Figure 42. Apparent Additional Mass of Flat Plates

(θ is the angle between the direction of motion and the normal to the plate) Reference 15.

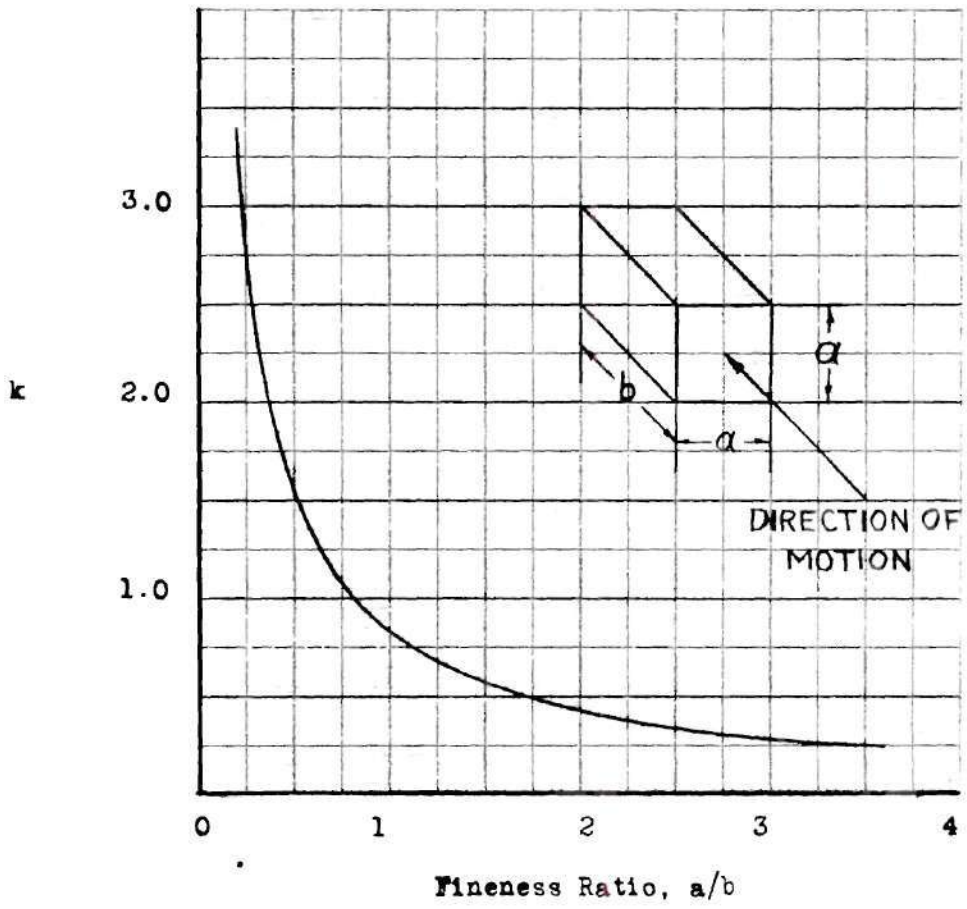


Figure 43. Estimated Apparent Additional Mass Coefficient for Rectangular Parallelepiped.

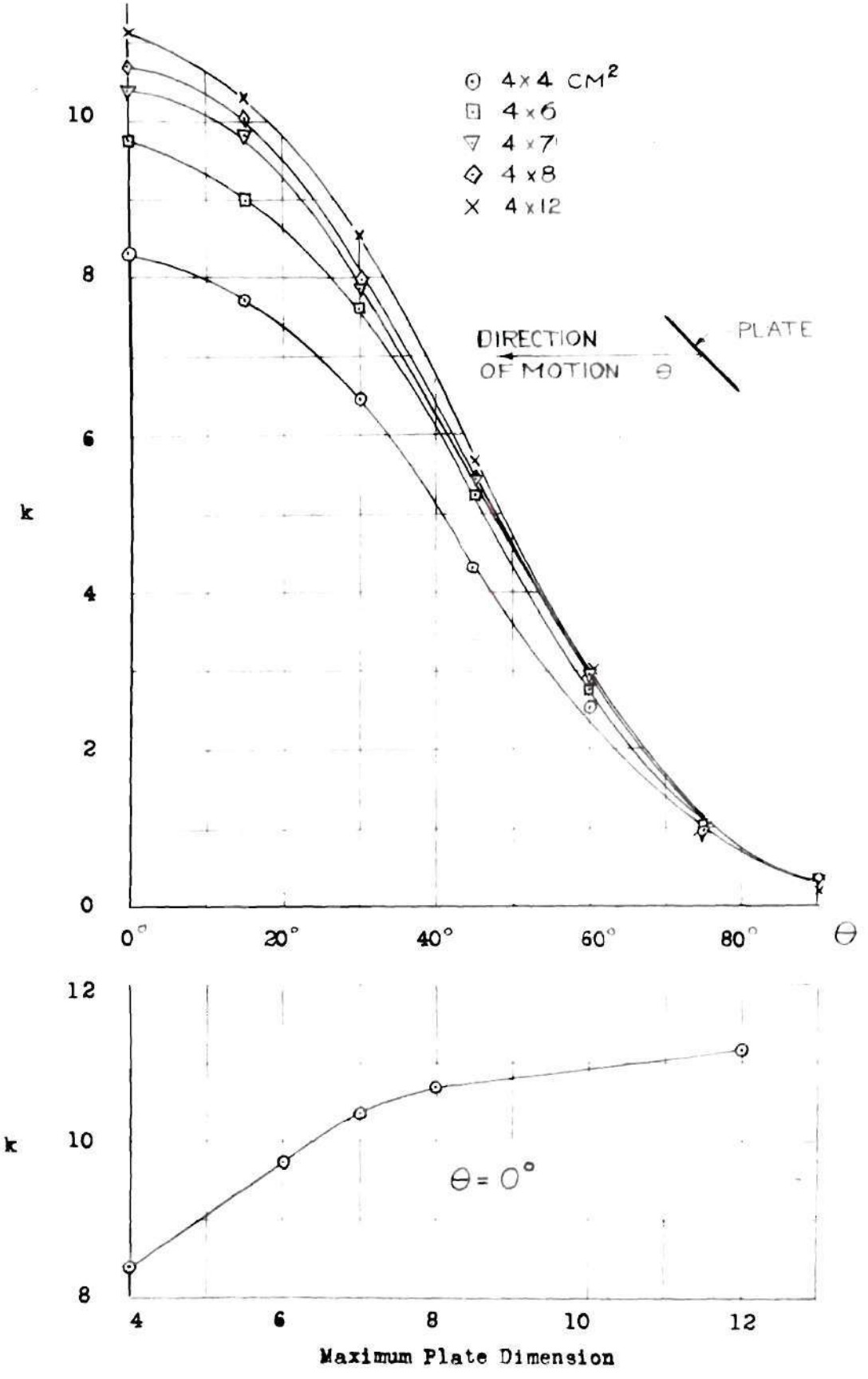


Figure 44. Apparent Additional Mass Coefficient of Flat Plates.

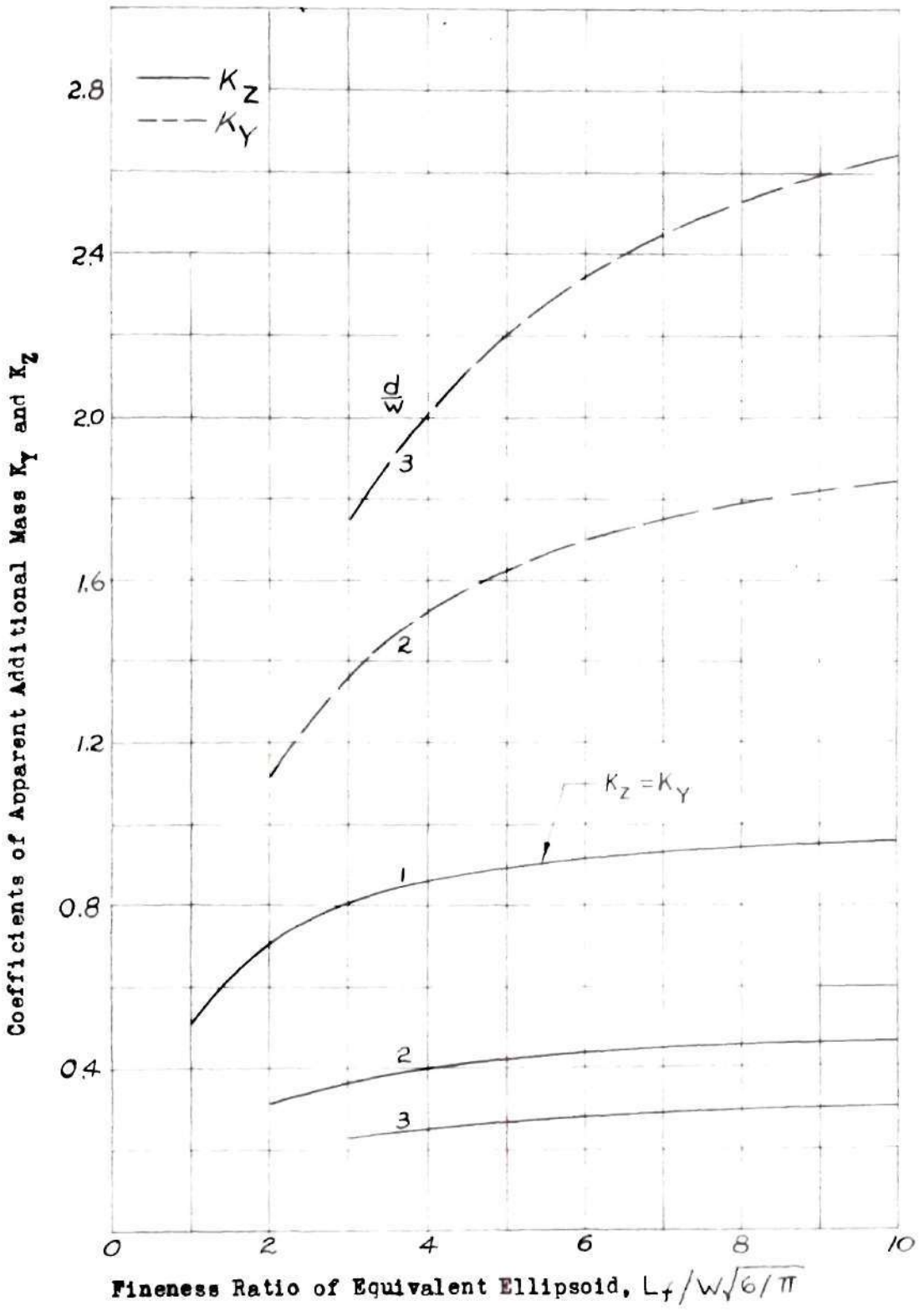


**Figure 45. Variation of Apparent Additional Mass Coefficients with Fineness Ratio of Equivalent Ellipsoid. (Reference 9)**

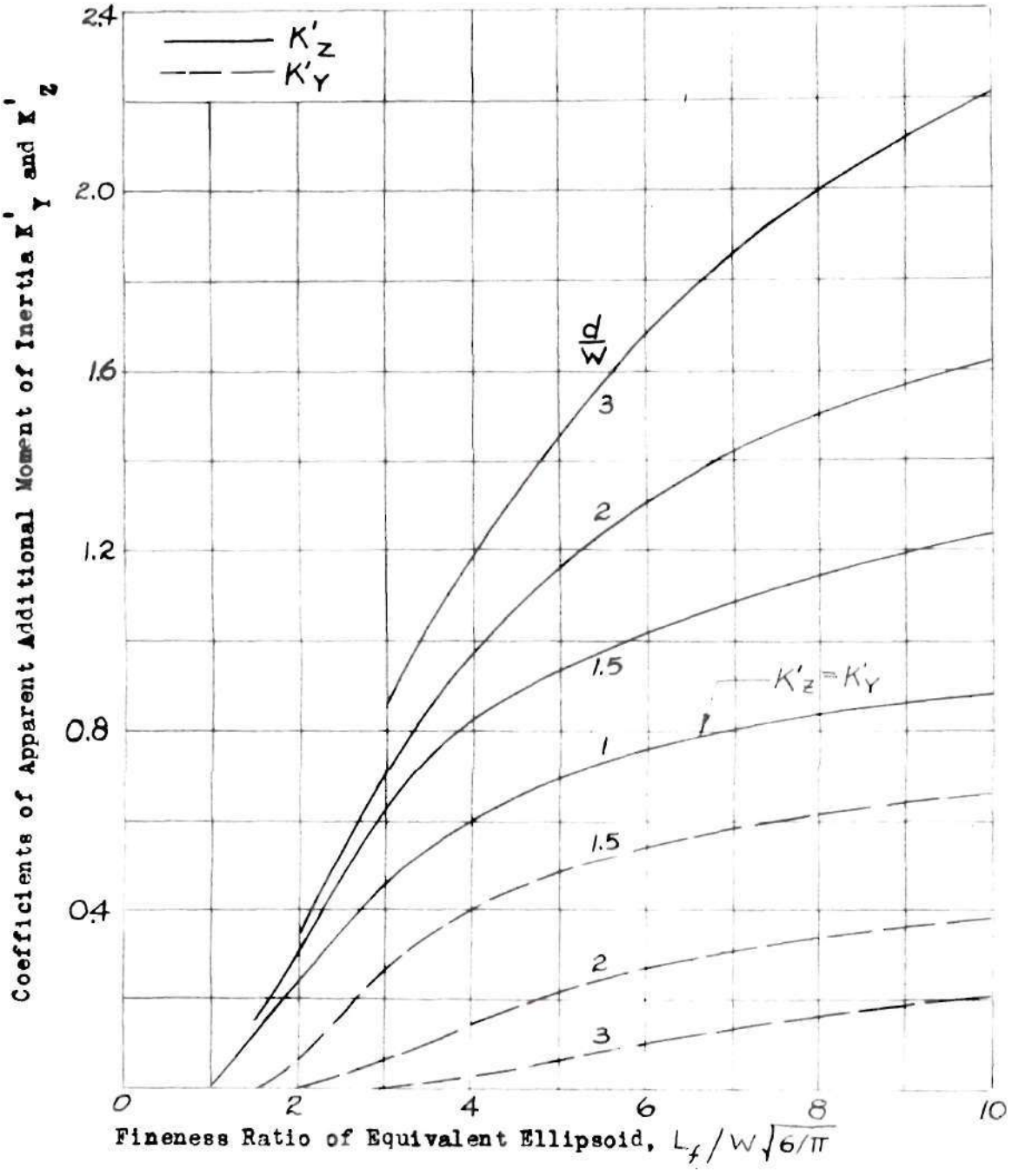


Figure 46. Variation of Apparent Additional Moment of Inertia Coefficients with Fineness Ratio of Equivalent Ellipsoid. (Reference 9)

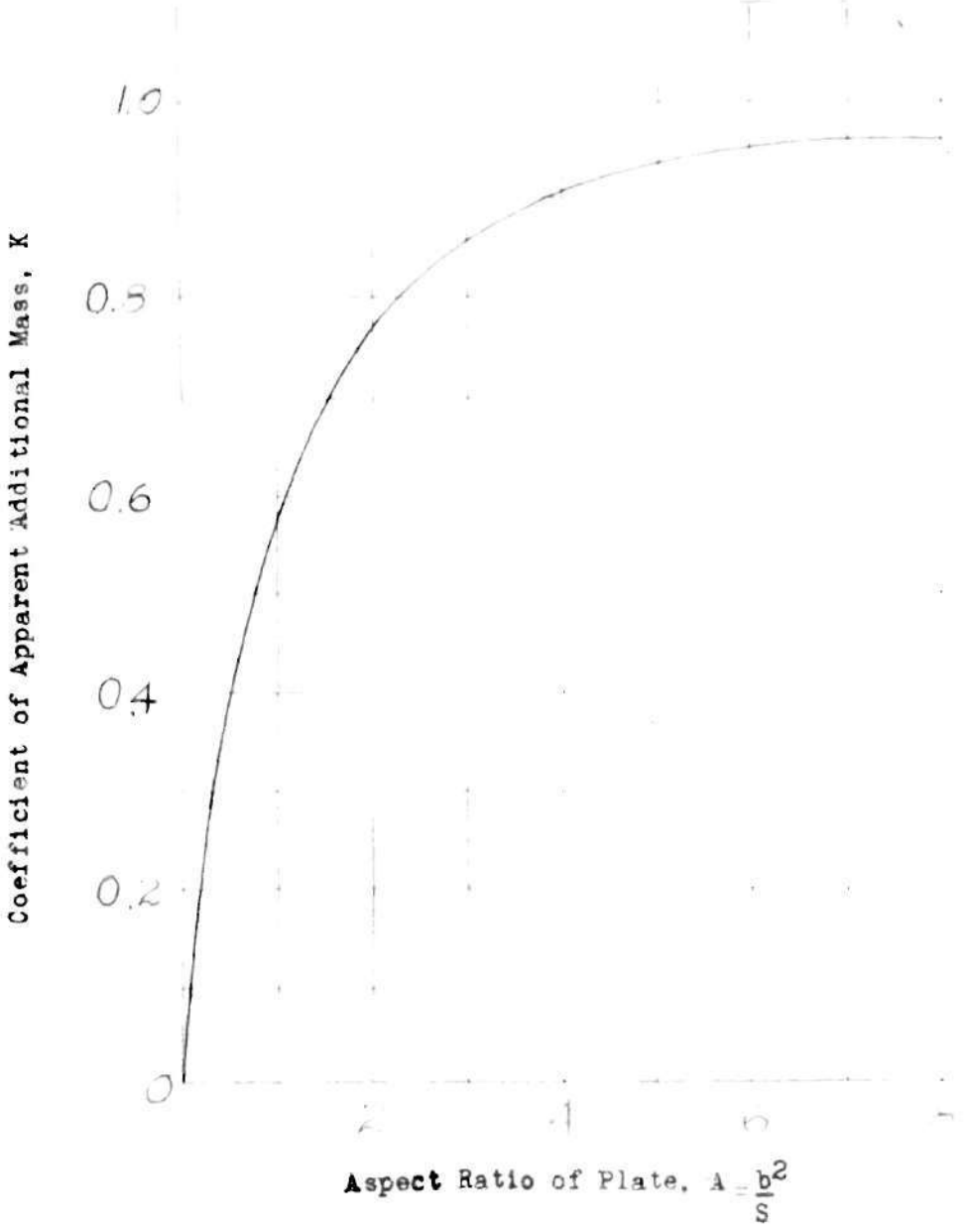


Figure 47. Coefficient of Apparent Additional Mass for Rectangular Plates. Curve is average of NACA 1933 and 1940 tests, (Reference 9)

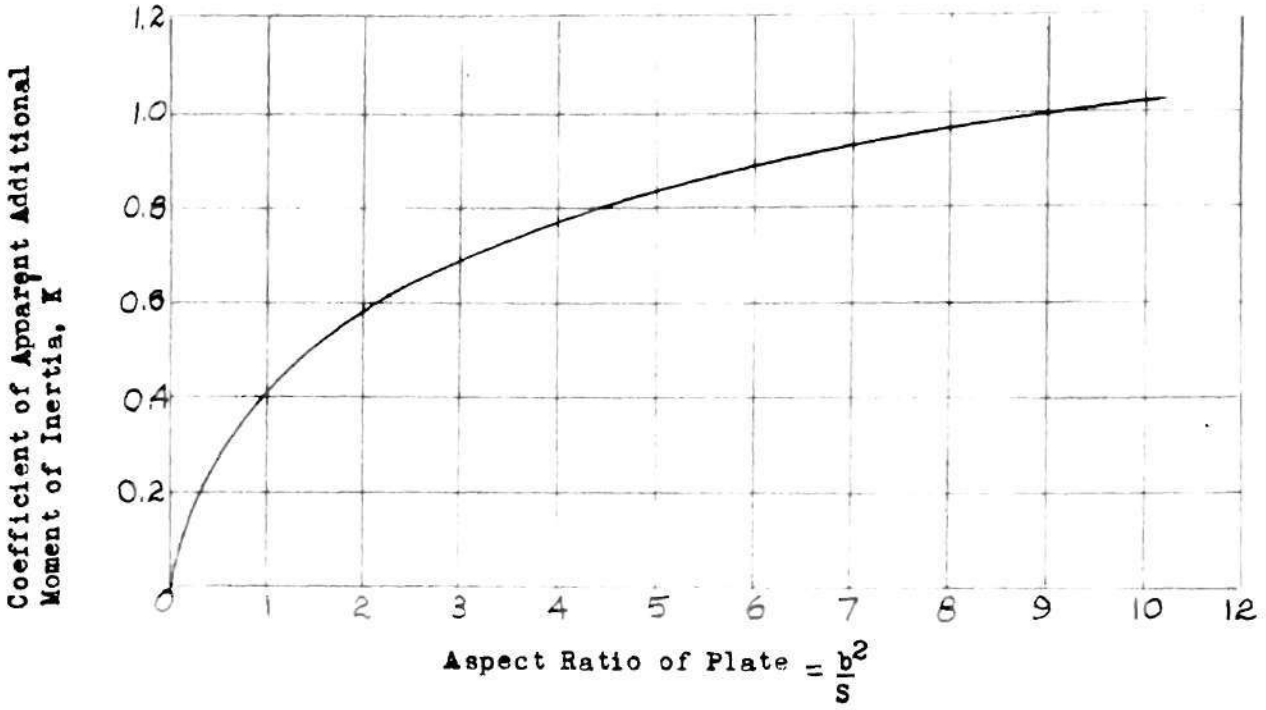


Figure 48. Coefficients of Apparent Additional Moment of Inertia for Rectangular Plates Curve is average of NACA 1933 and 1940 tests. (Reference 9)

# APPENDIX II

## Historical Sketch

About 160 years ago, Chevalier Du Buat discovered, while experimenting with spheres oscillating in water, that it was necessary to attribute to the sphere a mass greater than that of the sphere itself, or that the sphere had an apparent additional mass. Bessel made a similar observation in 1828 while working on the length of the seconds pendulum. He represented the increase of inertia by a mass, k times the mass of the displaced fluid. Swinging spherical pendulums in air and in water, he obtained values of k of approximately 0.9 and 0.6, respectively. Du Buat's experiments in water gave k = 0.585.

Sabine found the effects of hydrogen and air on the times of vibration were in the ratio of 1:5.25, and not in the ratio of the densities of the gases, as might be expected. Baily followed Sabine's experiments with experiments of spherical and cylindrical bobs of various sizes.

The mathematical study of the phenomenon was started by Poisson, who disregarded the viscosity of the fluid and obtained a value $k = 1/2$ for the sphere. This result was later confirmed by Green, Plana, Stokes, and Lamb, each using different methods. Both Du Buat and Sabine had suggested that the viscosity should be taken into consideration, and this seems reasonable, since the fluid does adhere to the body.

Stokes made a study of the effect of viscosity on the oscillations of a pendulum and obtained a correction to Poisson's formula which increases k and brings it into closer agreement with the values obtained by Baily and Du Buat. It is of interest to note that at this point Stokes suggested that the pendulum oscillations might be used to determine the viscosity of a gas. His experiments were reasonably successful in the

case of air, but such was not the case when the fluid was water because of the difficulty of making observations. McEwen, working with oil and water, obtained a better agreement.

Later, experiments were made by McEwen, Barnes and Krishnayar on oscillating spheres. The results are not in close agreement, but Krishnayar obtained values of 0.584, 0.585, and 0.580 for k, and these closely agree with Du Buat's value, 0.585. Stokes' theory gave 0.530, 0.536, and 0.530, respectively. Cook dropped a large sphere down a mine shaft and obtained a value $k = 0.46$, which disagrees with values obtained by the pendulum method. The fact that k is greater than $1/2$ for a sphere appeared to substantiate the theory that fluid adheres to the solid.

The important case of an ellipsoid in an infinite fluid was worked out by Green and computed by Lamb. Stokes learned that $k = 1$ for a cylinder with its axies perpendicular to the motion and that for a sphere oscillating in a spherical vessel filled with fluid the effect of the boundary is not negligible, as Poisson thought.

Taylor confirmed this conclusion for other boundaries, which limited the fluid about an immersed body. He found that a rigid boundary increases inertia.

After some decline in interest, the question of airship stability and performance became important. This led to a revival of work on apparent additional mass, since the apparent additional mass is such a large percent of the virtual mass of an airship. Munk was especially active in this work. Later, it was realized that the apparent additional effects must be taken into consideration for any accelerated motion where accurate

predictions are desired. This leads to the present day work already discussed in this paper.

The problem of apparent additional mass in a compressible fluid has not, to the author's knowledge, been investigated.

# APPENDIX III

## Green's Paper

Presented below is a copy of Green's original paper as published by the Royal Society of Edinburgh in 1836. This paper is presented here not only because of its historical interest, but also because it is the fundamental basis for a great portion of the later work concerning apparent additional effects.

The original paper contained several typographical errors. These have been noted and corrected.

---

Researches on the Vibration of Pendulums in Fluid Media. By George Green, Esq. Communicated by Sir Edward Ffrench Bromhead, Bart. M.A. F.R.SS. Lond. & Ed. (Read 16th Dec. 1833)

Probably no department of Analytical Mechanics presents greater difficulties than that which treats of the motions of fluids; and hitherto the success of mathematicians therein has been comparatively limited. In the theory of the waves, as presented by M. M. Poisson and Cauchy, and in that of sound, their success appears to have been more complete than elsewhere; and if to these investigations we join the researches of Laplace concerning the tides, we shall have the principal important applications hitherto made of the general equations upon which the determination of this kind of motion depends. The same equations will serve to resolve completely a particular case of the motions of fluids, which is capable of a useful practical application; and, as I am not aware that it has yet been noticed, I shall endeavour, in the following paper, to consider it as briefly as possible.

In the case just alluded to, it is required to determine the circumstances of the motion of an indefinitely extended non-elastic fluid, when agitated by a solid ellipsoidal body, moving parallel to itself, according to any given law, always supposing the body's excursions very small, compared with its dimensions. From what will be shown in the sequal, the general solution of this problem may very easily be obtained. But as the principal object of our paper is to determine the alteration produced in the motion of a pendulum by the action of the surrounding medium, we have insisted more particularly on the case where the ellipsoid moves in a right line parallel to one of its axes, and have thence proved, that, in order to obtain the correct time of a pendulum's vibration, it will not be sufficient merely to allow for the loss of weight caused by the fluid medium, but that it will likewise be requisite to conceive the density of the body augmented by a quantity proportional to the density of this fluid. The value of the quantity last named, when the body of the pendulum is an oblate spheroid, vibrating in its equatorical plane, has been completely determined, and, when the spheroid becomes a sphere, is precisely equal to half the density of the surrounding fluid. Hence in this case, we shall have the true time of the pendulum's vibration, if we suppose it to move "in vacuo", and then simply conceive its mass augmented by half that of an equal volume of the fluid, whilst the moving force with which it is actuated is diminished by the whole weight of the same volume of fluid.

We will now proceed to consider a particular case of the motion of a non-elastic fluid over a fixed obstacle of ellipsoidal figure, and thence endeavour to find the correction necessary to reduce the observed length of a pendulum vibrating through exceedingly small arcs in any indefinitely extended medium to its true length "in vacuo", when the body of the pendulum is a solid ellipsoid. For this purpose, we may, remark, that the equations of the motion of a homogeneous non-elastic fluid are

$$V - \frac{p}{\rho} = \frac{d\phi}{dt} + \frac{1}{2}\left\{\left(\frac{d\phi}{dx}\right)^2 + \left(\frac{d\phi}{dy}\right)^2 + \left(\frac{d\phi}{dz}\right)^2\right\} \qquad (1)$$

$$0 = \frac{d^2\phi}{dx^2} + \frac{d^2\phi}{dy^2} + \frac{d^2\phi}{dz^2} \qquad (2)$$

Vide. Mec. Cel. Liv. iii. Ch. 8. No. 33, where $\phi$ is such a function of the coordinates x, y, z of any particle of the fluid mass, and of the time t that the velocities of this particle in the directions of and tending to increase the coordinates x, y, and z shall always be represented by $\frac{d\phi}{dx}, \frac{d\phi}{dy}$, and $\frac{d\phi}{dz}$ respectively. Moreover, $\rho$ represents the fluid's density, p its pressure, and V a function dependent upon the various forces which act upon the fluid mass.

When the fluid is supposed to move over a fixed solid ellipsoid, the principal difficulty will be so to satisfy the equation (2) that the particles at the surface of this solid may move along this surface, which may be effected by making

$$\phi = \left(\lambda + \mu \int_{\infty} \frac{df}{a^3 bc}\right) \chi \; * \qquad (3)$$

supposing that the origin of the coordinate is at the centre of the ellipsoid: $\lambda$ and $\mu$ being two arbitrary quantities constant with regard to the variables x, y, z; and a, b, c, $f$ being functions of these same variables determined by the equations

$$a^2 = a'^2 + f, \; b^2 = b'^2 + f, \text{ and } \frac{x^2}{a^2} + \frac{y^2}{b^2} + \frac{z^2}{c^2} = 1 \qquad (4)$$

in which a', b', c' are the axes of the given ellipsoid.

To prove the expression (3) satisfies the equation (2), it may be remarked, that we readily get, by differentiating (3)

$$\frac{d^2\phi}{dx^2} + \frac{d^2\phi}{dy^2} + \frac{d^2\phi}{dz^2} = \frac{2\mu}{a^3bc}\frac{df}{dx} + \frac{\mu\chi}{a^3bc}\left(\frac{d^2f}{dx^2} + \frac{d^2f}{dy^2} + \frac{d^2f}{dz^2}\right)$$

$$- \frac{\mu\chi}{a^3bc}\left(\frac{3}{2a^2} + \frac{1}{2b^2} + \frac{1}{2c^2}\right)\left\{\left(\frac{df}{dx}\right)^2 + \left(\frac{df}{dy}\right)^2 + \left(\frac{df}{dz}\right)^2\right\}$$

Moreover, by the same means, the last of the equation (4) gives

---

*In my memoir on the Determination of the exterior and interior Attractions of Ellipsoids of Variable Densities, recently communicated to the Cambridge Philosophical Society by Sir Edward Ffrench Bromhead, Baronet, I have given a method by which the general integral of the partial differential equation $0 = \frac{d^2V}{dx_1^2} + \frac{d^2V}{dx_2^2} + \ldots\ldots \frac{d^2V}{dx_s^2} + \frac{d^2V}{du^2} + \frac{m-s}{u}\frac{dV}{du}$ may be expanded in a series of a peculiar form, and have thus rendered the determination of these attractions a matter of comparative facility. The same method applied to the equation (2) of the present paper, has the advantage of giving an expansion of its general integral, every term of

$$\frac{df}{dx} = \frac{\frac{2x}{a^2}}{\frac{x^2}{a^4} + \frac{y^2}{b^4} + \frac{z^2}{c^4}}, \quad \left(\frac{df}{dx}\right)^2 + \left(\frac{df}{dy}\right)^2 + \left(\frac{df}{dz}\right)^2 = \frac{4}{\frac{x^2}{a^4} + \frac{y^2}{b^4} + \frac{z^2}{c^4}}$$

$$\text{AND} \quad \frac{d^2f}{dx^2} + \frac{d^2f}{dy^2} + \frac{d^2f}{dz^2} = \frac{\frac{2}{a^2} + \frac{2}{b^2} + \frac{2}{c^2}}{\frac{x^2}{a^4} + \frac{y^2}{b^4} + \frac{z^2}{c^4}}$$

which values being substituted in the second member of the preceding equation, evidently cause it to vanish, and we thus perceive that the value (3) satisfies the partial differential equation (2).

We will now endeavour so to determine the constant quantities $\lambda$ and $\mu$ that the fluid particles may move along the surface of the ellipsoidal body of which the equation is

$$1 = \frac{x^2}{a^2} + \frac{y^2}{b^2} + \frac{z^2}{c^2} \qquad (5)$$

By differentiation, there results

$$0 = \frac{x\,dx}{a'^2} + \frac{y\,dy}{b'^2} + \frac{z\,dz}{c'^2}$$

And as the particles must move along the surface, it is clear that the last equation ought to subsist, when we change the elements dx, dy, and dz into their corresponding velocities $\frac{d\phi}{dx}$, $\frac{d\phi}{dy}$, and $\frac{d\phi}{dz}$. Hence, at this surface,

---

which, besides satisfying this equation, may likewise be made to satisfy the conditon (6). The formula (3) is only an individual term of the expansion in question. But in order to render the present communication independent of every other, it was thought advisable to introduce into the text a demonstration of this particular case.

$$O = \frac{X}{a'^2}\frac{d\phi}{dx} + \frac{y}{b'^2}\frac{d\phi}{dy} + \frac{z}{c'^2}\frac{d\phi}{dz} \qquad (6)$$

But the expression (3) gives generaly

$$\frac{d\phi}{dx} = \lambda + \mu\int_\infty \frac{df}{a^3bc} + \frac{\mu x}{a^3bc}\frac{df}{dx}, \frac{d\phi}{dy} = \frac{\mu y}{a^3bc}\frac{df}{dy}, \frac{d\phi}{dz} = \frac{\mu z}{a^3bc}\frac{df}{dz} \qquad (7)$$

and consequently, at the surface in question $f = 0$.

$$\frac{d\phi}{dx} = \lambda + \mu\int_\infty \frac{df}{a^3bc} + \frac{\mu x}{a'^3b'c'}\frac{df}{dx}, \frac{d\phi}{dy} = \frac{\mu y}{a'^3b'c'}\frac{df}{dy}, \frac{d\phi}{dz} = \frac{\mu z}{a'^3b'c'}\frac{df}{dz}$$

These values, substituted in (6) gives, when we replace $\frac{df}{dx}$, $\frac{df}{dy}$, and $\frac{df}{dz}$ with their values at the ellipsoidal surface

$$O = \lambda + \mu\int_\infty^\circ \frac{df}{a^3bc} + \frac{2\mu}{a'b'c'} \qquad (8)$$

which may always be satisfied by a proper determination of one of the constants $\lambda$ and $\mu$, the other remaining entirely arbitrary.

From what precedes, it is clear, that the equation (2), and condition to which the fluid is subject, may equally well be satisfied by making

$$\phi = \left(\lambda' + \mu'\int_\infty \frac{df}{ab^3c}\right)y \quad \text{AND} \quad \phi = \lambda'' + \mu''\int_\infty^\circ \frac{df}{abc^3} + \frac{2\mu''}{a'b'c'}$$

respectively. The same may likewise be said of the sum of the three values of $\phi$ before given. However, in what follows, we shall consider the value (3) only, since, from the results thus obtained, similar ones relative to the cases just enumerated may be found without the least difficulty.

Instead now of supposing the solid at rest, let every part of the whole system be animated with an additional common velocity $-\lambda$ in the direction of the coordinate x. Then it is clear, that the equation (2), and condition to which the fluid is subject, will still remain satisfied. Moreover, if x', y', z' are now referred to the three axes fixed in space, we shall have

$$x' = x - \int \lambda dt, \quad y = y', \quad z = z'$$

and if X' represents the coordinate of the centre of the ellipsoid referred to the fixed origin, we have

$$X' = -\int \lambda dt \qquad (9)$$

Adding now to the term - x due to the additional velocity, the expression (3) will then become

$$\phi = \mu x \int_{\infty} \frac{df}{a^3 bc}$$

and the velocities of any point of the fluid will be given, by means of the differentials of this last function. But $\phi$ and its differentials evidently vanish at an infinite distance from the solid, where $f = \infty$; and consequently, the case now under consideration is that of an

indefinitely extended fluid, of which the exterior limits are at rest, whilst the parts in the vicinity of the moving body are agitated by its motions.

It will now be requisite to determine the pressure p at any point of the fluid mass. But, by supposing, this mass free from all extraneous action V = 0, and if the excursions of the solid are always exceedingly small, compared with its dimensions, the last term of the second member of the equation (1) may evidently be neglected, and thus we shall have, without sensible error

$$-\frac{p}{\varrho} = \frac{d\phi}{dt} \qquad i.e. \qquad p = -\varrho\frac{d\phi}{dt}$$

or, by substitution from the last value of $\phi$

$$p = -\frac{d\mu}{dt}\varrho x\int_{\infty}\frac{df}{a^3bc}$$

Having thus ascertained all the circumstances of the fluid's motion, let us now calculate its total action upon the moving solid. Then the pressure upon any point on its surface will be had by making $f = 0$ in the last expression, and is

$$p_o = -\frac{d\mu}{dt}\varrho x\int^{o}\frac{df}{a^3bc}$$

Hence we may readily get for the total pressure on the body tending to increase, x

$$P = \int ds (p_o' - p_o'') = \frac{d\mu}{dt} \int_\infty \frac{df}{a^3 bc} x \int 2x ds = \frac{d\mu}{dt} \rho v \int_\infty^o \frac{df}{a^3 bc}$$

v representing the volume of the body, $p_o''$ the pressure on the side where x is positive, $p_o'$ the pressure on the opposite side, and ds an element of the principal section of the ellipsoid perpendicular to the axis of x.

If now we substitute for $\mu$ its value given from (8), the last expression will become

$$P = \frac{a'b'c' \int_o^\infty \frac{df}{a^3 bc}}{2 - a'b'c' \int_o^\infty \frac{df}{a^3 bc}} , \frac{d\lambda}{dt} \qquad (10)$$

Having thus the total pressure exerted upon the moving body by the surrounding medium, it will be easy thence to determine the law of its vibrations when acted upon by an exterior force proportional to the distance of its centre from the point of repose. In fact let $\rho_1$ be the density of the body, and, consequently, $\rho_1$ v its mass, gX' the exterior force tending to decrease X'. Then by the principles of dynamics,

$$0 = \rho_1 v \frac{d^2 X}{d^2 t^*} + gX - P$$

If, now, in the formula (10) we substitute for $\lambda$ its value drawn from (9), the last equation will become

---

*Note typographical error. Should be $d^2X'/dt^2$.

$$0 = \left( \rho_1 + \frac{a'b'c' \int_0^\infty \frac{df}{a^3bc}}{2 - a'b'c' \int_0^\infty \frac{df}{a^3bc}} \right) \nu \frac{d^2X}{dt^2} + gX$$

which is evidently the same as would be obtained by supposing the vibrations to take place "in vacuo" under the influence of the given exterior force, provided the density of the vibrating body were increased from

$$\rho_1 \text{ TO } \rho_1 + \frac{a'b'c' \int_0^\infty \frac{df}{a^3bc}}{2 - a'b'c' \int_0^\infty \frac{df}{a^3bc}} \rho \qquad (11)$$

We thus perceive, that, besides the retardation caused by the loss of weight which the vibrating body sustains in a fluid, there is a farther retardation due to the action of the fluid itself; and this last is precisely the same as would be produced by augmenting the density of the body in the proportion just assigned, the moving force remaining unaltered.

When the body is spherical, we have $a' = b' = c'$, and the proportion immediately preceding becomes very simple, for it will then only be requisite to increase $\rho_1$ the density of the body by $\rho/2$, or half the density of the fluid, in order to have the correction in question.

The next case in the point of simplicity is where $a' = c'$, for then

$$\int_0^\infty \frac{df}{a^3bc} = \int_0^\infty \frac{df}{a^4b} = 2 \int_{b'}^\infty \frac{db}{a^4} \qquad (12)$$

If a'>b', or the body, is an oblate spheroid vibrating in its equatorial plane, the last quantity properly depends on the circular arcs, and has for value

$$(a'^2-b'^2)^{-\frac{3}{2}}\left\{\frac{\pi}{2}-\text{ARC}\left(\text{TAN}=\frac{b'}{\sqrt{a'^2-b'^2}}\right)\right\}-\frac{b'}{a'^2(a'^2-b'^2)}$$

If, on the contrary, a'< b', or the spheroid, is oblong, the value of the same integral is

$$*-\frac{1}{2}(b'^2-a'^2)^{-\frac{3}{2}}\,\text{LOG}\frac{b'+\sqrt{b'^2-a'^2}}{b'-\sqrt{b'^2-a'^2}}+\frac{b'}{a'^2(b'^2-a'^2)}$$

Another very simple case is where c' = b', for then the first of the quantities (12) becomes, if a' > b'

$$(a'^2-b'^2)^{-\frac{3}{2}}\,\text{LOG}\,\frac{a'+\sqrt{a'^2-b'^2}}{a'-\sqrt{a'^2-b'^2}}-\frac{2}{a'(a'^2-b'^2)}$$

and if a' >b'**, the same quantity becomes

$$2(b'^2-a'^2)^{-\frac{3}{2}}\left\{\text{ARC}\left(\text{TAN}=\frac{a'}{\sqrt{b'^2-a'^2}}\right)-\frac{\pi}{2}\right\}+\frac{2}{a'(b'^2-a'^2)}$$

---

*This minus sign was not in the original paper. Correct results require its use.

**This should have been a' < b'.

By employing the first of the four expressions immediately preceding, we readily perceive, that, when an oblate spheroid vibrates in its equatorial plane, the correction now under consideration will be affected by conceiving the density of the body augmented from $\varrho_1$

$$\text{TO } \varrho_1 + \frac{\frac{\pi}{2}a'^2b' - a'^2b' \text{ ARC}\left(\text{TAN} = \frac{b'}{\sqrt{a'^2-b'^2}}\right) - b'^2\sqrt{a'^2-b'^2}}{2(a'^2-b'^2)^{3/2} - \frac{\pi}{2}a'^2b' + a'^2b' \text{ ARC}\left(\text{TAN} = \frac{b'}{\sqrt{a'^2-b'^2}}\right) + b'^2\sqrt{a'^2-b'^2}}\,\varrho$$

When b' is very small compared with a', or the spheroid is very flat, we must augment the density

$$\text{from } \varrho_1 \text{ to } \varrho_1 + \frac{\pi}{4}\frac{b'}{a'}\varrho \text{ nearly;}$$

and we thus see that the correction in question becomes less in proportion as the spheroid is more oblate.

In what precedes, the excursions of the body of the pendulum are supposed very small compared with its dimensions. For, if this were not the case, the term of the second degree in the equation (1) would no longer be negligible, and therefore the foregoing results might thus cease to be correct. Indeed, were we to attend to the term just mentioned no advantage would even then be obtained; for the actual motion of the fluid, where the vibrations are large, will differ greatly from what would be assigned by the preceding method, although this method consists in

satisfying all the equations of the fluid's motion, and likewise the particular conditions to which it is subject. It would be encroaching too much upon the Society's time to enter on the present occasion into an explanation of the cause of this apparent anomaly: it will be sufficient here to have made the remark, and, at the same time, to observe, that when the extent of the vibrations is very small, as we have all along supposed, the preceding theory will give the proper corrections to be applied to bodies vibrating in air, or other elastic fluid, since the error to which this theory leads cannot bear a much greater proportion to the correction before assigned, than the pendulum's greatest velocity does to that of sound.

---